University of Stavanger

Faculty of Science and Technology

MASTER'S THESIS

Study program/Specialization: Petroleum Engineering/Natural Gas Technology	Spring semester, 2021 Open
Writer: Ida Haug Færøy	Ida Haug Færøy (Writer's signature)
Faculty supervisor: Rune W. Time Herimonja A. Rabenjafimanantsoa	
Thesis title: Ocean & climate lab scale model – Thermal circulation with surface wind drive	
Credits (ECTS): 30	
Key words: Ocean circulation Thermohaline circulation Surface circulation Wind drive Stommel's model Flow measurement Heat flow dynamics	Pages: 81 + supplemental material: 29 Haugesund, 15.06.2021 Date/year

Acknowledgement

This thesis is a part of my Master of Science Degree Programme in Petroleum Engineering, Natural Gas Technology, from the University of Stavanger. The experimental work in this thesis was performed in the multiphase laboratory for the Department of Petroleum Engineering. The purpose of this thesis has been to design, build and test a new ocean and climate lab scale model. It has been both exciting and challenging to work with an experimental thesis, and I would like to express my sincere gratitude to the following people, whom without I would not have been able to complete this research:

Professor Rune W. Time, who gave me the opportunity to write an interesting experimental thesis, and whose insight and knowledge into the subject matter steered me through this research. I would also like to thank him for providing the MATLAB program used.

Senior Engineer Herimonja A. Rabenjafimanatsoa, for sharing his enthusiasm for working in the laboratory, his knowledge and many years of experience, and for guiding me throughout the project. Thank you for lending me a helping hand during the construction and testing of the model.

Rune J. Færøy, who took the time to help drill holes in the bottom plates of the model and lent me the equipment needed. Thank you for giving good guidance throughout the process of building the model.

Alf Kristian Haugland, for the optimism and enthusiasm he has shown for the project, for showing me that there is always a solution and then helped me find it. Thank you for helping with proof-reading and valuable feedback.

Caroline Haug, who spent her weekends helping me design the equipment in Autodesk Inventor, allowing my thesis to go the extra mile, and for proof-reading the thesis.

Special thanks to Bente Haug for helping with proof-reading the thesis, for giving valuable feedback throughout the entire writing process and for having put up with my stresses and moans for the past half year. None of this would have been possible without her encouragement and unwavering support.

And at last, I would like to thank my family and friends who has engaged in my work, asked questions and encouraged me while working on this thesis.

Ida Haug Færøy

Abstract

Background: The earth receives more heat from the sun at the equator than at the poles. This imbalance is offset by the fact that heat is continuously transported from low-latitude oceans by large-scale winds and ocean currents towards high-latitude oceans. The return current is dependent on the density difference created by the temperature and salt difference in the oceans. This plays a key role in our climate, but we still don't know much about how the system is affected by outside variables. The world is facing global warming issues, resulting in more ice melting and therefore a larger influx of freshwater to the high-latitude oceans, and stronger and more unstable wind patterns.

Purpose: The purpose of this thesis was to design, build and test a laboratory model for thermal circulation with surface wind. The model will be used by students, teachers and professors in the multiphase laboratory at the University of Stavanger. It was therefore also desired to have a detailed description of the components, equipment and techniques used.

Method: The thesis has an experimental design. Before building the model, a technical feasibility study was performed in order to find the best design. The feasibility study illuminates the down sides of the thermohaline circulation model currently situated in the multiphase laboratory, proposes different designs that satisfies requirements set by the faculty supervisors, together with measurement and conditioning systems.

Findings: Based on analysis of flow rate, it can be concluded that an air flow introduced in the same direction as a liquid surface moving due to thermal circulation would result in a positive impact on the flow rate. Air flow introduced in the opposite direction as a liquid surface moving due to thermal circulation would result in a negative impact on the flow rate. Experiments also proved that a higher wind speed introduced to a water surface allowed a higher amount of energy to be transferred from the wind to the liquid.

Conclusion: With the modifications done throughout the process, the final result was satisfactory relative to expectations. The experimental design functioned as intended, and the measurement data received during tests held a high quality due to the measurement equipment chosen.

Keywords: Ocean circulation, Thermal circulation, Surface circulation, Wind drive, Stommel's model, Flow measurement, Temperature measurement, Heat flow dynamics, Pasco, Sensirion.

Nomenclature

Abbreviations

THC	Thermohaline circulation
OD	Outer diameter
ID	Inner diameter
PIV	Particle image velocimetry
Re	Reynolds number

Roman letters

A	Area [m^2]
d	Diameter [m]
h	Height [m]
k	Thermal conductivity [W/mK]
L	Length [m]
g	Acceleration [m/s^2]
t	Time [s]
Q	volumetric flow [m^3/s]
T	Temperature [°C]
c	Temperature transfer coefficient [s^{-1}]
P	Pressure [Pa]
R	Resistance
h	Heat transfer coefficient [W/m^2K]
D	Characteristic length [m]
v	Velocity [m/s]
$\bar{v}$	Average velocity [m/s]
v_{max}	Max velocity [m/s]

Greek letters

μ	Viscosity [Ns/m^2]
ρ	Density [kg/m^3]
σ	Stefan-boltzmann constant [W/m^2]
ϵ	Emissivity

Contents

List of Figures

List of Tables

Chapter 1

Introduction

Ocean water is constantly moving in form of waves, tides and currents. Some ocean currents flow at the surface, others deep within the water, some flow for short distances while others flow across entire oceans. Climate variations and changes are strongly affected by these ocean circulations because they bring heat from the equator to the poles. If the ocean circulation were to be affected by the global warming experienced today, it could affect important circulation systems such as the Gulf Stream. Effects scientists had predicted in the past would result from global climate change are now occurring, such as loss of sea ice, accelerated sea level rise, longer, more intense heat waves, increase in the number, duration and intensity of tropical storms and larger changes in predictable wind patterns. [9] [10]

Designing and creating a model where one can introduce surface wind would allow studies on the influence of wind on the ocean circulation to be conducted. This could help better our understanding of how atmospheric impacts affects the ocean circulation. If we can understand the mechanisms of exchanging water, we will be better able to predict how the system will react to climate change, and how stable the circulation is against deviations predicted by scientists.

In this thesis, the objective was to develop an experimental model to conduct experiments concerning thermal circulation with surface wind, where temperature and wind speed could be altered. It was desirable to test how the temperature and fluid flow rate was affected by the surface air flow to see if the theoretical methods chosen actually worked as expected. An existing small-scale model for thermohaline circulation is located in the multiphase laboratory at the University of Stavanger. Due to multiple limitations identified in a feasibility study, it was decided to design and build a new model which would consist of larger volumes, but smaller heights.

A numerical model in form of a MATLAB program has been developed by Professor Rune W. Time, in order to calculate the maximum overturning flow when changing the setup and set conditions. With the results from this program, one has the opportunity to compare theory to the obtained experimental data and discuss how coherent they are.

After the new model was designed and approved by the supervisors, the model was built and tested. Modifications were done to improve the experimental data and simplify the usage. The fluid flow was measured by a Sensirion flow meter, and temperature was measured by fast responding temperature sensors from Pasco. The data was analyzed using programs such as Capstone, Microsoft Excel and MATLAB. A moving average was used to analyze the flow measurements due to the flow meters sensitivity.

As preparation for this thesis, different articles and books concerning ocean circulation, multiphase flow and measurement systems were read to gain background knowledge and a better understanding for how the model should be designed. An important part of the experiments was to study how the method chosen for introducing wind drive affected the circulation measured by the flow meter. A lot of useful information and inspiration was therefore taken from the subject Multiphase Flow in Pipes held by Professor Rune W. Time, Senior Engineer Herimonja A. Rabenjafimanantsoa and Associate Professor Tore H. Flåtten.

The thesis is organized as follows:
Chapter 2 introduces theory related to the designing and experimentation. It concerns topics like Ocean circulation, Stommel's model, the NORTH project, fluid flow in pipes and heat transfer.

Chapter 3 includes a feasibility study. The first part highlights faults and limitations with the old experimental model and introduces the requirements for the new model. Designs which satisfies these requirements are presented together with conditioning and measurement systems. The final part explains the different tests performed before the model could be built and used in experimentation.

Chapter 4 describes the experimental setup regarding the construction, use of measurement equipment and data analysis.

Chapter 5 presents the experimental results, including flow rate measured by Sensirion flow meter, temperature measured by Pasco equipment and how optimizing the model affected the measurement data.

Chapter 6 discusses the experimental data together with research limitations and future research propositions.

Chapter 7 is a summary of all the conclusion which may be drawn from the thesis.

Appendices A, B, C and **D** covers MATLAB scripts used in the model, different experimental results, a user guide for the model and various illustrations respectively.

Chapter 2

Theory

This chapter includes a short introduction of some relevant topics used for developing the new model, including information about ocean circulation, Stommel's theoretical model, the NORTH loop, fluid flow in pipes and heat transfer.

2.1 Key aspects of ocean circulation

Ocean circulation is often divided into surface circulation and thermohaline circulation (THC). Surface circulation includes surface currents from wind and tides appearing in the upper parts of the ocean due to the gravity of moon and sun. THC includes the part of the ocean circulation which is driven by fluxes of heat and freshwater. These two circulations interact with each other, and together they represent the ocean circulation. [1]

2.1.1 Thermohaline circulation

THC is used to describe how ocean circulation is driven by a difference in density, as density varies as a function of salinity and temperature. Warmer, saltier surface water will flow from low latitudes towards high latitudes, where some evaporation will happen and heat is lost to the atmosphere due to the strong temperature gradient. Losing its heat, the water becomes denser due to a higher salt content and sinks. In the North Atlantic Ocean the water becomes so cold that sea ice starts to form. The salt naturally present in seawater does not become part of the ice, but is left behind in the ocean water that lies just underneath the ice, making the water more dense. The increase in density links the warm surface flow to the cool, deep return flow, as the cold, dense water slowly spreads southward. The flows are also linked by upwelling, where a divergence of surface waters causes an upward flux of deep water, and the circulation is complete. [1]

Figure 2.1 shows a schematic representation of the global THC. Surface currents are shown in red, deep waters in light blue and bottom waters in dark blue. The main deep water formation sites are shown in yellow.

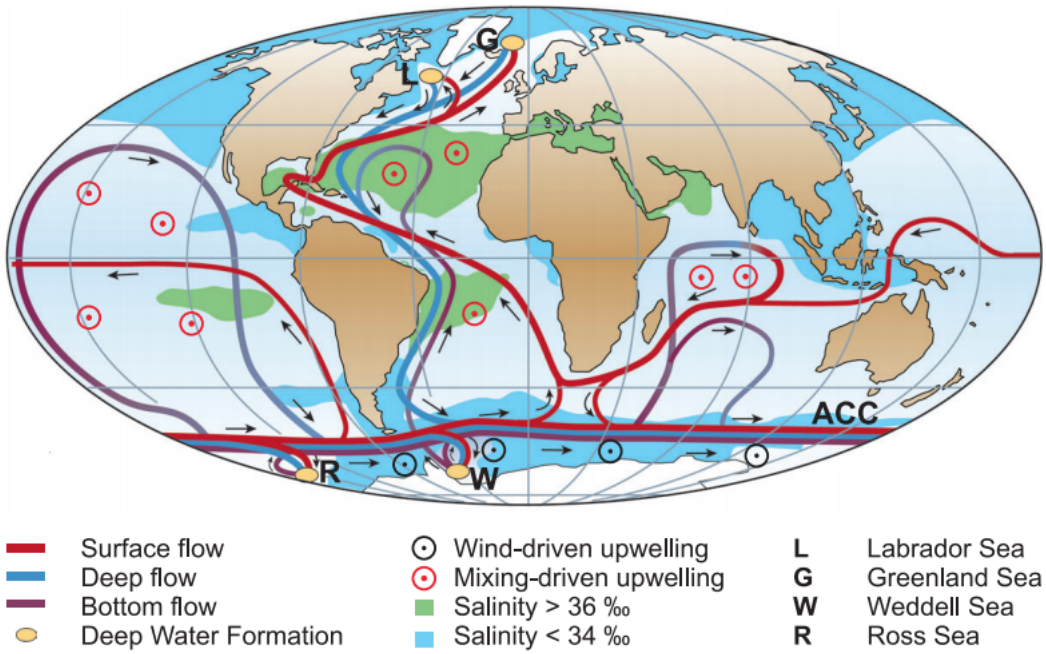

Figure 2.1: Schematic representation of the global thermohaline circulation [1]

Figure 2.2 shows the typical temperature profiles of high-, low-, and mid-latitude oceans. The temperature in a low-latitude ocean varies with depth, while the temperature in a high-latitude ocean is seen to be quite constant independent of depth. [11]

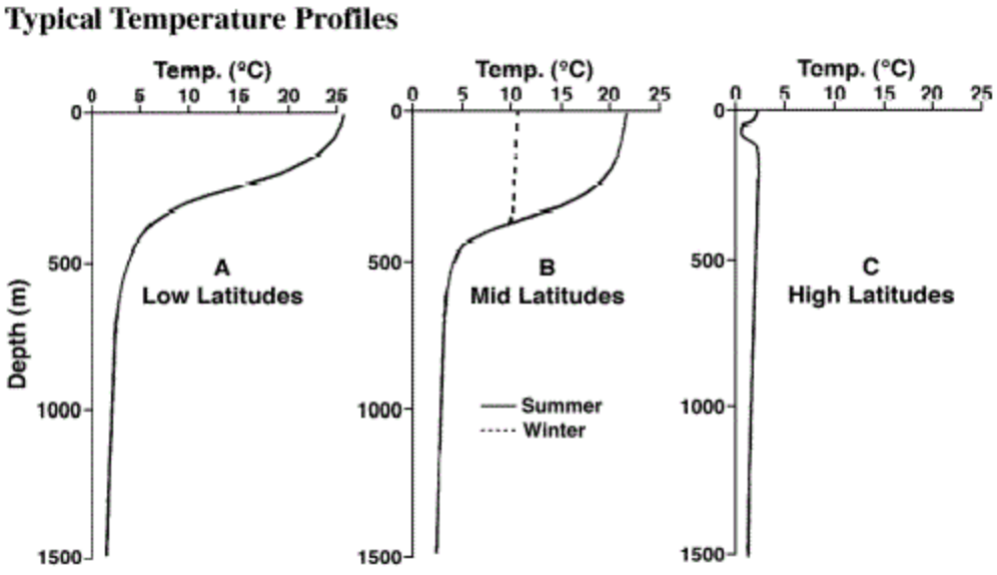

Figure 2.2: Schematic representation of the temperature gradient in oceans

There are 90 degrees of latitude. Low-latitude oceans are located between the Equator (0 degree latitude) and 30 degrees north/south. High-latitude oceans are located between the poles and 30 degrees north/south. The oceans in between (30 - 60 degree latitude) are referred to as mid-latitude. [12]

2.1.2 Surface circulation

Surface circulation is a combination of currents and tides. Tides contribute to coastal currents that travel short distances. Large-scale currents are driven by global wind systems that are fueled by energy from the sun and transfer heat from the tropics to the polar regions. Wind drags on the surface of the water as it blows, and the wind stress induces a circulation pattern that is similar for each ocean, crating gyres that stretch across the entire ocean. Currents do not simply track the wind, but is influenced by the shape of coastline and the seafloor and most importantly the rotation of the Earth. The depth penetration of the wind-driven currents depends on the intensity of ocean stratification. [13]

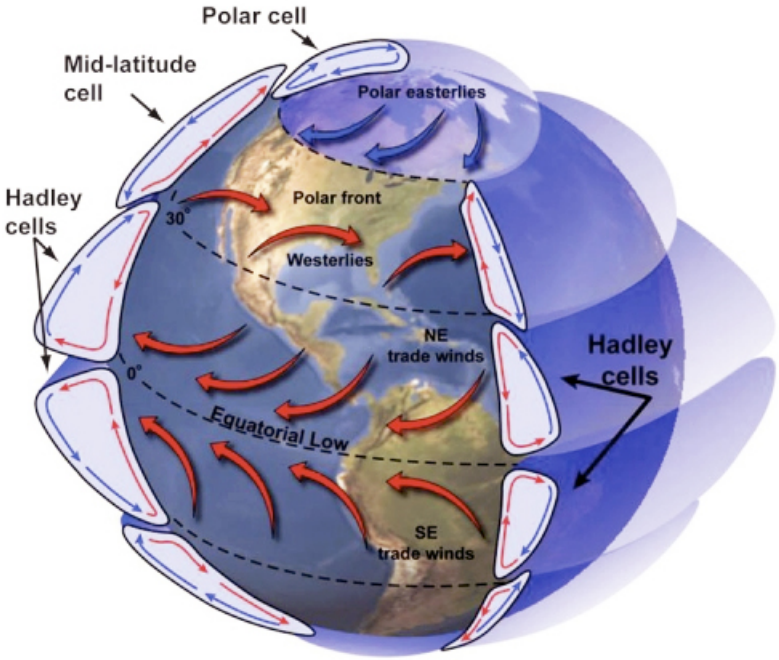

Figure 2.3: Schematic representation of the global wind belts [NASA]

Figure 2.3 shows a schematic representation of the global wind belts. In the Northern Hemisphere, predictable winds blow from east to west just above the equator, pulling surface water with them and creating currents. As these currents flow west, the Coriolis effect caused by Earths rotation deflects them, and bends them north. At about 30 degrees north latitude, a different set of winds push the currents back to the east, producing a closed clockwise loop. Below the equator, in the Southern Hemisphere, the same phenomenon takes place. The Coriolis effect bends surface currents south, producing a counter-clockwise loop. [13]

2.2 Stommel's two box model

Stommel's model (1961) is a widely known mathematical model for visualizing ocean circulation. The model consists of two waterfilled boxes representing one high-latitude ocean and the other a low-latitude ocean. The boxes were placed at the same level and connected with two tubes, one at the top and one at the bottom. The circulation was through these two tubes, overflow on the top and capillary flow, also known as overturn, on the bottom. The direction of the capillary flow was controlled by the density differences between the water in the two boxes. The two boxes had both porous, separating walls with a storage tank providing salt or heat to the water boxes. The box representing the low-latitude ocean contained warm saltwater, while the box representing the high-latitude ocean contained cold freshwater. Mixing propellers were used to ensure a uniform concentration as the fluid flowed between the two boxes. [2] [14]

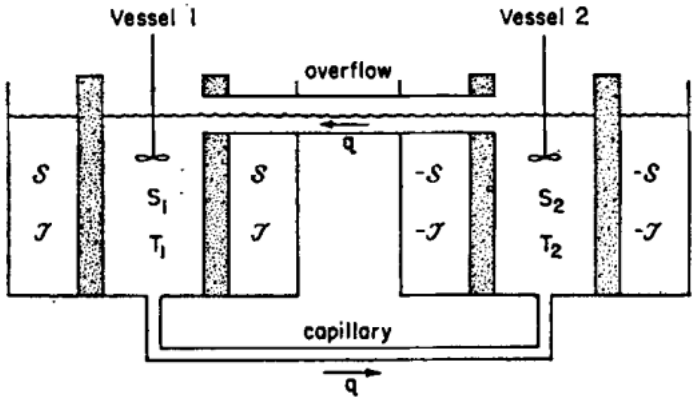

Figure 2.4: Stommel's two box model illustration [2]

Figure 2.4 shows an illustration of the Stommel's two box model. Rate of flow is given by q, and the arrow shows the direction through capillary determined by the density difference between the two boxes. The upper overflow is provided so that the surface level in each box remains the same.

2.3 The NORTH model

The NORTH project was a collaboration between the University of Stavanger and the Bjerknes Centre at the University of Bergen, which purpose was to assess the fundamental structure and operation of the Atlantic THC's northern limb. In relation to this project, the University of Stavanger developed and constructed an experimental model for THC. The experimental model was named the NORTH loop, figure 2.5, short for "northern constraints on the Atlantic thermohaline circulation".

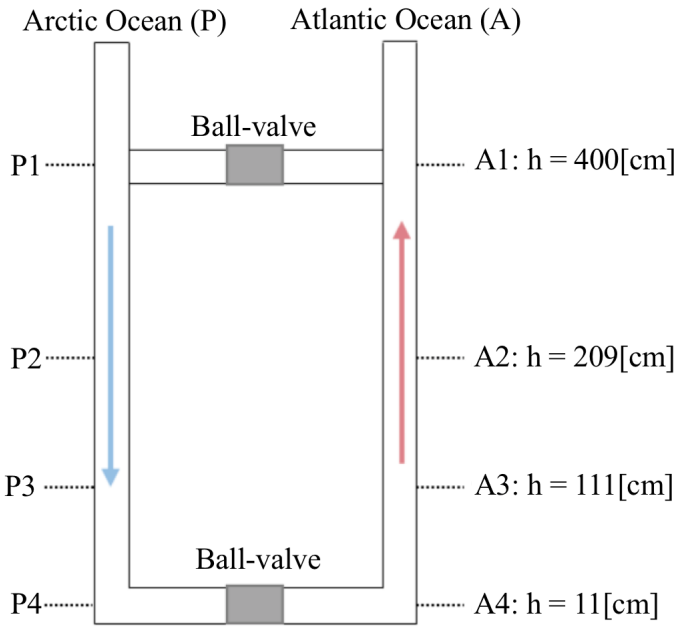

Figure 2.5: the NORTH loop with temperature sensor placement

The experimental model was made of two vertically placed transparent, acrylic pipes with a length of 4.5 m and an inner diameter of 0.05 m. At the bottom and a half meter from the top, passages were placed across, allowing the working fluid to circulate. Water with different temperature and salinity was placed in each vertical pipe to represent water from different latitudes.

2.4 Fluid flow in pipelines

Fluid flow in pipes is a comprehensive subject that builds on fluid mechanics and thermodynamics. Difficult areas are phase transitions, multiphase viscosity, internal flow in multiphase mixtures, compressibility effects and pressure gradients. [4] This section gives only a brief introduction to single phase flow and two phase flow in pipelines that are relevant to the thesis.

Flow is defined as the quantity of a given fluid that passes by a certain point within a unit of time, and is dependent on a pressure gradient between two points. The pressure gradient establishes the direction of flow, and the pressure difference the flow drive. [3] Flow is commonly expressed as:

$$Q = \frac{V}{t} \tag{2.1}$$

where Q is the flow, V is the volume and t is time.

The flow inside a pipe is related to velocity by the relationship:

$$Q = vr^2 \tag{2.2}$$

where Q is the fluid flow, v is the mean velocity and r is the fluid radius.

2.4.1 Single-phase flow in pipes

In single phase flow in pipes, the flow pattern of a fluid can be divided into laminar and turbulent flow, as well as a transitional zone between these two flow patterns.

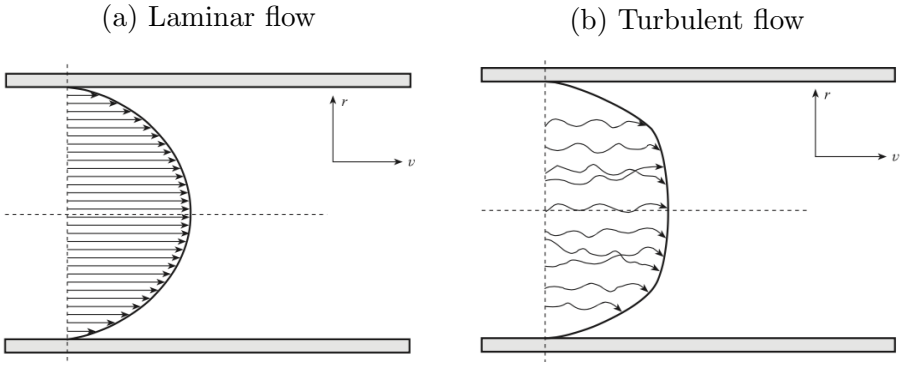

Figure 2.6: Flow profiles of fully developed laminar and turbulent flows [3]

Reynolds number (Re) is a dimensionless quantity used to differentiate between different flow regimes. The expression is based on the ratio of inertial forces to viscous forces, and is given by equation:

$$Re = \frac{\rho v D}{\mu} \tag{2.3}$$

where ρ is the fluid density, v is the average fluid velocity, D is the characteristic length of the geometry (diameter for pipes) and μ is the fluid dynamic viscosity. Density and dynamic viscosity depends on temperature. Table 2.1 shows some common values for water.

Table 2.1: Density and dynamic viscosity for water [7]

Temperature	ρ [kg/m^3]	μ [Ns/m^2 $\times 10^{-3}$]
0	999.85	1.787
10	999.70	1.307
20	998.21	1.002
30	995.65	0.798

Laminar flow:
Laminar flow in pipes can be described as flow following smooth streamlines in a highly ordered motion, resulting in a parabolic velocity profile shown in figure 2.6 (a). Although laminar flow moves in straight lines, each streamline has a different velocity. Molecules in the center of the flow has the highest velocity, whereas those at the periphery of the pipe are almost motionless due to frictional forces between the pipe surface and the fluid. For steady and fully developed flows the velocity profile remains unchanged in the flow direction. [3]

The velocity profile of a laminar flow can be expressed:

$$v(r) = 2\bar{v}(1 - \frac{r^2}{R^2}) \tag{2.4}$$

where $v(r)$ is the velocity profile, $\bar{v}$ is the is the average fluid velocity, r is the distance from pipe center to the stream line and R is the radius from centerline to the pipe wall. The average velocity for a fully developed laminar flow in a pipe is half the maximum velocity, $\bar{v}=\frac{1}{2}v_{max}$.

Flow in circular pipes with Re < 2300 are defined as laminar.

Fluids flow in a laminar pattern when they have low flow rates through smooth pipes with large cross-sectional areas. Laminar flow is directly proportional to the pressure gradient, and can according to Ohm's law be expressed by the linear relationship

$$Q = \frac{\Delta P}{R} \tag{2.5}$$

where Q is the fluid flow, ΔP is the differential pressure and R is the resistance.

Turbulent flow:
Turbulent flow in pipes is characterized by highly disordered motion and velocity fluctuations, shown in figure 2.6 (b). The molecules move in irregular directions due to eddy currents, and the disordered nature of turbulent flow increases resistance to flow. Unlike laminar flow, turbulent fluids have a nonlinear relationship between flow and pressure. The flow rate is proportional to the square root of the pressure gradient, resulting in a larger pressure gradient required to increase turbulent flow. This is why laminar flow patterns are preferable to turbulent ones. [3]

Flow in circular pipes with Re > 4000 are defined as turbulent.

Transition flow:
Transition flow, also known as transient flow, is the phase that occurs between laminar and turbulent flow. In this phase there is a mixture of laminar and turbulent flows present. Flow in circular pipes with Re between 2300 and 4000 are defined as transitional. [3]

2.4.2 Two-phase flow in pipes

Two-phase flow in pipes refers to the interactive flow of two distinct phases with common interfaces in a pipeline. Two-phase flow is discriminated between flow regimes that are characteristic for the time and space distribution of gas and liquid flow. [4]

Horizontal pipes
In horizontal pipes there are six flow regimes, as shown in figure 2.7, where the velocity is increasing from stratified, smooth flow to annular flow. At low velocities the gas and liquid is separated as in stratified flow. At high velocities gas and liquid become mixed. Slug flow is an example of a flow regime in between, representing both separation and mixing, and is consequently referred to as an intermittent flow regime.

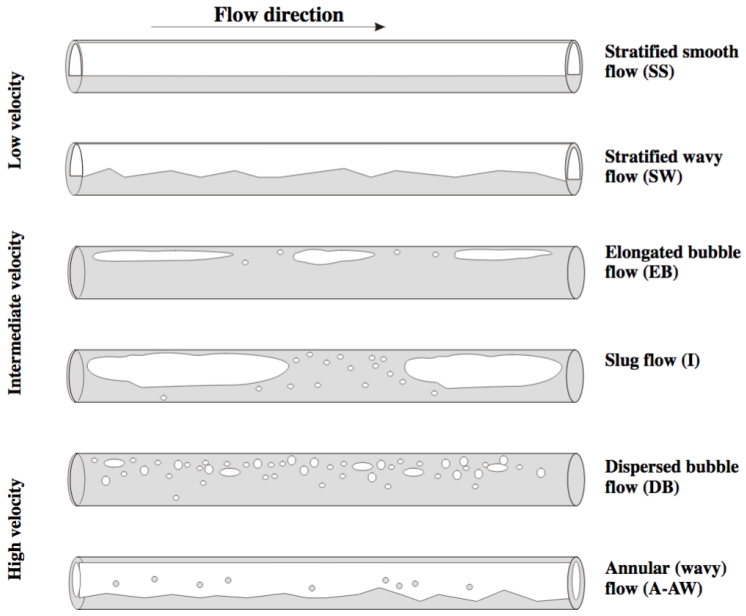

Figure 2.7: Horizontal pipe, two-phase flow regimes [4]

Vertical pipes

In vertical pipes there are four flow regimes, as shown in figure 2.8, where the velocity is increasing from slug flow to annular flow.

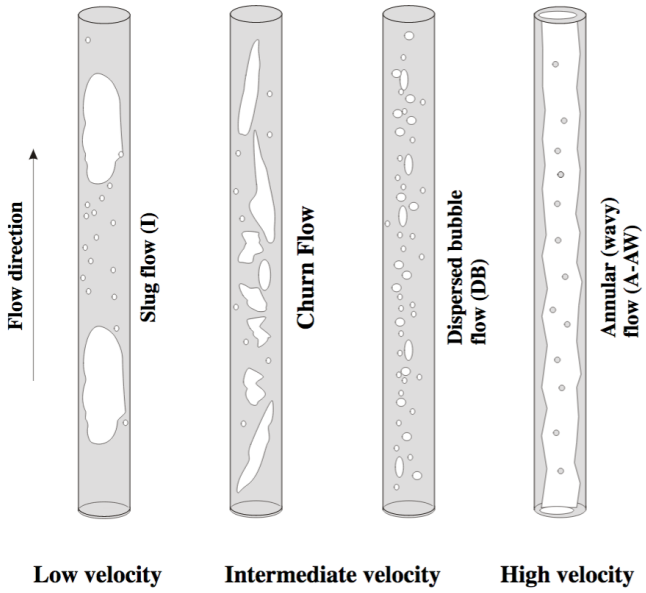

Figure 2.8: Vertical pipe, two-phase flow regimes [4]

2.5 Heat transfer

Heat is defined as energy transferred from one system to another as a result of a temperature difference. The transfer is always from a system of higher temperatures to a system of lower temperatures, and the heat transfer stops when the two systems reaches equilibrium. Heat transfer can be divided into three mechanisms: conduction, convection and radiation. [8]

2.5.1 Conduction

Conduction is defined as transfer of energy from more energetic particles of a substance to the adjacent, less energetic ones as a result of interaction between the particles. Conduction can take place in both solids and fluids. In solids, it is due to a combination of vibrations of the molecules in a grid and the energy transported by free electrons. In fluids, it is due to the collisions and diffusion of the molecules during their random motion. The rate of heat conduction through a medium depends on the geometry of the medium, its thickness and material as well as the temperature difference across the medium. [8]

The rate of heat conduction is expressed by Fourier's law:

$$Q_{cond} = -kA\frac{dT}{dx} \tag{2.6}$$

where Q_{cond} is the rate of heat conduction, k is the thermal conductivity of the material, A is the area and dT/dx is the temperature gradient.

Table 2.2: Thermal conductivities of some materials at room temperature [8]

Material	k [W/mK]
Copper	401
Aluminium	237
Acrylic	0.2
Water (liquid)	0.607
Air (gas)	0.026

Table 2.2 shows the thermal conductivities of some relevant materials at room temperature. A high conductivity value indicates that the material is a good heat conductor, and a low value the opposite. [8]

2.5.2 Convection

Convection is defined as heat transfer between a solid surface and an adjacent fluid in motion, and it involves the combined effects of conduction and fluid motion. Although fluid motion enhances the heat transfer between the solid surface and the fluid, it also complicates the determination of heat transfer rates. [8]

The rate of convection heat transfer is observed to be proportional to the temperature difference, and is conveniently expressed by Newtons law of cooling as:

$$Q_{conv} = hA_s(T_s - T_\infty) \tag{2.7}$$

where Q_{conv} is the rate of heat convection, h is the convection heat transfer coefficient, A_s is the surface area through which convection heat transfer takes place, T_s is the surface temperature and T_∞ is the temperature of the fluid sufficiently far from the surface. Typical values of h are given in table 2.3.

Table 2.3: Typical values of convection heat transfer coefficient [8]

Type of convection	h [W/m^2K]
Free convection of gases	2-25
Free convection of liquids	10-1000
Forced convection of gases	25-250
Forced convection of liquids	50-20 000
Boiling and condensation	2500-100 000

Convection is referred to as forced convection if the fluid is forced to flow over a surface by external means, and in contrast it is referred to as free convection if the fluid motion is caused by buoyancy forces induced by density differences due to the variation of temperature in the fluid. The convection heat transfer coefficient is not a property of the fluid, but an experimentally determined parameter whose value depends on the surface geometry, the nature of fluid motion, the properties of the fluid and the bulk fluid velocity. [8]

2.5.3 Radiation

Radiation is defined as energy emitted by matter in the form of electromagnetic waves as a result of changes in the electronic configurations of atoms or molecules. Radiation is considered the fastest transfer, suffers no attenuation in a vacuum, and are unlike the other mechanisms not dependent on the presence of an intervening medium. It is described as a volumetric phenomenon, and all solids and fluids emit, absorb or transmit radiation to varying degrees. [8]

The radiation emitted by a surface can be expressed by the Stefan-Boltzmann law as:

$$Q_{emit} = \epsilon \sigma A_s T_s^4 \tag{2.8}$$

where Q_{emit} is the rate of radiation heat, ϵ is the emissivity of the surface, σ = 5.670 x 10^{-8} [W/m^2 K^4] is the Stefan-Boltzmann constant, A_s is the surface area through which convection heat transfer takes place and T_s is the surface temperature.

Emissivity is a measure of how closely a surface approximates an idealized surface for which $\epsilon = 1$. The emissivities of some surfaces are given in table 2.4

Table 2.4: Emissivities of some materials at 300 K [8]

Material	Emissivity
Aluminum foil	0.07
Anodized aluminium	0.82
Polished copper	0.03
Water	0.96

The determination of the net rate of heat transfer by radiation between two surfaces depends on the properties of the surfaces, their orientation relative to each other and the interaction of the medium between the surfaces with radiation. The net radiation heat transfer between two surfaces is given by:

$$Q_{rad} = \epsilon \sigma A_s (T_s^4 - T_{surr}^4) \tag{2.9}$$

where T_{surr} is temperature of the surrounding.

2.6 Principles of measurement

While working on this thesis, some principles of measurement were seen as relevant to define.

2.6.1 Signals

A signal is defined as an electrical impulse or radio wave transmitted or received that is used to convey information. Signals can be described as deterministic or random. [3]

Deterministic signals: is one whose value at any further time can be exactly predicted, based on recordings of the signal for an observation period. [3]

Random signals: is one whose value at any further time can not be exactly known, based on recordings of the signal for an observation period. [3]

Noise signals: are unwanted random signals. A method of reducing the noise signals is moving averages. [3]

Moving average: is a method used to reduce the noise signals in experimental data. A running average will smooth out the measured data by creating a series of averages, giving a more clear indication of the results. The amount of noise reduction is equal to the square-root of the number of points in the average. [3]

2.6.2 Time series analysis

Analysis of experimental data often involve processing of time series. Data recorded in time series can be described as evenly spaced or unevenly spaced. [3]

Evenly spaced time series: is experimental data recorded with a constant sampling rate, meaning the time between each measured value is constant. [3]

Unevenly spaced time series: is experimental data recorded with an uneven sampling rate, meaning the data needs adjustment to be able to be compared with data of even time series. [3]

Chapter 3

Feasibility study

A technical feasibility study with multiple tests were performed when designing the model. Disadvantages with the NORTH model was identified and a set of requirements for the new model were made together with the supervisors. Multiple designs were proposed together with conditioning techniques and measurement systems. The feasibility study with its tests were used in order to choose the overall best design.

3.1 Faults and limitations with the NORTH model

The new model was not only supposed to be based on Stommel's two-box model, showed in chapter 2, but also on the old NORTH loop. Therefore, its faults and limitations needed to be identified in order to avoid getting them in the new model. Old reports were read and the model was tested. Also part of the preparation for the thesis was emptying, cleaning and dismantling the different equipment used in the NORTH model, as well as checking the measurement equipment to determine if they were still usable.

3.1.1 Leakage points

During testing of the model, there were identified multiple leakage points. The NORTH model had drilled holes in the acrylic pipes for temperature sensors, salinity sensors, flow meters and water inlets. The amount of drilled holes increased the chance of leakage, and the model had to be resealed multiple times in between experiments. During the tests it was discovered a leak in one of the salinity sensor connections, a pump connection and in the bottom valve. Although the water lost from the system was considered to be a small amount, it would still affect the circulation, especially during experiments running through a long period of time.

3.1.2 Conditioning techniques

To achieve a desired temperature inside the NORTH model, a circulatory system depending on peristaltic pumps were used. Two water baths set to the desired temperature were used as temperature regulators, and the liquid would flow from the inlet via a capillary pipe in the circulation system, through a heating coil located in the temperate water bath inside the regulator, and back into the pipe system. The circulation system can be seen in figure 3.1.

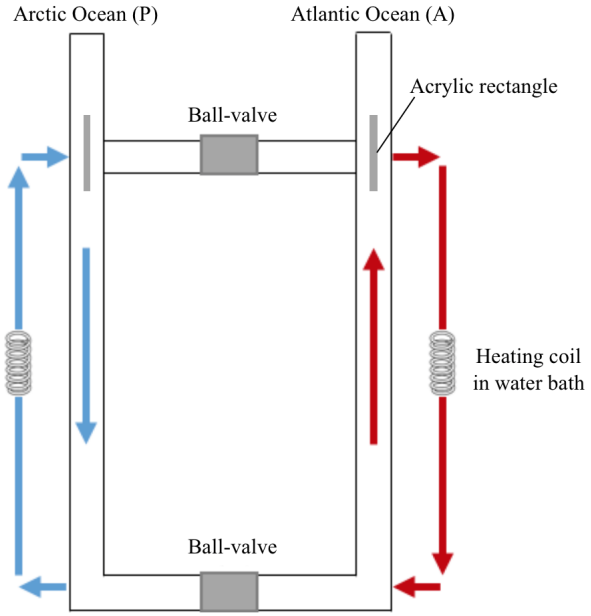

Figure 3.1: Temperature regulation system, NORTH loop

The system was based on an ideal situation without any cross-flow due to temperature regulation. To reduce the potential of cross-flow, rectangular plates of acrylic material were put inside each vertical pipe after the inlet to force the fluids direction away from the cross-pipes, ref. figure 3.1. Although this proved to be helpful, there were still some cross-flow influencing the flow meters, and the acrylic plates would further limit the models versatility. Peristaltic pumps has pulsation as an important side effect. From fluid measurements found in old reports, it could clearly be seen that this influenced the results. [15] Collecting reliable data from experiments proved therefore to be difficult [5].

The fluid flow from the circulation system would also impact the sensitive temperature sensors used, which can clearly be seen from figure 3.2 where sensor P1 was situated near the liquid inflow [5]. The placement of each sensor seen in figure 3.2 may be found in figure 2.5.

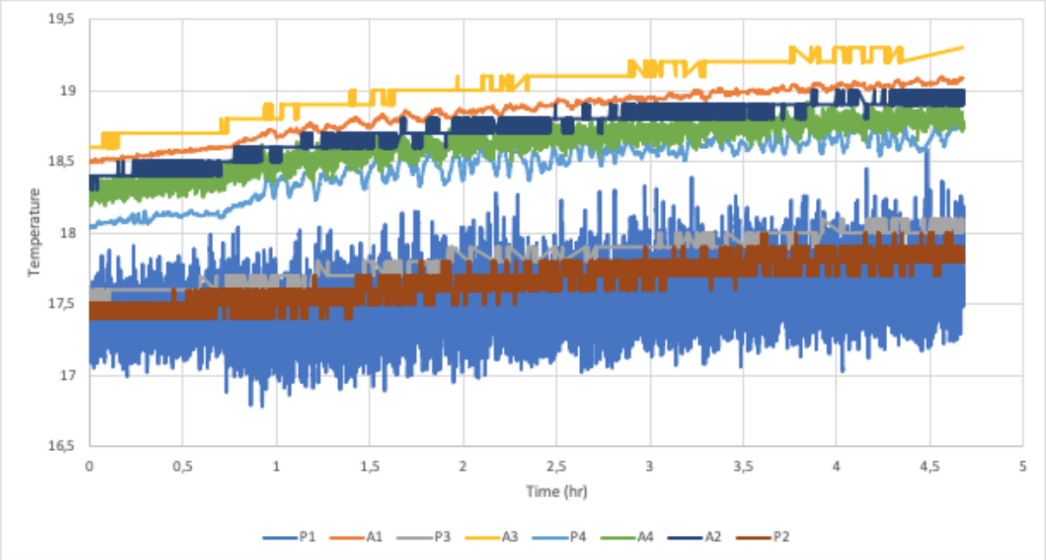

Figure 3.2: Temperature behaviour in NORTH model [5]

To replicate the evaporation happening in ocean circulation, an external evaporation system was implemented. A mass balance of salt content was expected to be preserved throughout experiments, but proved inaccurate. It was observed reduced values in the fluid circulating and a salt accumulation in the evaporation system resulting in an ineffective salt drive. [5]

3.1.3 Experimental limitations

The NORTH model design introduced a number of limitations in terms of conditioning, which in turn affected the overall versatility of the model. The small volume compared with the large height made it unfavorable to exchange the current temperature regulation system with heating/cooling coils directly inserted into the model, as it would take up too much space. From figure 3.2 it can also be seen how the temperature in both vertical pipes increased during experiments. The circulatory system gave the model an almost homogeneous temperature in each vertical pipe, which corresponds well with Stommel's model, but removes an important feature of the real ocean circulation system in which there is a temperature gradient. Achieving a realistic temperature gradient without additional cooling/heating could be hard. The design had also not taken into account wind drive. The acrylic plates mentioned in the section above, together with the temperature regulation systems inlet, was situated in a way that made it hard to introduce air flow into the system. All of this combined made it more favorable to create a new model instead of trying to change the NORTH model.

3.2 Model designs that meet the new requirements

After discussing the ineffective areas of the NORTH model with the supervisors, some requirements were set for the new model:

- A method for introducing surface wind
- An effective temperature conditioning technique
- A flexible design where the heights and lengths could be altered
- Few leakage points
- Enable easy disassembly and consequently preservation of equipment

The new model should also be based on two PE100 plates and two PMMA cast tubes ordered by the faculty supervisors. Information about these parts may be found in Appendix C together with Inventor drawings. Appendix C includes a detailed description of how they were connected and sealed. After connection, each bottom plate connected to a tube is referred to as a tank, as the item is now sealed at the bottom while it is open at the surface. Pipes connected to other pipes, bends or valves are referred to as pipelines or systems. For time and financial reasons, the equipment and materials used should be readily available in the laboratory. This introduced some limitations when designing and building the new model, which increased the desire to have a mobile and flexible design in order to make it possible to perform changes later.

This section is divided into top circulation and bottom circulation. The different designs proposed are presented by illustrations with a short explanation and compressed list of the designs advantages and disadvantages. Both illustrations and lists may be used later in the event of changing the design.

3.2.1 Top circulation

Top circulation refers to the pipeline connecting the two tanks at the top. The main goal was to find a flexible and simple design where an air flow could be introduced to simulate wind on ocean surface. Two different designs were presented together with information on how they could be altered in terms of different measurement techniques.

Top Circulation A:
Figure 3.3 shows an illustration of top circulation design A. The design is based on a pipeline resting on top of the water tanks, making it completely mobile. In order for liquid to circulate, the pipeline is dependent on the principle of vacuum. Air can be removed by a vacuum pump, which will drag the liquid up and into the pipeline. Closing the inlet/outlet will ensure a vacuum inside the pipeline, so long as it is airtight. Wind can be introduced by connecting the vacuum pump to both sides of the pipeline. The vacuum will be maintained, and the air which is pushed into the pipeline will equally be removed from the pipeline at the opposite side, making a closed loop of air circulation. The direction of wind can easily be altered based on which side the outlet of the pump is connected to. The fluid flow can be measured using particle image velocimetry (PIV), or by introducing a valve in the pipeline the fluid flow can be measured by a flow meter. This is shown in figure D.1 found in appendix D.

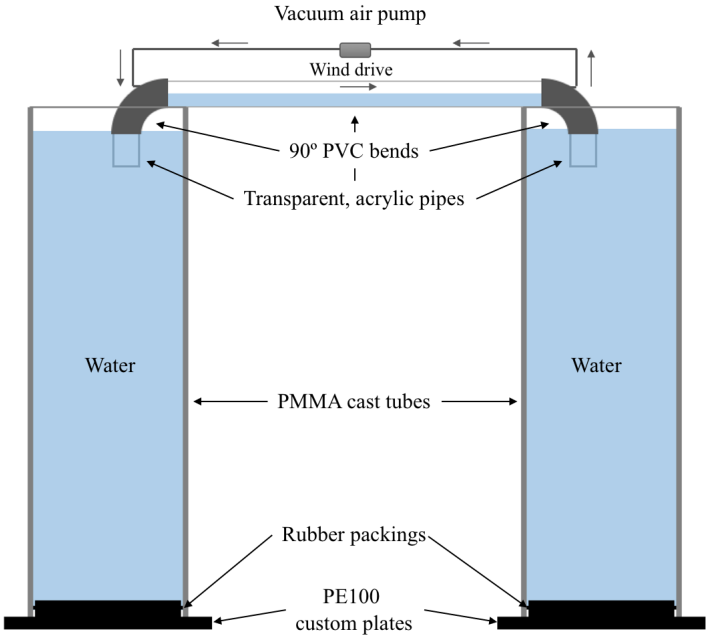

Figure 3.3: Illustration of Top Circulation A design

Advantages and disadvantages with Top Circulation A

Advantages	**Disadvantages**
• No holes in PMMA tubes	• Must be airtight
• Multiple measurement techniques	• Hard to regulate temperature inside
• Theoretically possible to introduce wind drive on surface	• Two liquid heights to deal with
• Theoretically possible to introduce evaporation directly inside pipeline	
• Easily disconnected for cleaning, maintenance, etc..	
• No need for a valve to separate the fluids when tempering liquid	
• Lengths, diameters and shapes can easily be changed	

Top Circulation B:

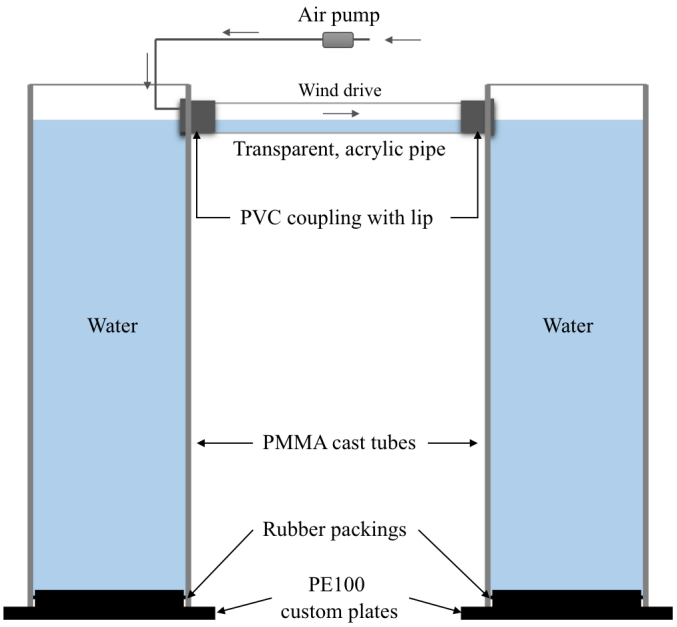

Figure 3.4: Illustration of Top Circulation B design

Figure 3.4 shows an illustration of top circulation design B. The design is based on a pipeline directly connected to the PMMA cast tubes. An air flow can be directly introduced to the liquid surface, and the air flow direction can easily be changed based on which side it is introduced. Ideally, the cross pipe needs to include a valve to ensure no circulation between the two tanks while tempering the water. This can be seen in figure D.2 found in appendix D, where it is also shown how one can introduce a flow meter. Flow speed can be measured the same way as proposed in design A.

Advantages and disadvantages with Top Circulation B

Advantages	**Disadvantages**
• Easy to introduce air to surface	• Large holes in the PMMA tube
• Can use different measurement techniques	• Difficult to change lengths, diameters and shapes
• Can still introduce a vacuum pipeline	• Hard to seal completely without glue
• Only one liquid height to deal with	• Need to introduce a valve, which gives one more possible leakage point

3.2.2 Bottom circulation

Bottom circulation refers to the pipeline connecting the two tanks at the bottom. The main goal was to find a flexible and simple solution where a good measurement technique could be applied. Four different designs were presented together with information of how they could be altered in terms of different measurement techniques.

Bottom Circulation A:

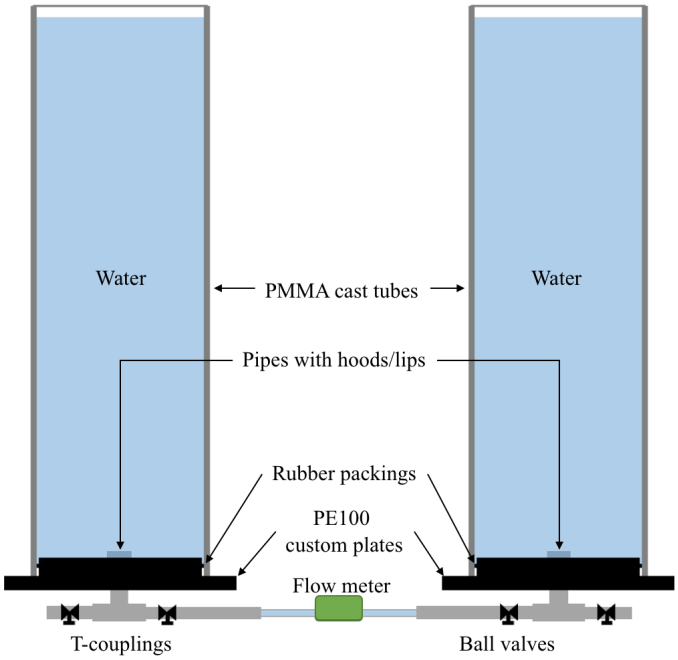

Figure 3.5: Illustration of Bottom Circulation A design

Figure 3.5 shows an illustration of bottom circulation design A. The design is based on a pipeline going through the bottom plates. Using flexible silicon as sealant ensures that the pipeline can easily be disconnected. The T-couplings and ball valves makes it possible to empty each tank independently without removing or altering the setup. In the illustration a flow meter is shown, but PIV can easily be introduced by exchanging the flow meter with a clear, acrylic pipe.

Advantages and disadvantages with Bottom Circulation A

Advantages	Disadvantages
• No threaded parts in the PE100 plates	• Pressure in multiple directions, danger of parts being plugged out
• Multiple measurement techniques	• Drilled holes in the PE100 plates
• Easy to change lengths and shapes	• Multiple leakage points
• Easy to increase heights to increase hydrostatic pressure	
• Easy to empty the model, simplifying cleaning	
• Can introduce other designs by closing the valves	

Bottom Circulation B:

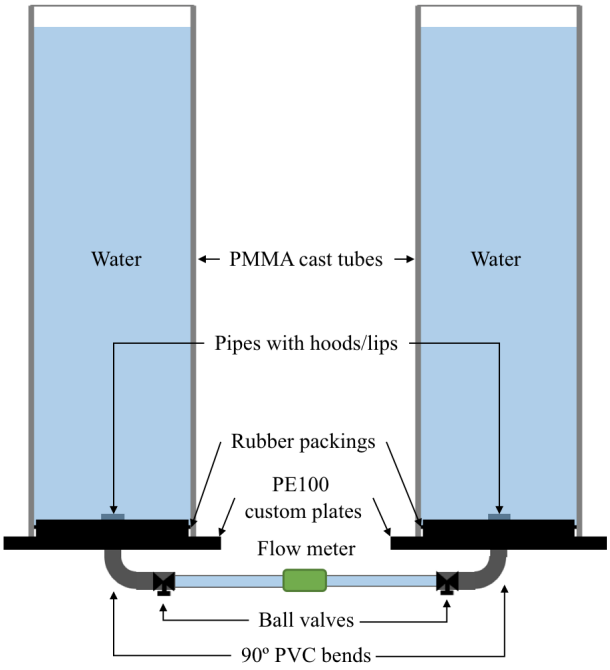

Figure 3.6: Illustration of Bottom Circulation B design

Figure 3.6 shows an illustration of bottom circulation design B. The design is based on a pipeline going through the bottom plates. Using flexible silicon as sealant ensures that the pipeline can easily be disconnected. Flow meter can easily be changed with an acrylic pipe so PIV can be used as measurement technique.

Advantages and disadvantages with Bottom Circulation B

Advantages	**Disadvantages**
• No threaded parts in the PE100 plates	• Remove flow meter/measurement pipe to empty the tanks
• Easy to change lengths and shapes	• Drilled holes in the PE100 plates
• Good pressure distribution	• Multiple leakage points
• Easy to increase heights to increase pressure	
• Multiple measurement techniques	
• Can introduce other designs by closing the valves	

Bottom Circulation C:

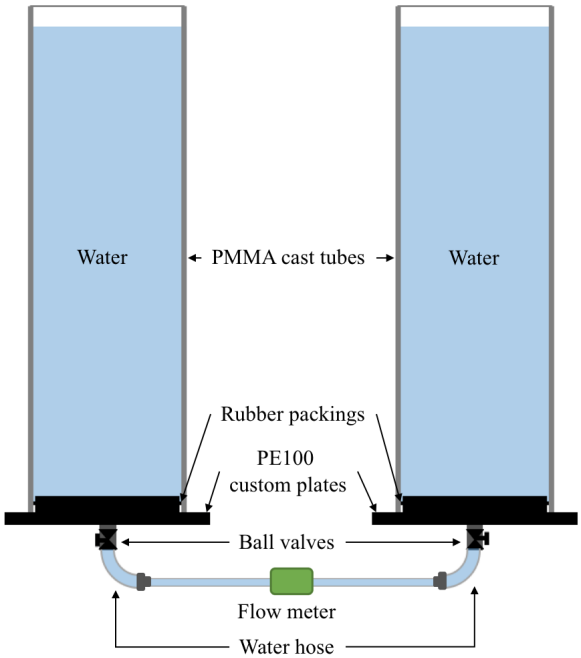

Figure 3.7: Illustration of Bottom Circulation C design

Figure 3.7 shows an illustration of bottom circulation design C. The design is based on a pipeline being directly connected to the bottom plates. Measurement techniques and method for emptying the tanks are similar to design B.

Advantages and disadvantages with Bottom Circulation C

Advantages	**Disadvantages**
• Multiple measurement techniques	• Remove flow meter/measurement pipe to empty the tanks
• Easy to increase lengths and heights	• Drilled holes in the PE100 plates
• Good pressure distribution	• Threaded parts in the PE100 plates
• Fewer leakage points than A and B	• Water hose could introduce movement affecting flow meter

Bottom Circulation D:

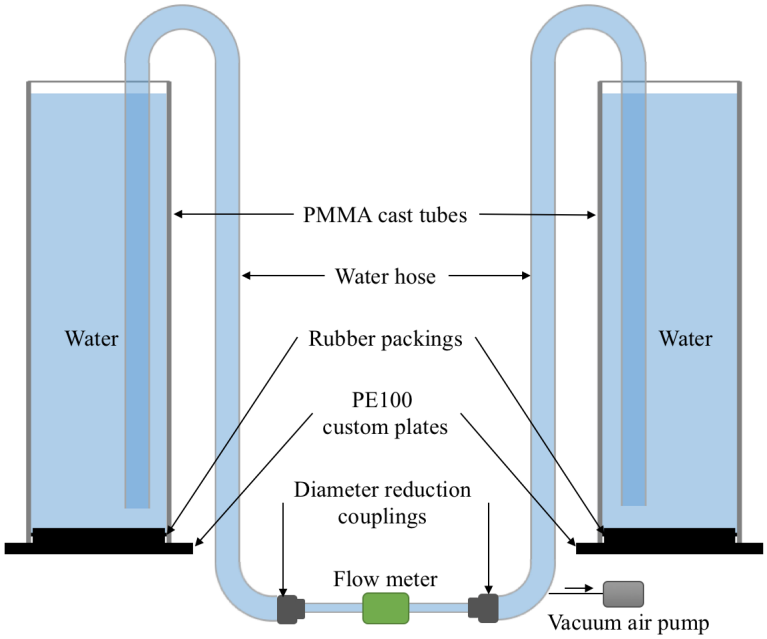

Figure 3.8: Illustration of Bottom Circulation D design

Figure 3.8 shows an illustration of bottom circulation design D, which was proposed by Professor Rune W. Time. The design was based on a pipeline which did not have to interfere with the bottom plate. A long hose is used to circulate fluid from the bottom of a tank and to the bottom of the other tank. A pump must be attached in order to drag out the air and create vacuum.

Advantages and disadvantages with Bottom Circulation D

Advantages	**Disadvantages**
• Easy to change diameters/lengths	• Hose can get pinched
• Possible few leakage points	• Long lengths = more friction
• No holes required	• Siphon tube to empty tanks
• No threaded parts	• Long lengths = increased heat loss
	• Multiple heights to deal with

3.3 Possible measurement techniques for fluid flow

Measuring fluid flow for slow moving fluids are often considered difficult due to the small pressure differences involved. Multiple measurement techniques have been discussed and the two most relevant methods are briefly explained in this section, amongst them a specific fluid flow meter available in the multiphase laboratory. This section can be used later should another measurement technique be desired.

3.3.1 Flow meter for small fluid flows

Sensirion SLQ-QT500 Liquid Flow Sensor is specially designed to measure small liquid flows with a high sensitivity, but is confined to a measurement area of +/- 120 ml/min. [6]

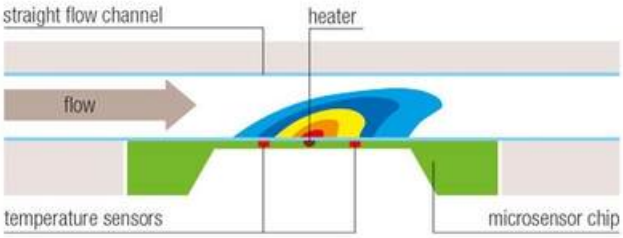

Figure 3.9: Sensirion Liquid Flow meter measuring technology [6]

The flow meter operates with a micro-thermal measurement principle with a coil around the capillary. The flow meter has an extremely fast, miniaturized thermal sensor with all of the high-precision signal-conditioning circuitry on a single CMOS microchip. A heating element on the microchip adds a minimal amount of heat to the medium. Two temperature sensors, symmetrically positioned above and below the source of the heat, detect even the slightest temperature differences. This provides the basic information about the spread of the heat, which itself is directly related to the flow rate. Integration on a single chip ensures that the sensitive analog sensor signals can be amplified with high precision, digitized and further processed. [6]

Advantages and disadvantages of a Sensirion Liquid Flow Meter

Advantages	**Disadvantages**
• Direct measurement technique	• Limited measurement range
• Highly sensitive down to the lowest flow rates	• Very sensitive to outside movements/disturbances
• For high- and low-viscosity liquids or for liquids with small particles	• The small diameters limits the fluid speed due to large friction
• Fast response time (50 ms)	• Limited operating pressure
• Non-invasive measurement	
• No moving parts	

3.3.2 Optical method (PIV)

PIV is an optical, non-intrusive measurement technique which principle is to measure the movement of seeding particles injected into a fluid during a time laps to derive velocity vectors. PIV measures whole velocity fields by taking two images shortly after one another and calculating the distance the individual particles travelled within the known time. From the known time difference and the measure displacement, the fluid flow velocity can be calculated. [16]

$$v = \frac{\Delta L}{\Delta t} \tag{3.1}$$

where v is the fluid velocity, ΔL is the measured displacement and Δt is the known time difference.

Seeding particles are injected into a fluid to make it possible to see the flow directly. The area of interest is illuminated with a light sheet and a high-speed camera is used to record the flowing particles. The recorded video is split into single picture frames, which is used for further analysis. In the analysis, the images are decided into small subsections called interrogation areas, which are cross-correlated with each other. The correlation results is a signal peak, which indicates the common particle displacement. An accurate measure of displacement is achieved with sub-pixel interpolation. When the cross-correlation analysis is executed on all frames, a velocity vector magnitude over the whole target area is obtained. This is illustrated in figure 3.10. [17]

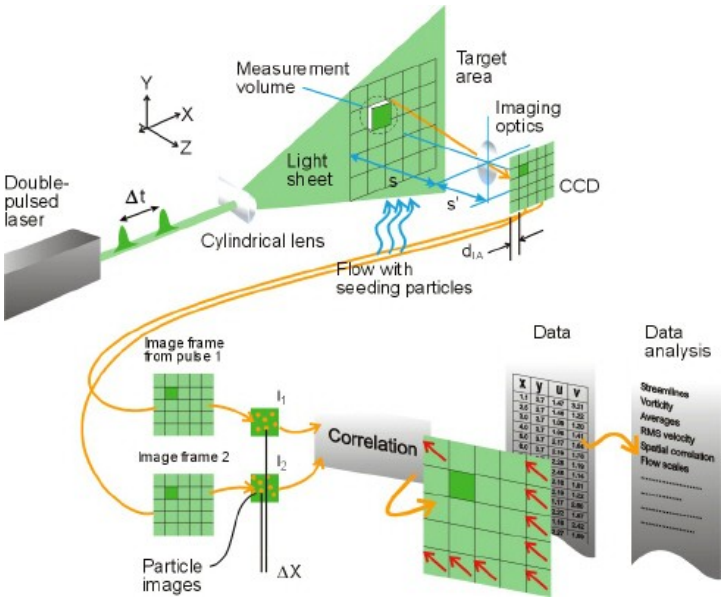

Figure 3.10: Measurement principles of PIV, [Dantec Dynamics]

The particles added generally cause negligible distortion of the fluid flow if they are properly chosen. The most difficult part about PIV is choosing the proper particles which are naturally buoyant. Since density of water changes with the temperature, particles that will fit with warm water may not fit with cold water.

Advantages and disadvantages with PIV using particles

Advantages	**Disadvantages**
• To a large degree, non-intrusive.	• Difficult to find neutral particles
• No limit to measurement range	• Requires data processing
• High degree of accuracy	• Does not measure components along z-axis (towards/away from camera)
• No restriction on fluid	• IV lasers introduce safety constraints
	• Can be costly due to IV lasers and high-speed cameras

Using PIV for the top circulation would also let the observer see how surface wind drive would affect the velocity profile of the fluid circulating.

3.4 Possible conditioning techniques

This section describes methods for regulating the temperature inside the model and the air flow inside the top circulation pipeline.

3.4.1 Temperature regulation system

To avoid having peristaltic pumps in the new experimental model that would interfere with the measurement equipment or give unwanted effects on the circulation, a different temperature conditioning technique from what was used in the NORTH model was desired. Given the large volume inside each tank, it was possible to heat up, cool down and regulate the water temperature using heating/cooling elements directly connected to water baths. This is showed in figure 3.11. The water inside the model would then be either warmed up or cooled down as a result of heat transfer through the heating/cooling element by conduction. The heat loss from the heating element would also be sufficient to keep the water at a desired temperature as long as size, placement and material was taken into account.

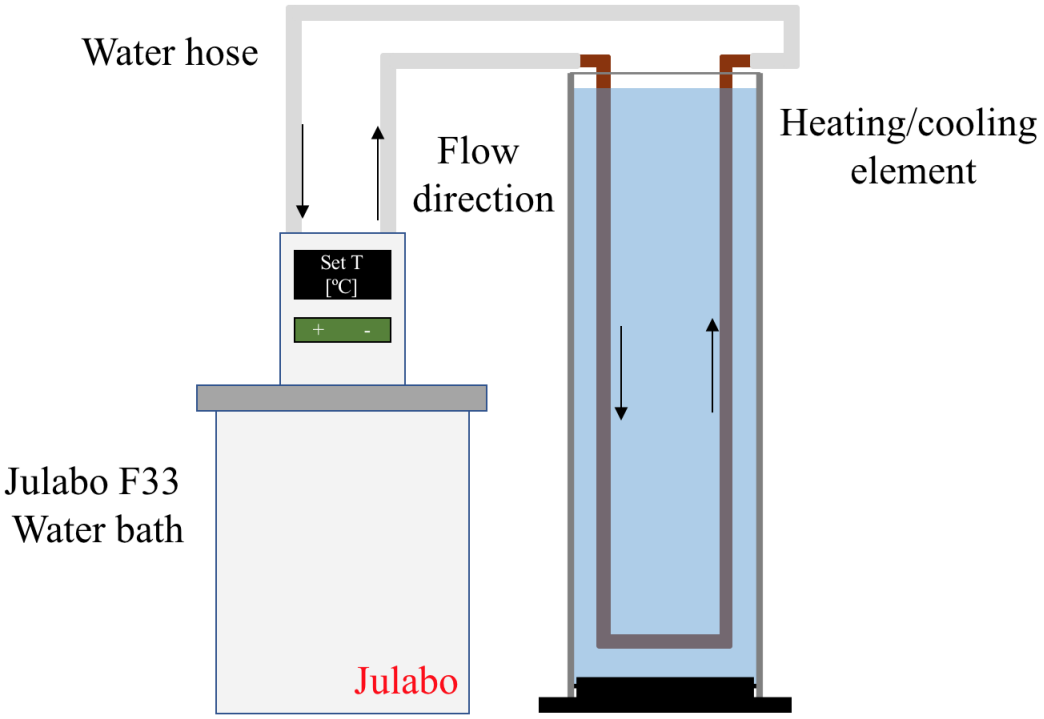

Figure 3.11: Illustration of temperature regulation principle, new model

The time it takes to heat/cool water to a specific temperature depends on the dimension of heating/cooling element and the material used. In figure D.3, found in appendix D, it is shown two alternative shapes, dimensions and lengths for heating/cooling elements compared to figure 3.11.

A good suggestion for heating/cooling element is copper pipes, which are economically favorable both because they are cheap and because they are readily available at the laboratory. Copper is durable and recyclable, the lightweight and malleable material is easy to work with and minimal tools are needed to fit and join copper pipes. Copper pipes conducts heat well, so the pipes get warm during exposure to hot water and cold during exposure to cold water. The water inside the pipe will therefor keep a consistent temperature while heating/cooling the water around the pipe. Copper pipes are safe unless the water is overly acidic or alkine, which must be taken into consideration if the model was to be used for something other than thermally driven circulation of tap or distilled water. [18]

3.4.2 Surface wind regulation system

Surface wind can be introduced using an air vacuum pump in order to be able to use it for both top circulation designs.

A motor driven air pump needs to be connected to a power source. To be able to relate the wind speed to the power supply, an experiment was performed using the top circulation pipeline A and Pasco Weather/Anemometer sensor, showed in figure 3.12. More information about this sensor may be found in appendix C.

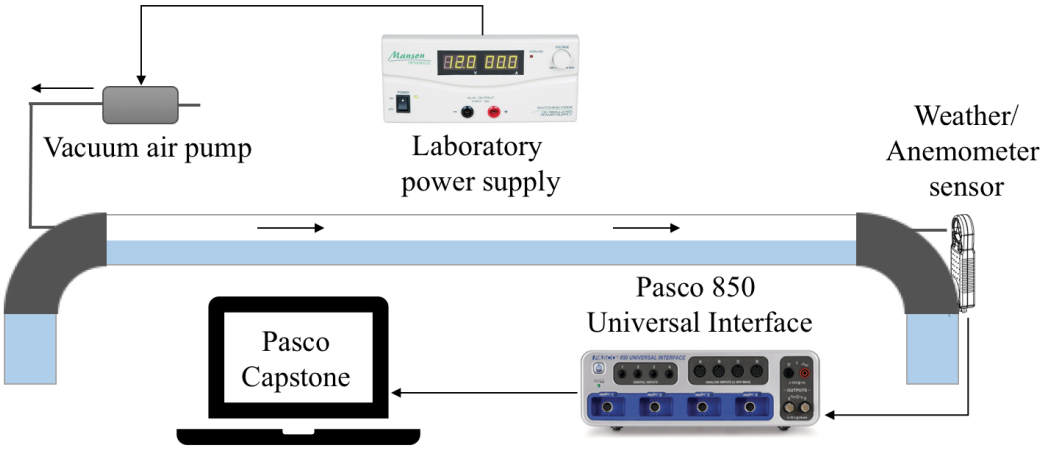

Figure 3.12: Relating wind to the power input

Wind speed into the pipeline was tested by holding the Pasco sensor straight in front of the hose connecting the pump outlet to the inlet of the top circulation pipeline. To test how the wind speed would behave inside the pipeline during experiments, the pipeline used for top circulation in the model was filled with the same amount of water that would be used in experiments to achieve the same liquid height and therefore the same flow volume. Wind speed out of the pipeline was measured by holding the Pasco sensor straight in front of the pipeline outlet, showed in figure 3.12. The wind speed was measured for a range of power levels in order to relate them to each other. The area of the sensor was much larger than the area of the outlet hoses, resulting in the output values differing based on where the air hit the sensor. The experiment is therefore only performed to get an indication of the wind speed, and the result can be found in figure 3.13.

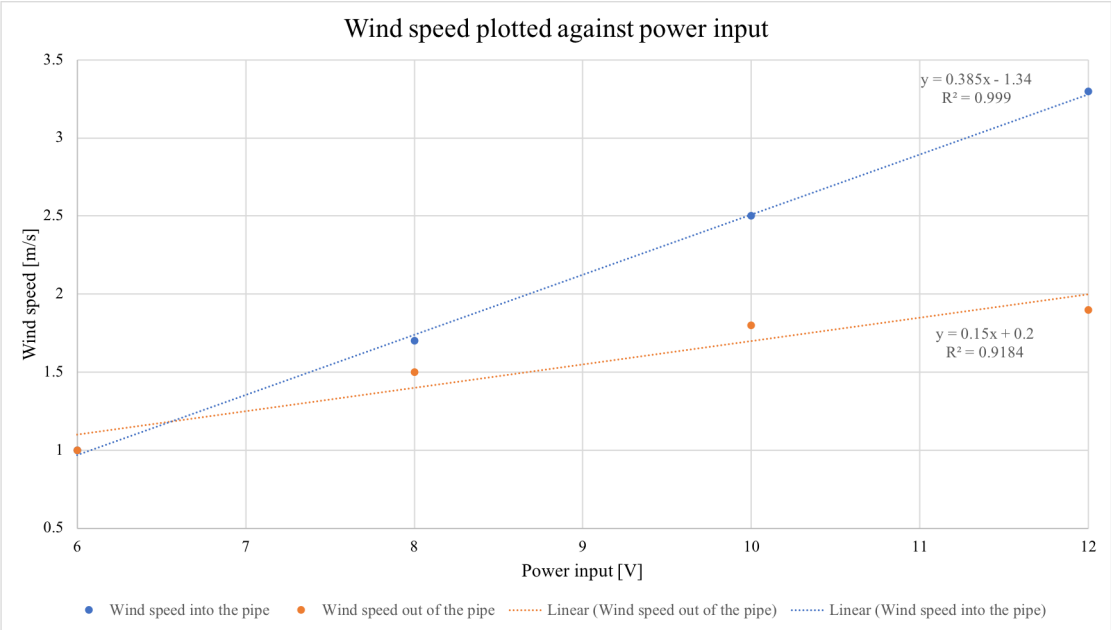

Figure 3.13: Graph showing wind speed plotted against power input

From the graph shown in figure 3.13 one can see how the wind speed into the pipe follows a linear pattern. The wind speed out of the pipe also follows a linear pattern in the start, before the wind speed acceleration is reduced when the power input is increased. This might be due to more energy going into the water when the wind speed gets large enough to create ripples and small waves on the water surface, see figure 3.14. The black arrows represent the air flow velocity profile. When the wind speed is small the surface is close to undisturbed. As wind speed increases, the surface becomes disturbed and small ripples form. The wind catches these ripples and creates larger waves, resulting in less of the wind going out of the pipeline.

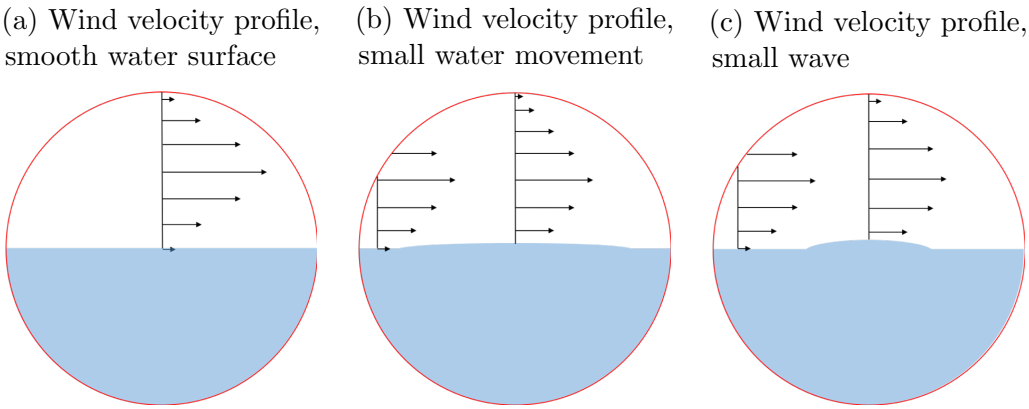

Figure 3.14: Wind velocity profiles in pipes with water

Once wind speed can be related to the power input, the wind speed into the pipeline can be selected based on the voltage.

3.5 Feasibility tests

Three tests were done in order to choose the best design and measurement technique. Two of the tests were performed prior to building the model, and the final one were performed to approve the final design.

3.5.1 Volumetric flow measurement technique

Based on the advantages and disadvantages of the measurement techniques mentioned, it was clear that a volumetric flow meter would be the easiest, most economically favorable and most accurate method. Using the equation of continuity for an incompressible fluid flowing in a system of varying cross-section, the volumetric flow rate is only needed to be measured at one place, which enables one to use only one flow meter.

In order to estimate how the small diameter would affect the flow rate in a new model, a MATLAB program was designed by Professor Rune W. Time. The program can be found in appendix A. The program could also be used for conditioning, and to estimate how changing lengths and diameters could influence the volumetric flow.

After checking that the thermally driven flow would be inside the measuring range of Sensirion SLQ-1500 liquid flow meter with the different designs proposed, it was also decided to investigate how low flow rates the flow meter could measure. This was done using a small U-pipe (figure D.4). The result can be found in Appendix B. From the graph seen in figure B.1 one can see how the flow meter measures all the way down to +/- 0.5 $\mu l/s$. Based on these two tests the flow meter was deemed a fitting measuring technique.

3.5.2 Over pipe vs cross-pipe

To check whether the circulation would be the same when using a pipeline situated above the tanks compared to a normal cross-pipe, an experiment was performed using Pascos Density Circulation Model ME-6816. The same temperature was used in all experiments and food colouring was used to visualize the circulation. Two PVC water hoses with different diameter were used. The purpose of the experiment was only to check that the placement of the pipe would not influence the thermal drive, and to get a better understanding of how the thermal driven fluid would flow before building the final model. An illustration is shown in figure 3.15.

(a) Pasco model (b) Pasco model with modified pipe

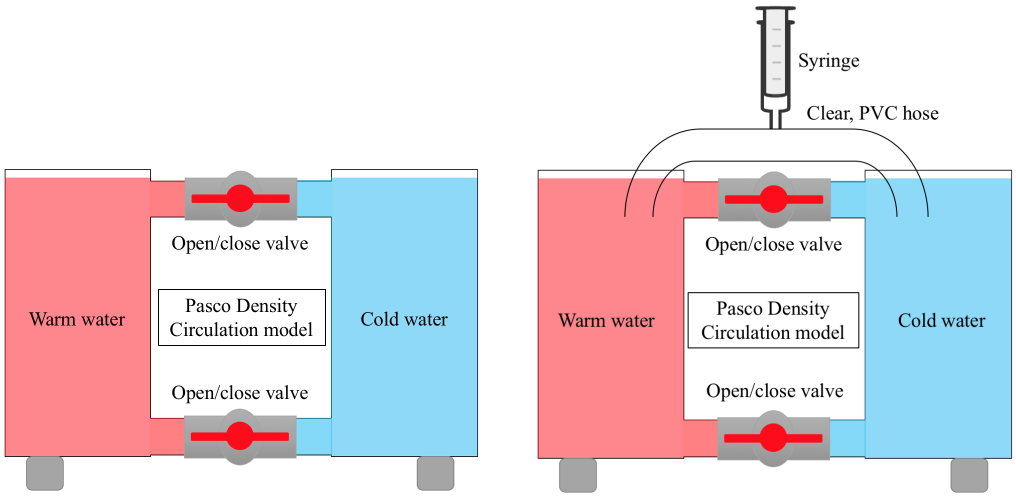

Figure 3.15: Pasco small scale circulation model

Before starting the experiment, both valves were kept closed. Warm water was poured into one side of the model to warm up the tank, while cold water with ice cubes was poured into the other side to cool down the tank. The warm water used in the experiment was heated up to about 40 °C, before being poured into the models already pre-warmed tank in order to get a uniform temperature. Cold, refrigerated water with a temperature of about 4 °C was used on the other side. The bottom valve was kept open during all experiments. In the first type of experiment, see figure 3.15 (a), both valves were opened simultaneously, In the second type of experiment, see figure 3.15 (b), the air was drawn out of the tube using a syringe before the bottom valve was opened. The experiments were filmed, and the coloured water was used as reference.

Some still images from the experiment can be found in figure D.5, D.6 and D.7 in Appendix D. From the experiments there could not be registered an interference in the circulation due to the pipeline placement. The diameter of the PVC hoses did however influence the flow rate. In the experiment where the PVC hose had a smaller diameter compared to the cross-pipe in the model, the flow rate appeared to be smaller. In the experiment where the PVC hose had a larger diameter than the cross-pipe, the flow rate appeared to be similar to the flow rate where only the cross-pipes were used. From the still images in appendix D, one can also see how the large temperature difference resulted in a large volumetric flow, as the red coloured water gets circulated into the blue colored water in a jet stream. From the MATLAB script it was seen that volumetric flow when using a Sensirion liquid flow meter would be quite small. Using a free-standing pipeline with much larger inside diameter than the Sensirion flow meter will therefore not impact the circulation in any notable way.

3.5.3 Pressure tests

The bottom circulation system had to be pressure-tested with full water tanks in order to be accepted before experiments. Based on the lists made for each model design, bottom circulation design A was pressure tested first. Some leakage was discovered in the threaded parts between PVC pipes and valves, which were easily fixed using thread tape. During the pressure test, it became clear that the water pressure pushed out parts in a horizontal direction. The flow meter or acrylic pipe situated between the two T-couplings would offset the pressure between them, but the part used to connect the valves to the other sides of the T-coupling were continuously being pushed out. A solution could be to glue the parts together, but since one of the desired criteria was for the model to be flexible, it was decided to test bottom design B instead. The bent PVC pipes had a better pressure distribution, and since the two tanks are connected, the horizontal pressure inside the system would virtually offset each other. Bottom circulation design B was pressure tested through 24 hours with no leakage before being accepted.

Chapter 4

Experimental method

The aim of the following experiments were to test how the model worked for thermal circulation, and to test if the method chosen for introducing a wind drive to the liquid surface would impact the flow rate. Multiple experiments were performed for purely thermal drive and two experiments with wind drive.

This chapter includes a description of the new model, equipment and procedures used during experimentation and data processing. An in-depth description of how the model was built and how sensors and programs were set up and calibrated may be found in appendix C, which serves as a companion guide on how to use the model for future experimentation.

4.1 Experimental model

The model was based on information gathered in the the feasibility study in chapter 3. Based on tests and general advantages and disadvantages, the best design was determined to be a combination of top circulation A (figure 3.3) and bottom circulation B (figure 3.6). The new model is presented in figure 4.1, the different components listed in table 4.1 with their respective dimensions, and some special components highlighted in figure 4.2.

Table 4.1: Component and pipe dimensions for the new model

Item	Description	OD [mm]	ID [mm]	Length [mm]
1	PMMA cast tube	300	284	1000
2	Clear, acrylic pipe	50	46	800
3	Clear, acrylic pipe	50	46	100
A	PE100 black plates	400	280	50
B	PVC with 90° bend	59	50	85x85 (wxh)
C1	PVC with 45° bend	36	32	
C2	PVC with 45° bend	36	32	
D	PVC pipe with hood	32	30	110
E	Ball valve	32	25	80
F	Diameter reduction	25/20	21/16	40

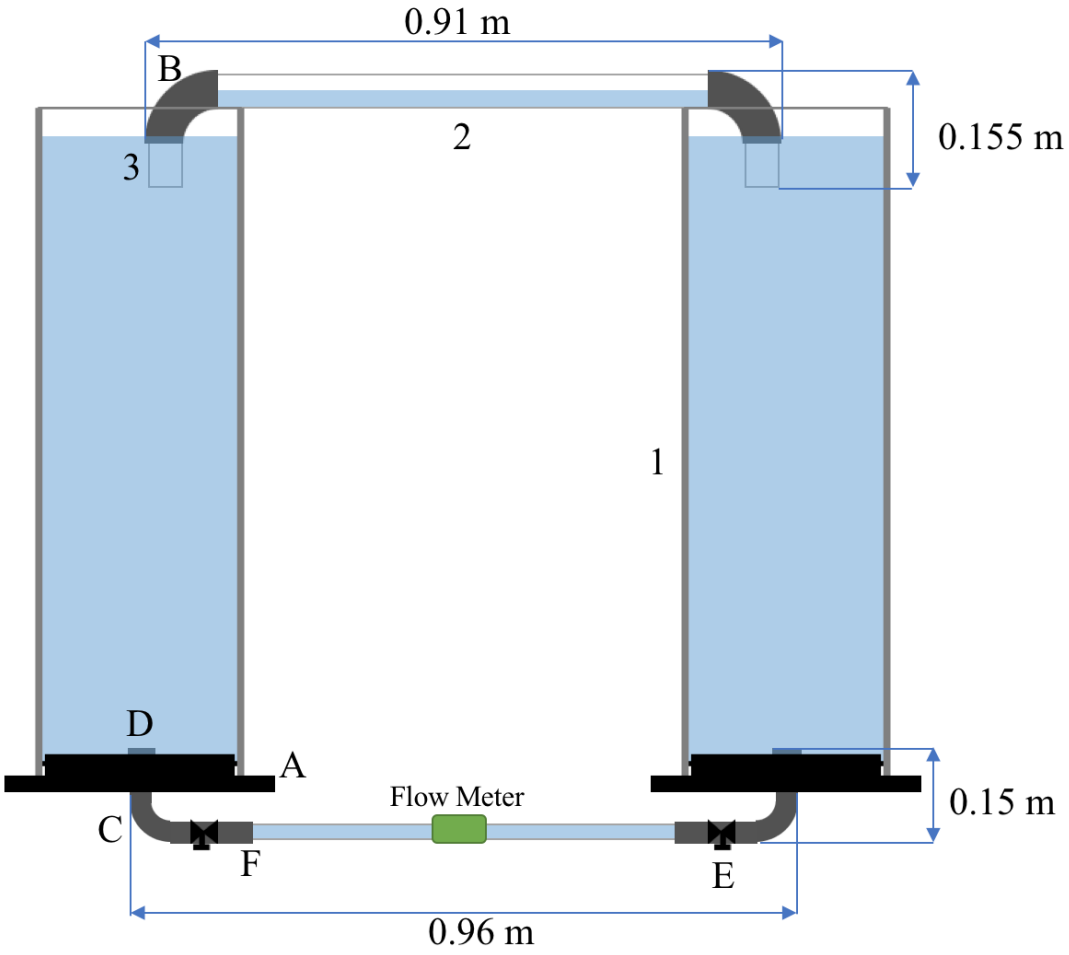

Figure 4.1: Illustration of the new model with lengths

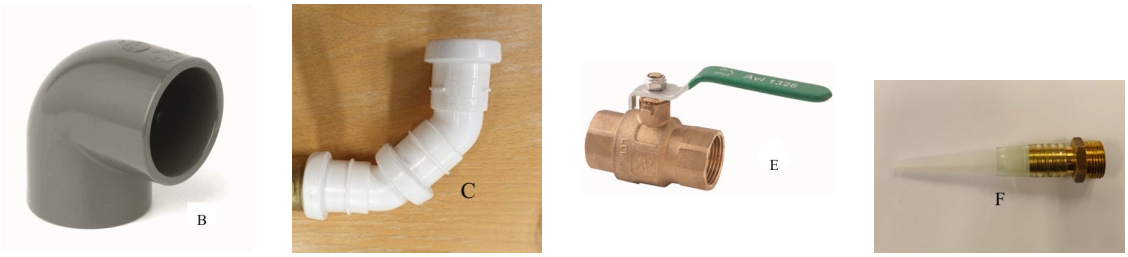

Figure 4.2: Model components highlighted from the model

Some of the components used in the new model had previously been used in other experimental setups, and had to be sealed before they could be implemented in the new model. To reduce the diameter in an effective way, a plastic cartridge was used together with a brass hose connector, (figure 4.2 F). The bottom plates were connected to the cast tubes using both rubber packing seals adapted in the laboratory and clear, flexible silicone. PVC parts were attached to acrylic pipes using silicon, and to other PVC parts using rubber packing. Thread tape was used to reduce the chance of leakage in threaded parts. Holes were drilled in the PVC 90° bends, threaded, and plastic hose connectors were inserted in order to connect the air regulation system to the top circulation pipe.

4.2 Conditioning systems

The model was equipped with two independent regulation systems, both of which premise has been touched upon in the feasibility study found in chapter 3.

4.2.1 Temperature regulation system

The temperature regulation system used for both tempering the water before experiments and regulating the temperature during experiments consisted of:

- One Julabo F34-HE Refrigerated/heating circulator
- One Julabo F33-HL Refrigerated/heating circulator
- Two copper pipes (2 m length, 0.8 mm thickness, 10 mm ID)
- Four water hoses (1 m length, 12 mm ID)
- Four water hoses (1 m length, 16 mm ID)
- Four plastic garden hose connectors

From theory about ocean temperature gradients, the desired temperature in the low-latitude ocean was 25 °C and in the high-latitude ocean 5 °C. From calculations on heat exchange, the area needed to cool down the liquid volume inside the high-latitude ocean had to be considerably larger than the area provided by the copper pipes available in the laboratory. Considering these experiments were merely tests to see how the new model operated, the copper pipes were used despite this knowledge.

Due to the length of the copper pipes, they were bent in U-shapes, shown in figure 3.11. In figure 4.4 the distance between the copper pipe and bottom plate can be seen. Because the connection points on the Julabo waterbaths had a larger circumference than the copper pipes, water hoses of different diameter were used together with plastic garden hose connectors. The water hoses were heated up when connecting them to other components, and hose clamps were used to seal the connections.

4.2.2 Air flow regulation system

The air flow regulation system was used to introduce a wind drive to the liquid surface in the model during experiments as well as create the vacuum needed inside the top circulation pipe. The system consisted of:

- Two silicone tubes (1 m length, 1 mm thickness, 4.5 mm ID)
- One AirPro DC 12V vacuum pump
- One Manson SPS-9602 power supply
- Two power cables for power supply
- Two connectors for power supply

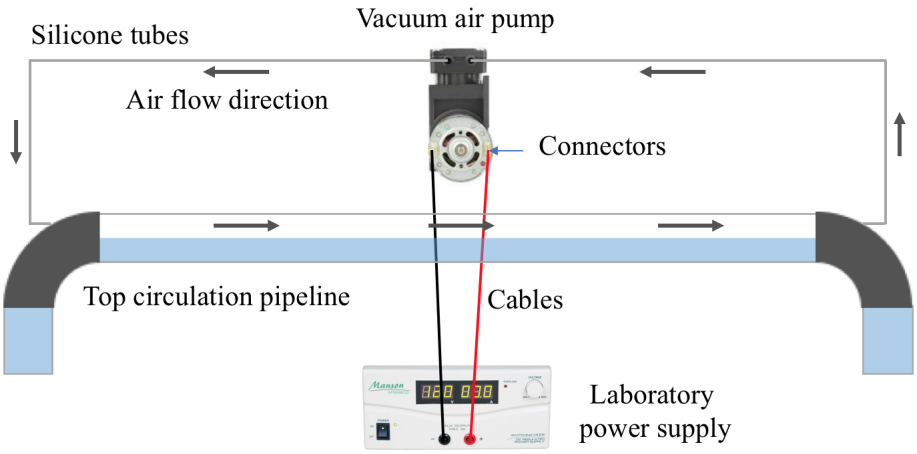

Figure 4.3: Air flow regulation system

Figure 4.3 shows the system. The wind speed was regulated using the power supply, made possible by the test performed in the feasibility study. The result from the wind tests are presented in table 4.2.

Table 4.2: Wind speed based on power supply

Power input [V]	Wind speed in [m/s]
6	1
8	1.7
10	2.5
12	3.3

To change the air flow direction, the connection point for each silicon tube were simply swapped.

4.3 Measurement techniques

Two parameters were seen as important to measure during the experiments, namely fluid flow rate and temperature. The quantitative data was collected using measurement and control systems described in the feasibility study. Figure 4.4 shows an illustration of both the conditioning systems and the measurement and control systems used in the new model.

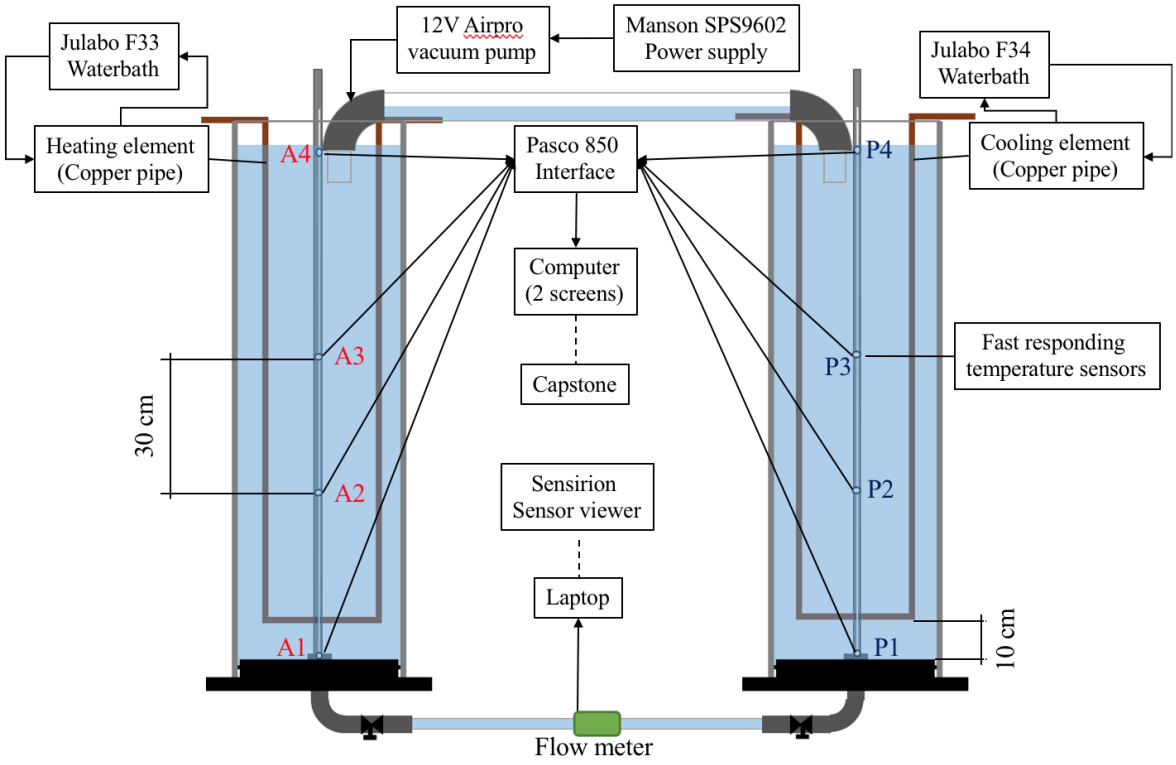

Figure 4.4: Illustration of the external measurement and control systems

4.3.1 Fluid flow rate

The best measurement technique was determined to be a volumetric flow meter inserted in the bottom circulation pipeline as shown in figure 4.1. Fluid flow rate was therefore measured using the Sensirion QLS-QT500 liquid flow meter introduced in the feasibility study (chapter 3). The flow meter was connected to a laptop with a USB sensor cable and the Sensirion flow viewer was used for logging the data. The flow meter is highly sensitive, making it important that neither flow meter, cable or laptop is moved during logging.

The sensor was set to measure twice every second.

4.3.2 Temperature

Fast responding temperature sensors were used together with PASPORT quad temperature sensors from Pasco. During testing, it was discovered that the sensors did not just measure from the tip of the cable, where the sensor was placed, but measurements could also be seen registered almost 10 cm up the cable. Therefor, the cables were wound around a pole to ensure that the measurements were taken from an exact point in the model. This can be seen in figure C.7 in appendix C. The first sensor was placed at the bottom of the pole, and the next three were placed with an interval of 30 cm, shown in figure 4.4. The sensors for the low-latitude ocean were marked with A's and the sensors for high-latitude ocean were marked with P's, with increasing numbering from the bottom. The PASPORT sensors were connected to Pasco 850 Universal Interface, which was in turn connected to a computer with two screens. The software Capstone was used to gather the temperature data and visualize real-time data from the sensors. Temperature data was saved every hour in case something were to go wrong during the experiments.

Having all the sensors for one tank coiled around the same rod made it possible to easily remove the sensors from the model, even while it was still filled with water. During testing of the sensors used in the NORTH model, it was seen that the sensors had been damaged by lying in water over long periods of time. The new method ensured that changing a defect sensor will be easy, and the sensors can be re-calibrated when needed.

The temperature sensors were set to measure once every 10 seconds, as the temperature inside the model would not be as rapidly effected as the flow rate.

4.4 Experimental procedure

Due to the large water volume, it was decided to use tap water during these experiments. The model was filled with tap water and left to temperate by the conditioning system over night. The ball valve between the low-latitude ocean and the flow meter was kept closed while the water was heating/cooling to the desired temperature. The valve between the high-latitude ocean and the flow meter was kept open. The same water was used in multiple experiments, each time being left to re-temperate for a minimum of 12 hours.

Figure C.10 in appendix C shows the best procedure for emptying the model.

4.4.1 Thermal drive

Purely thermal drive is in this report defined as circulation due to the hydrostatic pressure difference in the two tanks due to temperature difference.

All experiments were started the same way:

1. The inlet of the vacuum air pump was connected to one of the hose connectors in the top circulation pipe by a soft silicon tube. The other hose connector was closed by a laboratory steel tubing clamp.

2. The pump was turned on and a power supply of 6 volt was used to drag the air out of the pipeline until the liquid reached a reference water height. The reference height chosen was roughly 50 % of the pipe used in the top circulation pipeline. The hose connector was then closed to create an airtight system.

3. Capstone and Sensirion logging were stated at the same time.

4. The valve between the low-latitude ocean and Sensirion flow meter was opened to start the experiment.

5. The valve between the low-latitude ocean and Sensirion flow meter was closed to end the experiment.

The experiments were run between 8-9 hours to see how the circulation developed over time. Illustrations of the top circulation pipe with the plastic hos connections and silicon tubes connected may be seen in figure C.5 found in appendix C.

4.4.2 Positive wind drive

Positive wind drive is in this report defined as air introduced from the low-latitude side of the top circulation pipe, making the surface wind flow in the same direction as the thermally driven flow.

The experiments were started by following step 1 to 4 for purely thermal circulation. For experiments where positive wind drive was introduced, the additional following steps were taken:

1. The inlet of the pump was connected to the high-latitude side of the top circulation pipe, while the outlet of the pump was connected to the low-latitude side, effectively creating a closed system. Air sucked out of the pipeline by the pump would also be blown back into the pipeline, maintaining the vacuum.

2. The plastic connectors were opened, the air pump was turned on and the power supply set to 8.0 volt after 1 hour.

3. The power supply was increased after a total of 6 hours to 11.5 volt.

4. The power supply was turned off after a total of 7 hours and the connectors were closed.

5. The experiment was ended by closing the valve between the low-latitude ocean and the flow meter again.

4.4.3 Negative wind drive

Negative wind drive is in this report defined as air introduced from the high-latitude side of the top circulation pipe, making the surface wind flow in the opposite direction as the thermally driven flow.

The experiment was started by following step 1 to 4 for purely thermal circulation. For experiments where negative wind drive was introduced, the additional following steps were taken:

1. The inlet of the pump was connected to the low-latitude side of the top circulation pipe, while the outlet of the pump was connected to the high-latitude side, effectively creating a closed system. Air sucked out of the pipeline by the pump would also be blown back into the pipeline, maintaining the vacuum.

2. The plastic connectors were opened, the air pump was turned on and the power supply set to 8.0 volt after 2 hour.

3. The power supply was increased after a total of 5 hours to 11.5 volt.

4. The power supply was turned off after a total of 8 hours and the connectors were closed.

5. The experiment was ended by closing the valve between the low-latitude ocean and the flow meter again.

4.5 Data processing and analysis

After temperature and fluid flow data had been collected, it was processed using Pasco Capstone, Microsoft Excel and MATLAB.

The Pasco temperature sensors gave experimental data recorded with an evenly spaced time series, measuring once every 10 seconds. The Sensirion flow meter gave experimental data recorded with an unevenly spaced time series. Although the sensor was set to measure twice per second, the time between each measurement was not constant. To even out the time series, an average of the two measurement data per second was implemented.

When the flow meter was exposed to physical movement, either by movement from the cable connecting it to the laptop or movement from the surroundings, it results in an inaccurate measurement. These measurements appears as large peaks, either positive or negative relative to the average flow. Because the Sensirion flow meter was so highly sensitive, reacting to every outside movement, a moving average was used when processing these data to reduce the amount of noise. The moving average was taken over 20 points, corresponding to 10 seconds of measurement. The result was then overlapped with the original data, so both can be seen in the results.

The different results obtained were compared to each other, and the average flow rate for thermal circulation was compared to the theoretical flow rate calculated using the MATLAB script introduced in the feasibility study.

4.6 Modifications and optimization

The model was modified and optimized along the way, in consultation with the supervisors, as better solutions were found during testing.

After the first thermal circulation test, the model was insulated using bubble wrap. An illustration is showed in figure C.4, found in appendix C. The water tanks were insulated using two to three layers, while the bottom circulation pipeline was insulated using four to six layers. To strengthen the natural environment, the top circulation pipeline was left without insulation, as warm water from a low-latitude ocean would loose heat freely when flowing towards a high-latitude ocean in a natural environment.

During some experiments, the vacuum pump stopped due to the clips connecting the power supply to the pump falling off. The clips used to connect the vacuum pump to the power cables were switched from crocodile clips to clamps with a closing mechanism, both showed in figure C.6 in appendix C. To ensure that the silicon tubes used to connect the vacuum pump did not get pinched during experiments, a box was put underneath the tubes close to the pump.

Two wireless temperature sensors were originally used together with six fast responding temperature sensors during the first tests. To simplify everything, and to ensure that the sensors were measuring at the same time, the wireless sensors were exchanged with another set of fast responding temperature sensors. This resulted in there being four fast responding temperature sensors in each tank (figure 4.4). The placement of the rod with temperature sensors were moved from the middle of each tank to the side where the bottom inlet and outlet pipes were situated. To ensure the rod would not move during experiments, due to the fluid flow in and out of the bottom circulation pipeline, a weight was fastened to both rods. This can be seen in figure C.8 in appendix C.

The low-latitude water bath was originally set to 35°C in order to obtain the temperature difference seen in a natural environment, but this induced too much air bubbles in the model which interfered with the vacuum in the top circulation pipeline. It was therefore decided to reduce the temperature to 25°C, which ultimately corresponded better with the true ocean water temperatures as well. The high room temperature ensured that the heating elements used for tempering the water had a large enough area to heat up the water.

After the first thermally driven circulation test a clear, flexible silicone was added to the threads connecting the plastic hose connectors to the top circulation pipeline in order to ensure no air-leakage during experiments.

Chapter 5

Results

This chapter presents the results obtained from the experiments performed in the new model. A discussion of the results can be found in chapter 6. The data presented consists of flow and temperature measurements from thermal circulation with and without wind drive, and a comparison of the temperature before and after the model was insulated.

5.1 Effect of insulating the model

The model was insulated to reduce heat transfer between the model and its surroundings. The stable temperature in each tank was measured before and after the model was insulated, and are presented in Table 5.1.

Table 5.1: Temperature comparison, before and after insulation

Sensor	Before insulation [°C]	After insulation [°C]	ΔT [°C]
A T1	23.9	24.6	+0.7
A T2	24.4	24.6	+0.2
A T3	24.5	24.7	+0.2
A T4	24.4	24.6	+0.2
P T1	9.3	8.4	-0.9
P T2	10.4	9.4	-1.0
P T3	12	10.6	-1.4
P T4	13.6	12.6	-1

Table 5.1 shows the temperature in the model under the same set conditions, before and after it was insulated. A denotes a low-latitude ocean while P denotes a high-latitude ocean. Numbers (1-4) represents where the sensors were located inside each tank. T1 was placed at the bottom of the tanks, while T4 was placed 7 cm from the top of the tanks. Every sensor was placed with a 30 cm interval from the bottom up. From the table, one can clearly see how the bubble wrap reduced the heat transfer between the model and its surroundings.

5.2 Thermal drive

Long running experiments for purely thermal driven circulation were performed three times. As the temperature profile followed the same trend, only one of the temperature graphs is shown in this chapter, while the other two can be found in figure B.2 and B.3 in appendix B. Since the fluid flow data differed between each experiment, they are all presented in this chapter with comments.

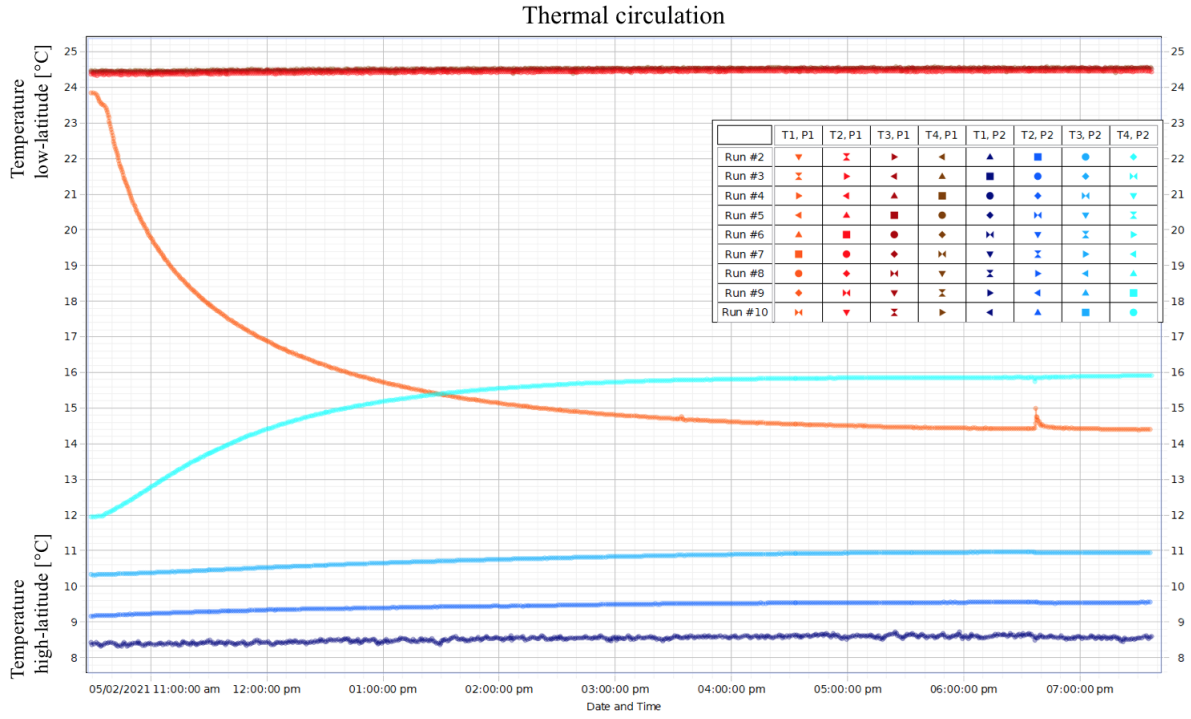

Figure 5.1: Temperature development, thermal circulation 3

Figure 5.1 shows the temperature development during the third experiment on thermally driven circulation. P1 stands for port 1, which was the sensors placed in the low-latitude ocean. These sensors were given a red-toned colour. P2 stands for port 2, which was the sensors placed in the high-latitude ocean. These sensors were given a blue-toned colour. The temperature in the bottom of the low-latitude ocean is directly affected by the temperature of the water circulating in from the high-latitude ocean, just as the temperature in the top of the high-latitude ocean is directly affected by the temperature of the water circulating in from the low-latitude ocean.

The MATLAB script, provided by Professor Rune W. Time, was used in order to ensure the flow rate would not surpass the measuring range of the Sensirion flow meter with the chosen temperatures. For thermal circulation with the given start temperatures, the calculated flow rate using the program was 559.5 $\mu l/s$ and an average flow rate of 472.9 $\mu l/s$ after the temperature had stabilized. The temperatures used were the average temperature in the model before and after experiments.

5.2.1 Thermal circulation experiment 1

The first thermally driven circulation experiment was performed 27.04.2021, from 10:44 to 18:44. The room temperature and water temperature inside the model at the start and end of the experiment is presented in table 5.2. The flow rate measured by the flow meter is presented in figure 5.2.

Table 5.2: Temperature at start and end, thermal circulation 1

Temperature sensor	T_{start} [°C]	T_{end} [°C]	ΔT [°C]
A T1	24.56	14.74	-9.82
A T2	24.55	24.66	+0.11
A T3	24.65	24.76	+0.11
A T4	24.61	24.70	+0.09
P T1	8.50	8.80	+0.3
P T2	9.37	9.48	+0.11
P T3	10.56	10.96	+0.4
P T4	12.62	16.46	+3.84
Room T	24.9	25.4	+0.5

Table 5.2 shows how much the temperature changed during the 8 hour long experiment.

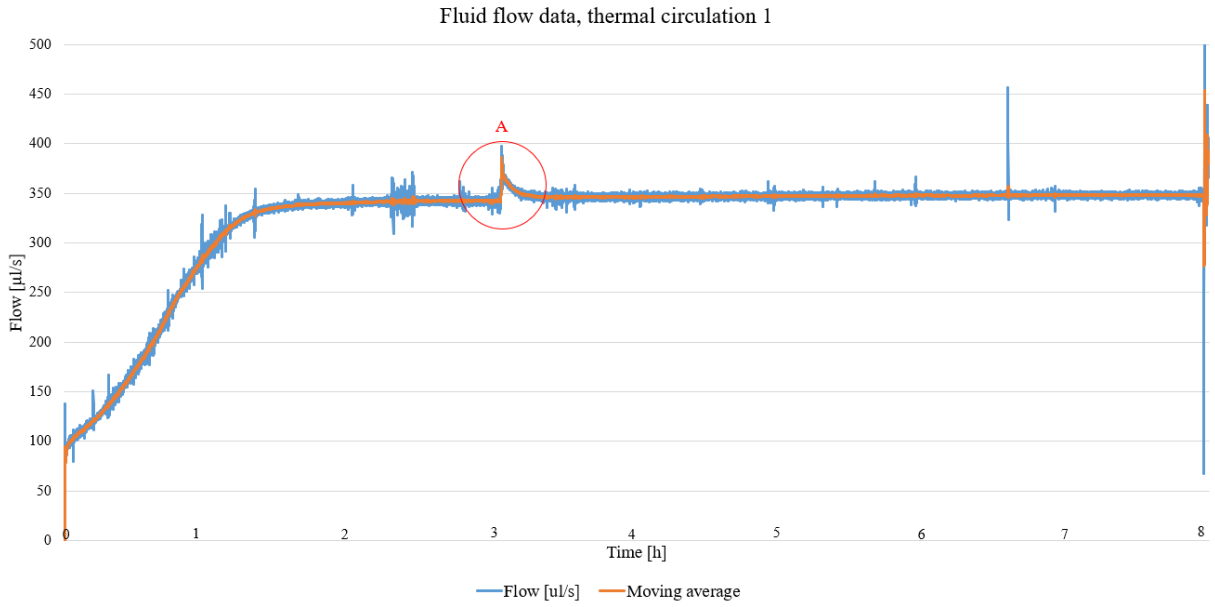

Figure 5.2: Thermal circulation 1, fluid flow data

Figure 5.2 shows how the flow rate developed during the 8 hour long experiment. The vacuum inside the top circulation pipe was not constant during the experiment, and the air had to be dragged out using the air pump after 3 hours to increase the liquid height back to original height, marked with an A in the figure.

The original water height was 1mm below 50% of the top circulation pipe, equivalent of 22 mm water height inside the pipe. The height was reduced by almost 40% the first 3 hours. After the height was increased by the pump, the water height was again reduced by 20% over the next 5 hours. From the graph one can see how the flow rate was effected by both the reduction in liquid height as well as the increase performed after roughly 3 hours. From start to 1.5 hours into the experiment, the flow is increasing. The flow evens out after about 2 hours. The flow is then seen to be close to constant after the liquid height has been increased. An excerpt of the flow data showing the time where liquid height was increased is shown in figure 5.3.

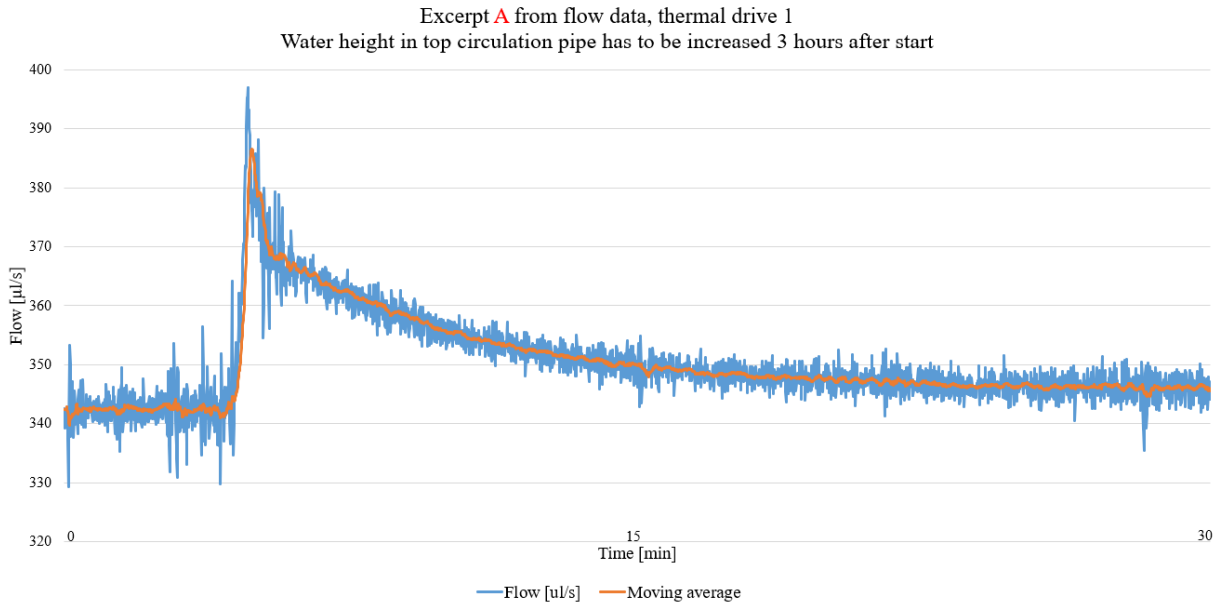

Figure 5.3: Thermal circulation 1, excerpt A from flow data

Figure 5.3 shows a 30 minute excerpt of the flow data. From the graph one can see how the flow is directly affected by the liquid height in the top circulation pipe. The fluid flow increased from 342.3 $\mu l/s$ to 346.1 $\mu l/s$ when the liquid height was increased by roughly 6 mm in the top circulation pipe. The flow was calculated from an average taken right before the height was increased and after the flow rate is seen to even out after.

5.2.2 Thermal circulation experiment 2

The second thermally driven circulation experiment was performed 01.05.2021, from 11:00 to 20:00. The room temperature and water temperature inside the model at the start and end of the experiment is presented in table 5.3. The flow rate measured by the flow meter is presented in figure 5.4.

Table 5.3: Temperature at start and end, thermal circulation 2

Temperature sensor	T_{start} [°C]	T_{end} [°C]	ΔT [°C]
A T1	23.87	14.27	-9.6
A T2	24.36	24.52	+0.16
A T3	24.44	24.61	+0.17
A T4	24.45	24.57	+0.12
P T1	8.43	8.73	+0.3
P T2	9.03	9.58	+0.55
P T3	10.08	11.00	+0.92
P T4	11.89	16.11	+4.22
Room T	23.1	23.8	+0.7

Table 5.3 shows how much the temperature changed during the 9 hour long experiment.

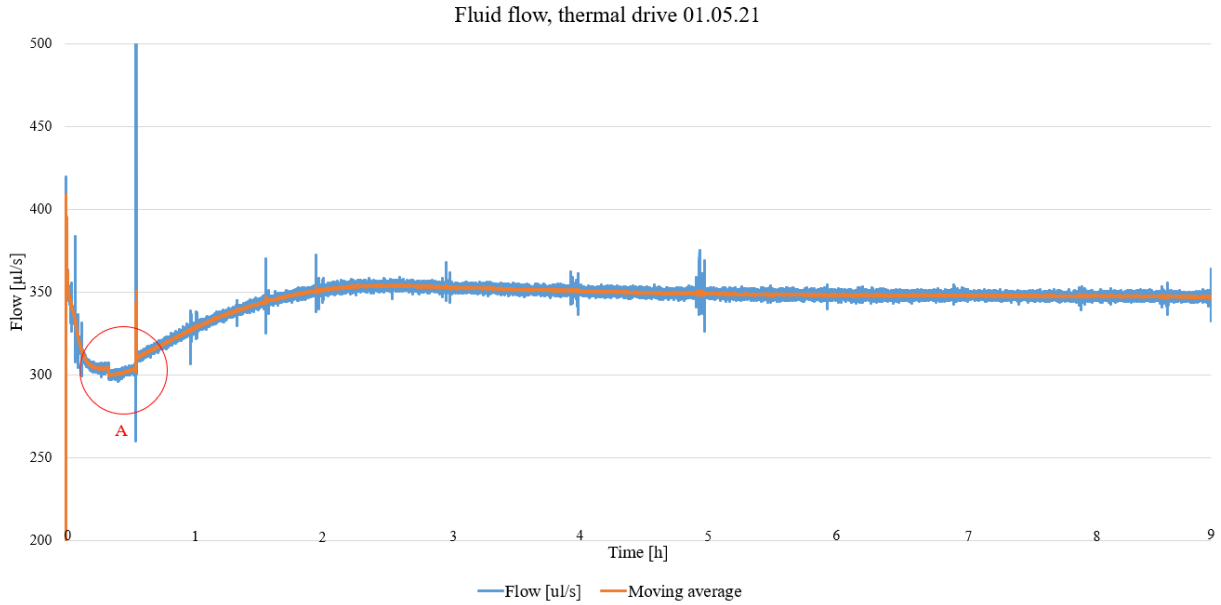

Figure 5.4: Thermal circulation 2, fluid flow data

Figure 5.4 shows how the flow rate developed during the 9 hour long experiment. The liquid height inside the top circulation pipe was 1mm above 50% of the diameter, equivalent of 24 mm. The vacuum was constant throughout the experiment.

The flow was rapidly reduced from start to roughly 20 minutes into the experiment, before something happens that affects the fluid flow abruptly. The flow starts to increase, before it evens out after 2.5 hours and reduces slowly towards the end of the experiment. The unexpected change in flow rate is marked by an A in the figure. An excerpt from this period is shown in figure 5.5.

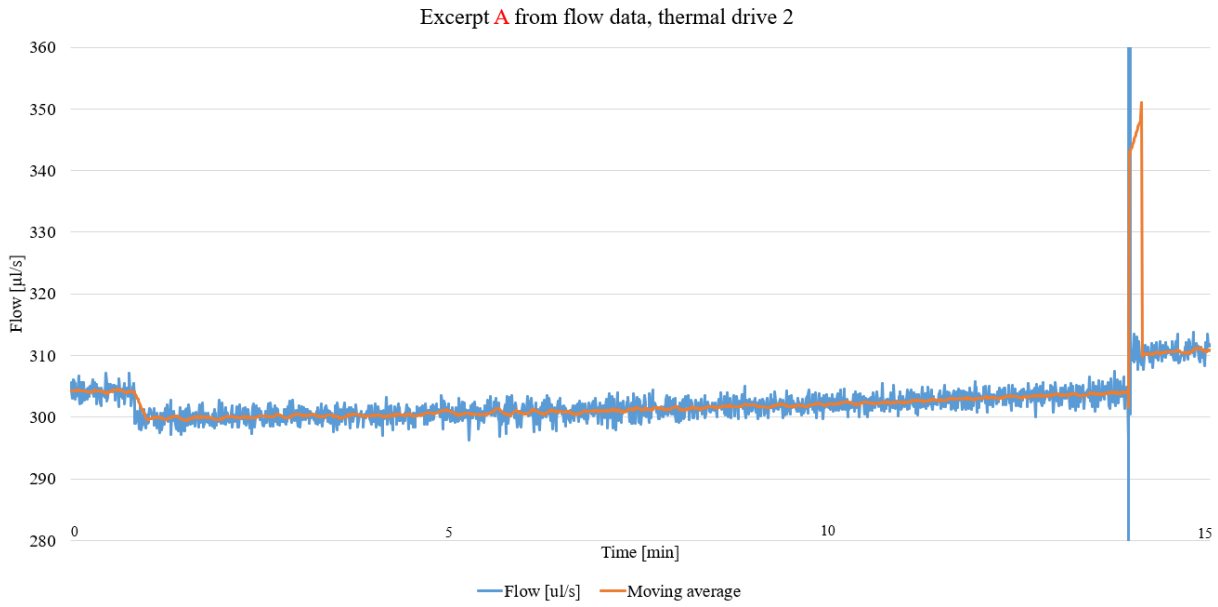

Figure 5.5: Thermal circulation 2, excerpt A from flow data

Figure 5.5 shows a 15 minute expert of the flow data. From the graph one can see how the flow is suddenly reduced from 305 $\mu l/s$ to 300 $\mu l/s$ and then back to 310 $\mu l/s$.

5.2.3 Thermal circulation experiment 3

The third thermally driven circulation experiment was performed 02.05.2021, from 10:30 to 19:30. The room temperature and water temperature inside the model at the start and end of the experiment is presented in table 5.4. The flow rate measured by the flow meter is presented in figure 5.6.

Table 5.4: Temperature at start and end, thermal circulation 3

Temperature sensor	T_{start} [°C]	T_{end} [°C]	ΔT [°C]
A T1	23.84	14.42	-9.42
A T2	24.36	24.44	+0.08
A T3	24.42	24.53	+0.11
A T4	24.47	24.53	+0.06
P T1	8.43	8.67	+0.25
P T2	9.17	9.55	+0.38
P T3	10.32	10.96	+0.64
P T4	11.95	15.86	+3.91
Room T	23.4	24.0	+0.6

Table 5.4 shows how much the temperature changed during the 9 hour long experiment.

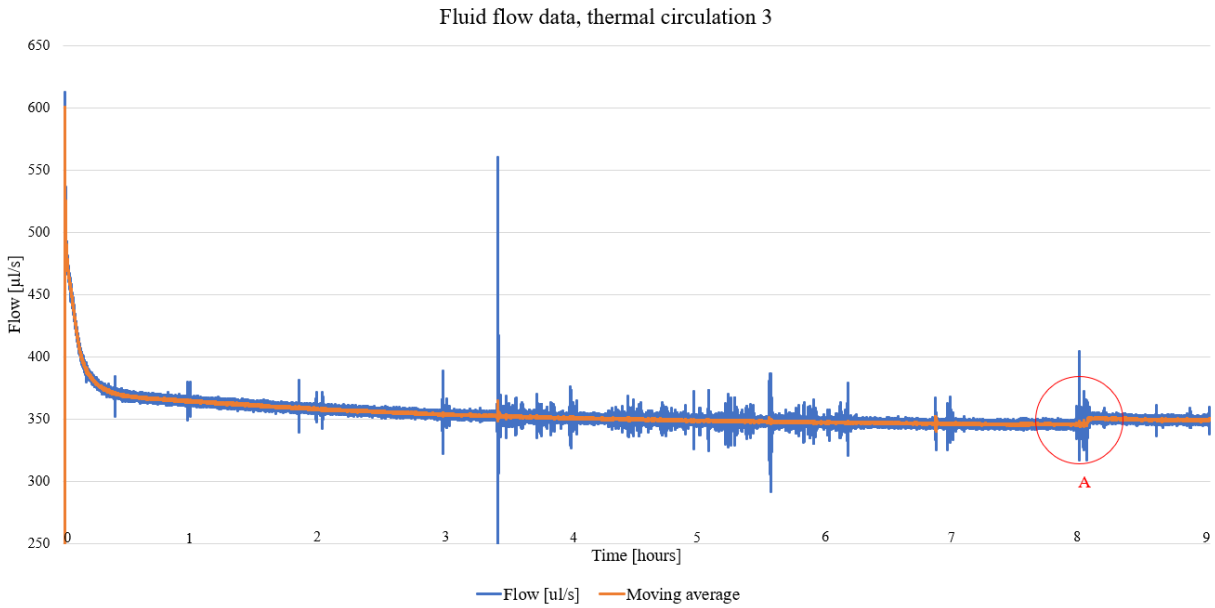

Figure 5.6: Thermal circulation 3, fluid flow data

Figure 5.6 shows how the flow rate developed during the 9 hour long experiment. The liquid height inside the top circulation pipe was 1 mm below 50% of the diameter, equivalent of 22 mm. The vacuum inside the top circulation pipe was constant throughout the experiment.

The flow was rapidly reduced the first 30 minutes before it evens out and reduces slowly the rest of the experiment. Between 3.5 hours and 6.5 hours, the sensor was subject to noise from the surroundings due to movement around the cable connecting the flow meter and the laptop. After 8 hours a positive wind drive with a power supply of 10 volt was introduced, marked by A in the figure, and the flow can be seen increasing. An excerpt of this time period is shown in figure 5.7.

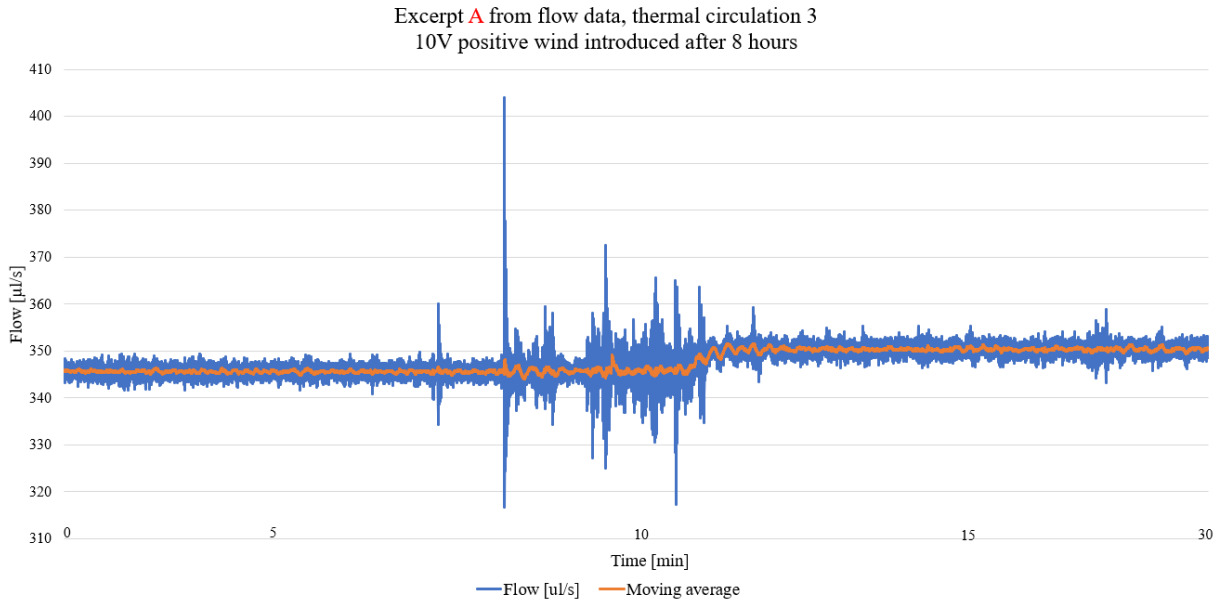

Figure 5.7: Thermal circulation 3, excerpt A from flow data

Figure 5.7 shows a 30 minute excerpt of the flow data. From the graph, one can see how the flow is increased from 345.7 $\mu l/s$ to 350.1 $\mu l/s$ due to the positive wind drive introduced.

5.3 Thermal drive with positive wind

One long running experiment was performed for thermal circulation with positive wind 28.04.21, from 10:45 to 18:45. The room temperature and water temperature inside the model at the start and end of the experiment is presented in table 5.5. The temperature measured by Pasco sensors is presented in figure 5.8, and the flow rate measured by the flow meter is presented in figure 5.9.

Table 5.5: Temperature at start and end, thermal circulation with positive wind

Temperature sensor	T_{start} [°C]	T_{end} [°C]	ΔT [°C]
A T1	24.74	14.90	-9.84
A T2	24.68	24.75	+0.07
A T3	24.78	24.84	+0.06
A T4	24.75	24.82	+0.07
P T1	8.67	8.90	+0.23
P T2	9.30	9.70	+0.4
P T3	10.47	11.22	+0.75
P T4	12.57	17.13	+4.56
Room T	25.9	26.3	+0.4

Table 5.5 shows how much the temperature changed during the 8 hour long experiment.

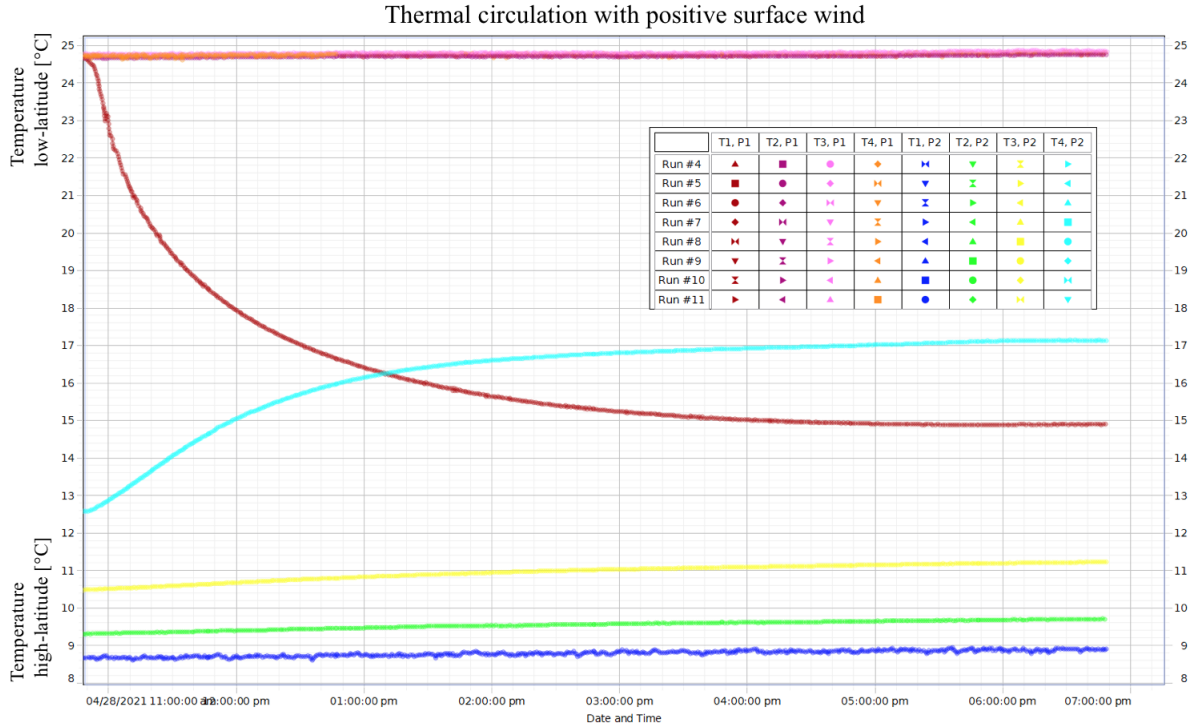

Figure 5.8: Temperature development, thermal circulation with positive wind

Figure 5.8 shows the temperature development during the 8 hour long experiment. The temperature development followed the same form as for purely thermally driven experiments, but the temperature reduction at the bottom of the low-latitude ocean and the temperature increase in the top of the high-latitude ocean is seen to happen faster compared to purely thermal drive.

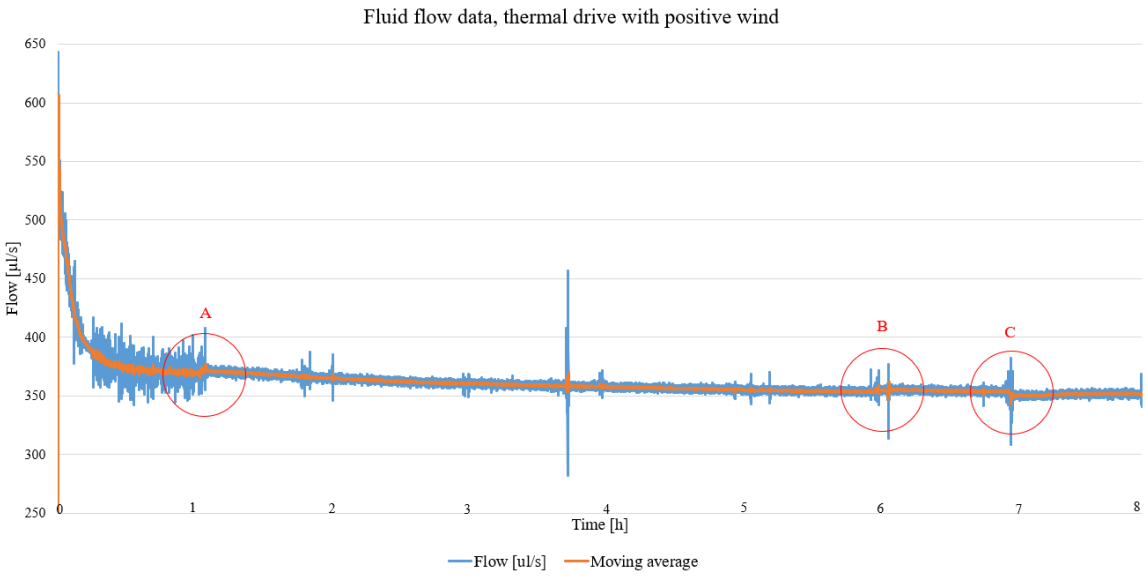

Figure 5.9: Thermal circulation with positive wind drive, fluid flow data

Figure 5.9 shows how the flow rate developed during the 8 hour long experiment. The liquid height inside the top circulation pipe was roughly 50% of the diameter, equal to 23 mm. Positive wind with a power supply of 8 volt was introduced after 1 hour, marked by A in the figure. The wind speed was increased from a power input of 8 volt to 11.5 volt after 6 hours, marked by B in the figure. After 7 hours the air pump was turned off, marked by C in the figure.

The flow was rapidly reduced the first 20 to 30 minutes before it evens out and reducing slowly the rest of the experiment. After 1 hour the flow was increased slightly due to the introduction of wind drive. An excerpt of this period is shown in figure 5.10. After 6 hours the flow was increased again due to the increase of power supply to the pump, shown in figure 5.11. After 7 hours the flow reduces due to the pump being stopped, shown in figure 5.12.

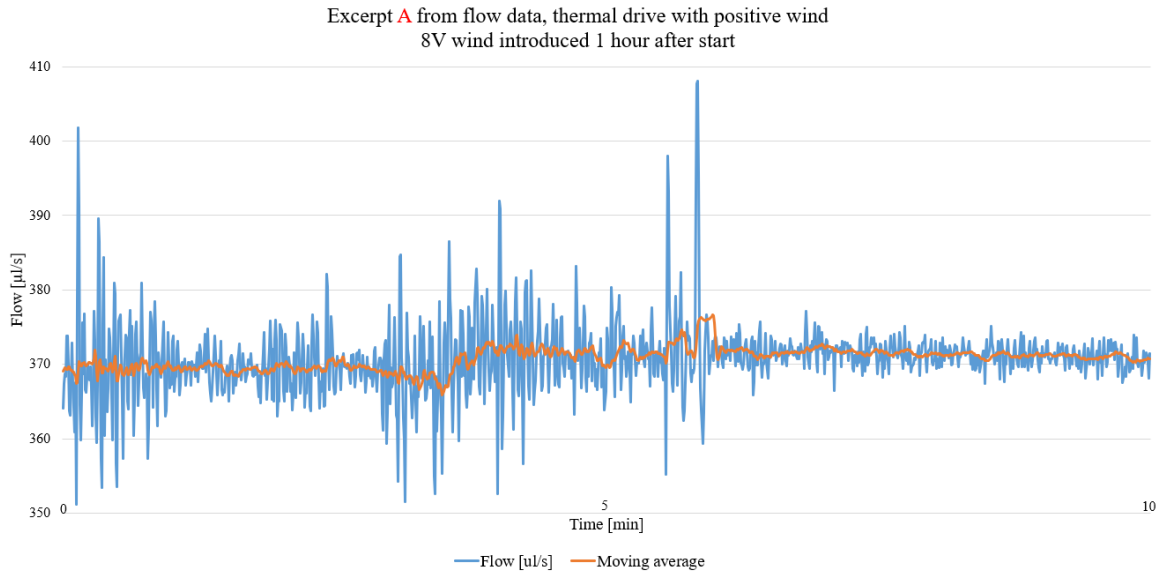

Figure 5.10: Thermal circulation with positive wind drive, excerpt A from flow data

Figure 5.10 shows a 10 minute excerpt of the flow data where positive wind drive was introduced. From the graph, one can see how the flow is increased from 370.0 $\mu l/s$ to 370.8 $\mu l/s$.

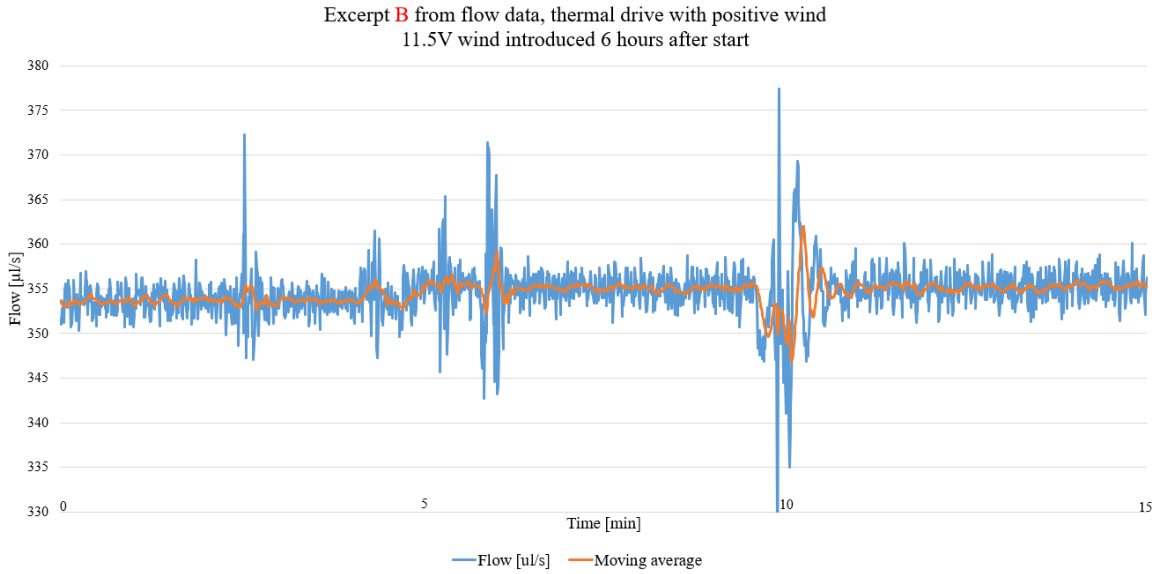

Figure 5.11: Thermal circulation with positive wind drive, excerpt B from flow data

Figure 5.11 shows a 15 minute excerpt of the flow data where power supply to the pump was increased. From the graph, one can see how the flow is increased from 353.8 $\mu l/s$ to 355.1 $\mu l/s$.

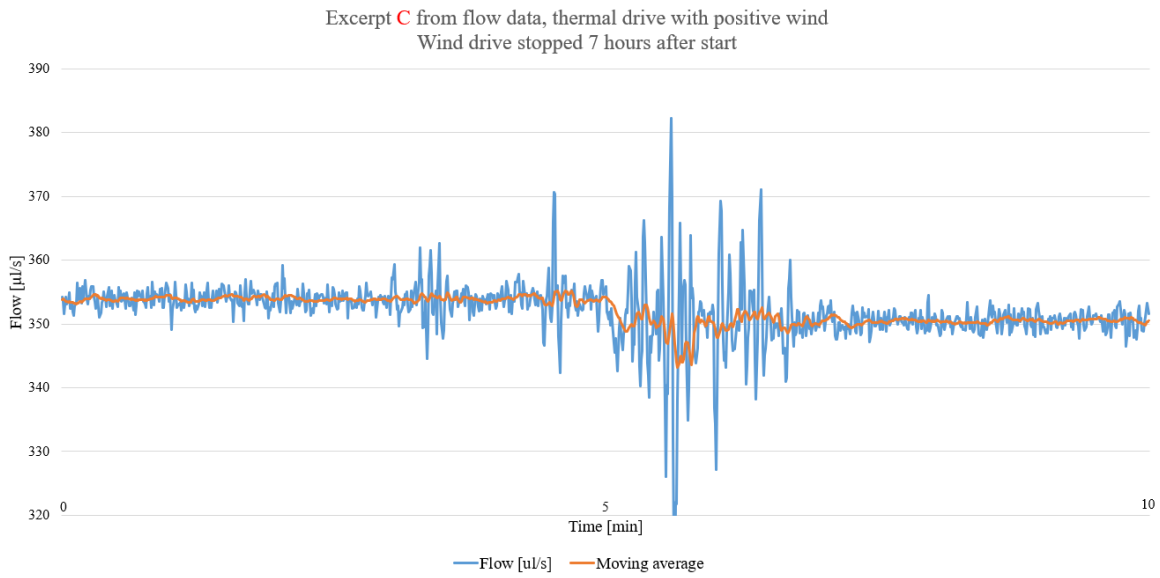

Figure 5.12: Thermal circulation with positive wind drive, excerpt C from flow data

Figure 5.12 shows a 10 minute excerpt of the flow data where the wind drive is stopped. From the graph, one can see how the flow is decreased from 354.0 $\mu l/s$ to 350.5 $\mu l/s$.

5.4 Thermal drive with negative wind

One long running experiment was performed for thermal circulation with negative wind 29.04.21, from 09:45 to 17:45. The room temperature and water temperature inside the model at the start and end of the experiment is presented in table 5.6. The temperature measured by Pasco sensors is presented in figure 5.13, and the flow rate measured by the flow meter is presented in figure 5.14.

Table 5.6: Temperature at start and end, thermal circulation with negative wind

Temperature sensor	T_{start} [°C]	T_{end} [°C]	ΔT [°C]
A T1	24.71	15.13	-9.58
A T2	24.70	24.78	+0.08
A T3	24.78	24.90	+0.12
A T4	24.73	24.84	+0.11
P T1	8.74	8.99	+0.25
P T2	9.47	9.81	+0.34
P T3	10.69	11.37	+0.68
P T4	12.89	17.35	+4.46
Room T	26.1	26.4	+0.3

Table 5.6 shows how much the temperature changed during the 8 hour long experiment.

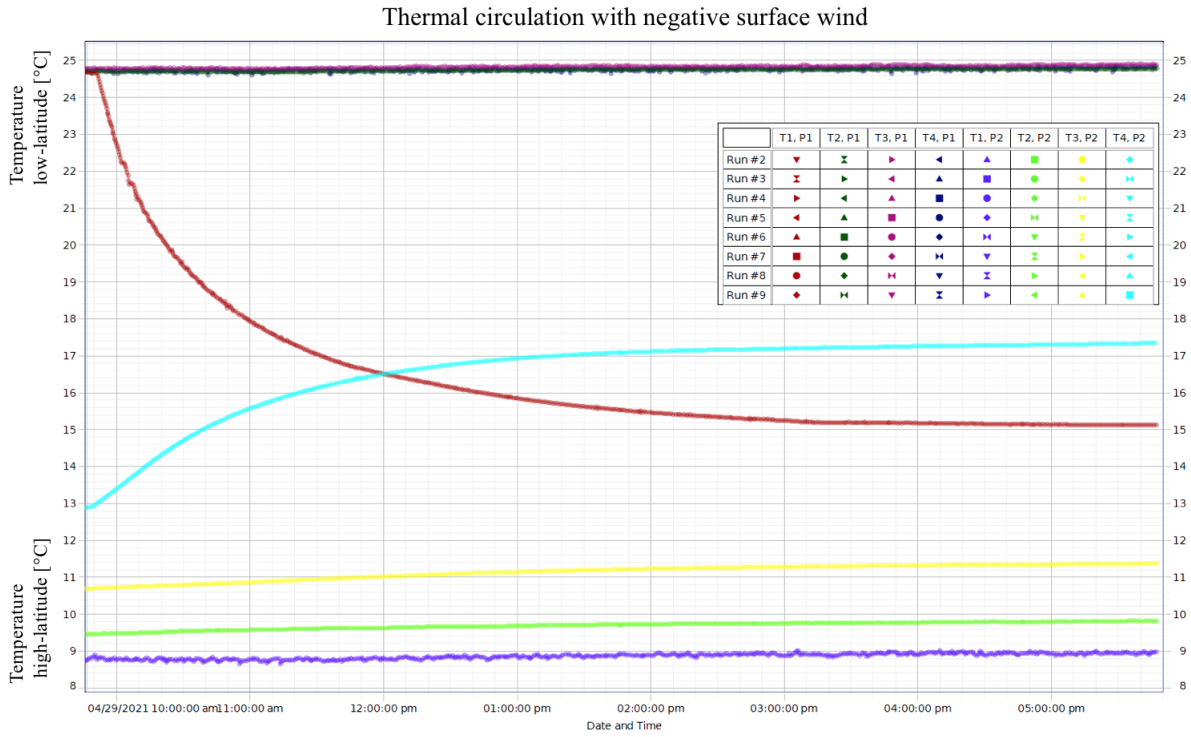

Figure 5.13: Temperature development, thermal circulation with negative wind

Figure 5.13 shows the temperature development during the 8 hour long experiment. The temperature development followed the same form as for purely thermally driven experiments.

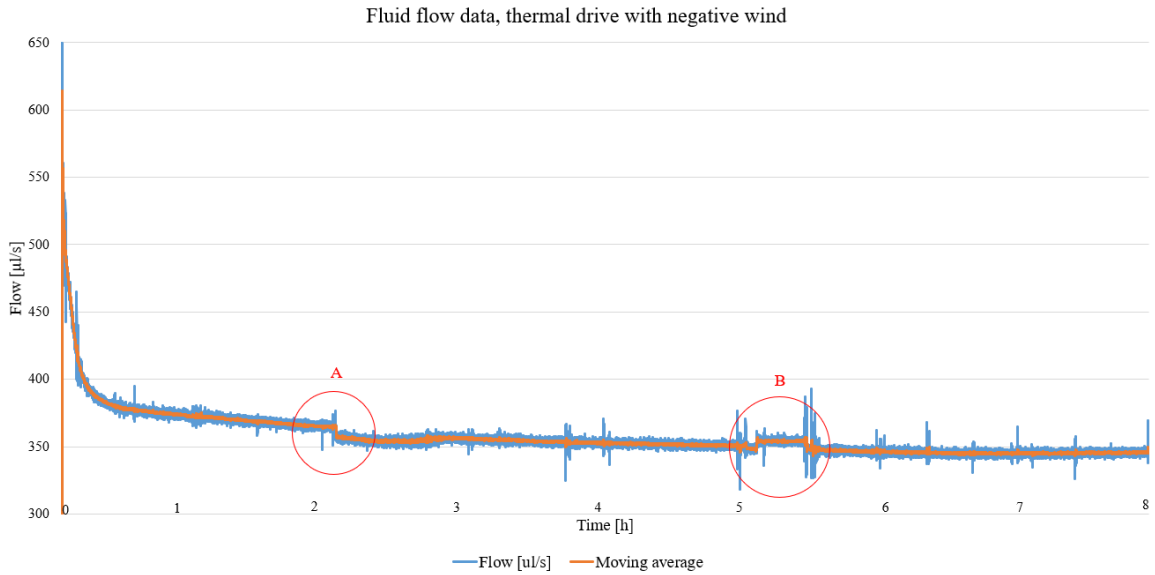

Figure 5.14: Thermal circulation with negative wind drive, fluid flow data

Figure 5.14 shows how the flow rate developed during the 8 hour long experiment. The liquid height inside the top circulation pipe was roughly 50% of the diameter, equal to 23 mm. Negative wind drive was introduced with a power supply of 8 volt after 2 hours, marked by A in the figure. After 5 hours, the power supply was increased from 8 volt to 11.5 volt, marked by B in the figure. The pump fell out for roughly 30 minutes of the experiment straight after the negative wind drive was introduced.

The flow was rapidly reduced the first 20 to 30 minutes before it evens out and reducing slowly the rest of the experiment. After 2 hours the flow was reduced due to the introduction of wind drive. An excerpt from this time period is shown in figure 5.15. After 5 hours the flow was reduced more due to the increase of wind. Between 5 and 5.5 hours the flow is seen increasing for a period before it is reduced again due to the pump falling out. An excerpt from this time period is shown in figure 5.16.

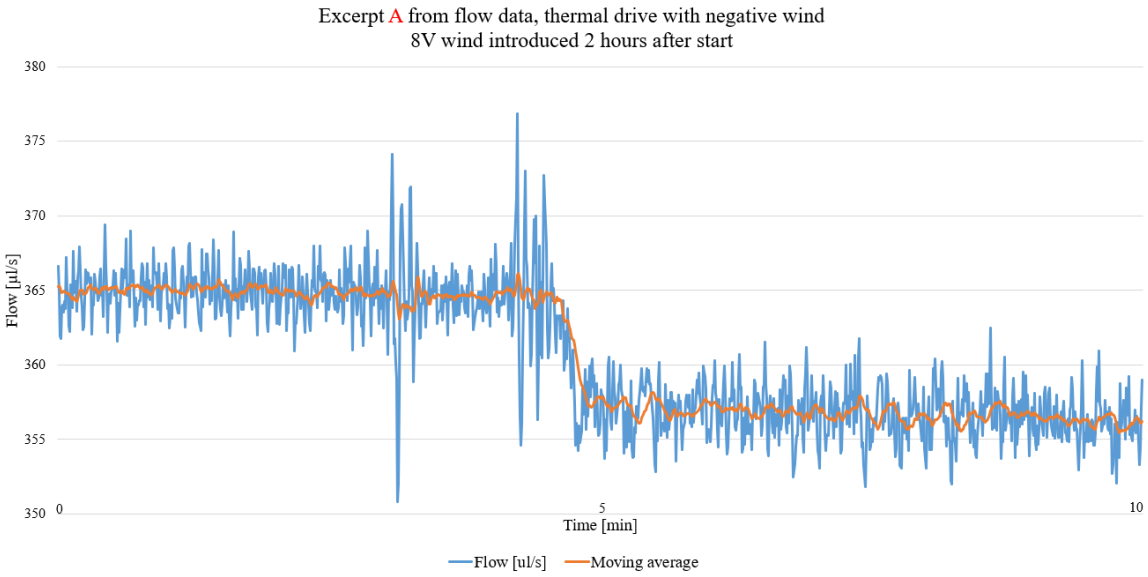

Figure 5.15: Thermal circulation with negative wind drive, excerpt A from flow data

Figure 5.15 shows a 10 minute excerpt of the flow data where negative wind is being introduced. From the graph, one can see how the flow was decreased from 365.0 $\mu l/s$ to 356.0 $\mu l/s$.

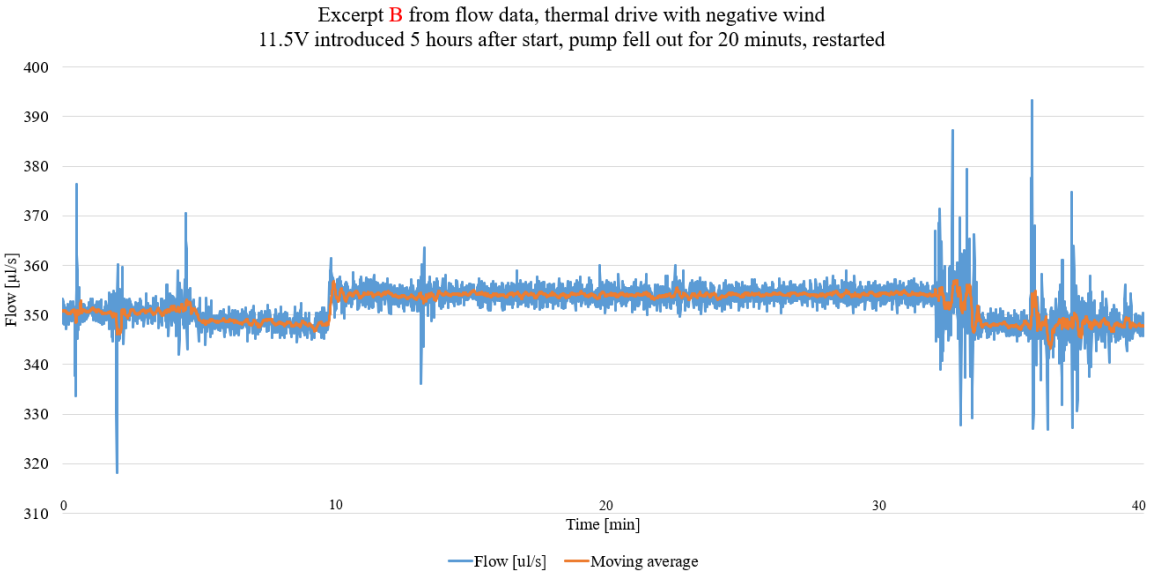

Figure 5.16: Thermal circulation with negative wind drive, excerpt B from flow data

Figure 5.16 shows a 40 minute excerpt of the flow data where power supply first is increased before it stops abruptly. From the graph, one can see how the flow was decreased from 350.9 $\mu l/s$ to 348.3 $\mu l/s$ due to the wind drive being increased. From 10 to 30 minutes of the excerpt one can see that the flow is increased back to 354.0 $\mu l/s$ due to the pump falling out and the wind drive being stopped. Once the pump was restarted, the flow was decreased back to 347.1 $\mu l/s$.

Chapter 6

Discussion

Development and testing of the new model has involved a wide spectre of ideas, unexpected results and new possibilities. In this chapter, the results presented in chapter 5 will be discussed, together with research limitations and future research propositions.

6.1 Heat transfer in the model

Heat transfer is an important aspect of the new model. This section is divided into three subsections: the effect isolating the model had on the temperature, the influence of the room temperature and the size and placement of the heating/cooling element.

6.1.1 The effect of isolating the model

From the comparison of liquid temperature inside the model before and after it was insulated proved that wrapping a hot or cold element in an insulating material reduces the rate of heat loss from the element. The thicker the insulation, the smaller the heat loss. From the temperature profiles introduced in chapter 2 (figure 2.2), it was desired to create a temperature gradient in the low-latitude ocean. The bottom circulation pipe was therefore insulated to reduce the amount of heat loss between the model and the surroundings when cool water circulated. Although the insulation proved to be effective, there were still a large amount of heat transfer between the bottom circulation pipe and the surroundings, proven by how the temperature in the bottom of the low-latitude ocean always stabilized at a much higher temperature than in the bottom of the high-latitude ocean.

Bubble wrap is considered an excellent insulator thanks to the small pockets of air within each bubble creating a barrier between an element and its surrounding which tends to resists temperature changes. Wrapping it around a hot element will prevent heat from moving out, and wrapping it around a cold element will prevent the heat from moving in. To better insulate the model, especially the high-latitude side, the amount of bubble wrap should be increased.

6.1.2 The influence of ambient temperature

From comparing the temperature inside the model before starting experiments to the ambient temperature before each experiment, it is clear that hot elements loses heat at a higher rate when the temperature of the room housing the element is lowered. In the same way, a cold element would gain more heat at a higher rate when the room temperature is increased. The model was placed in a small laboratory which allegedly had a good climate and temperature regulation system. During experimentation the temperature regulator proved to be defect, as the set room temperature was $21°C$, but the true room temperature was measured to be a lot higher, ranging from 23.1 - 26.4 $°C$ during experiments. As there were multiple people working in the laboratory, and a different number of machines were on during the various days the experiments were performed, the ambient temperature differed enough to impact the experiments. This was fixed on the last day of laboratory work.

6.1.3 Heating/cooling element in the model

The copper pipes used as heating/cooling element were chosen only based on their availability and not size. It was discussed that the area would be too small to properly cool down the water inside the high-latitude ocean to the desired temperature, as well as too small to effectively cool down the temperature of the water circulating from the low-latitude ocean into the high-latitude ocean. The true temperature profile in the ocean shows how the temperature in the high-latitude ocean is between 0-5 $°C$ independent of the depth. There should therefore be a much smaller temperature gradient in this ocean, and the water circulating in from the high-latitude ocean should immediately have been cooled down. During experiments it became clear that the copper pipes used should either be longer and shaped in a coil, or both be longer and larger in diameter in order to properly cool down the water. Another possible method would be to exchange the distilled water inside the cool waterbath with ethanol in order to use a lower set temperature. To get a more realistic temperature gradient in the high-latitude ocean, more cooling elements should be introduced either around the top of the high-latitude ocean, or directly around where the water from the low-latitude ocean flows in.

6.2 Water height inside top circulation pipe

The volumetric liquid flow through the model is based on the thermal circulation theory, where flow is proportional to the difference in hydrostatic pressure between the two water tanks due to temperature differences. Hydrostatic pressure can be expressed as:

$$P_{hyd} = \rho(T, S)gh \tag{6.1}$$

where P_{hyd} is the hydrostatic pressure, ρ is the density of the liquid which depends on both the temperature and the salinity, g is gravity and h is the liquid height.

In the new model, the potential for an unstable liquid height is high as the model depends on an air tight top circulation pipe. To ensure that something is air tight is difficult when it comes to opening/closing connections. In figure 6.1 the top circulation pipeline is shown together with the most probable leakage points. If these connections were not completely closed, air would leak into the pipeline, affecting the liquid height.

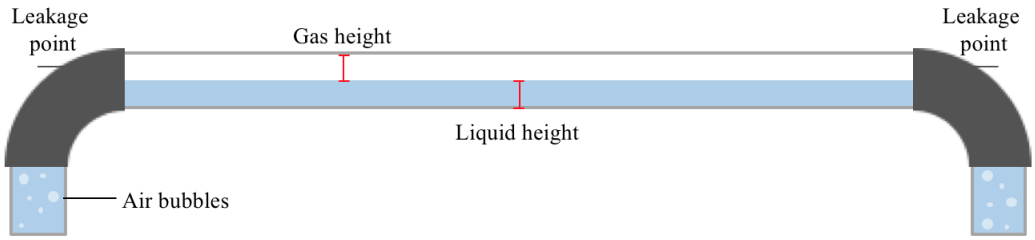

Figure 6.1: Closeup of the top circulation pipeline and its leakage points and air bubbles

In thermal circulation experiment 1 the affect of increasing the liquid height during an experiment can be seen. Increasing the liquid height gave an immediate increase in flow rate. Comparing the other experiments where the water height varied by 3 mm total, it is seen that the experiments where liquid height was higher also had the overall largest flow rate.

In thermal circulation experiment 1, the liquid height inside the top circulation pipe was not constant, but reduced over time. There are multiple possibilities why the liquid height changed during this experiment, but the most realistic one being the pipe was not air tight. Another explanation may have been the placement of the pipe. Air bubbles are less dense than water and will be pushed up to the surface, but they may get stuck to the pipe walls due to friction on their journey upwards. When the liquid inside the model starts to move, air bubbles may loosen from the pipe walls and thus rise to the surface. Air bubbles tend to be larger near the pipe wall as compared to those in the central region of the pipe [19], and since the bubbles are subject to the surrounding pressure, they will also be able to increase in size as they move towards the surface. If a large amount of bubbles enters the top circulation pipe, it might expand the air inside pipe, forcing liquid back into the the tanks. In figure 6.1 one can also see an illustration of air bubbles entering the pipeline.To limit the possibilities of air bubbles entering the top circulation pipe, the pipe should not be placed directly in contact with the PMMA cast tubes. It is also important to properly tighten the tube clamps used to prevent air from entering/leaving the pipe at the two leakage points shown in 6.1.

6.3 Different results using the same procedure

Based on the theory of thermal circulation, the flow rate was expected to be at its highest from the start, decreasing rapidly due to the small volume of the bottom circulation pipe and then decreasing slowly throughout the experiment before reaching a constant flow rate. Figure 6.2 shows one of the water tanks with the pipe connecting the tank to the bottom circulation pipe. The same height is marked two places on the figure to more easily explain the expected flow rate development.

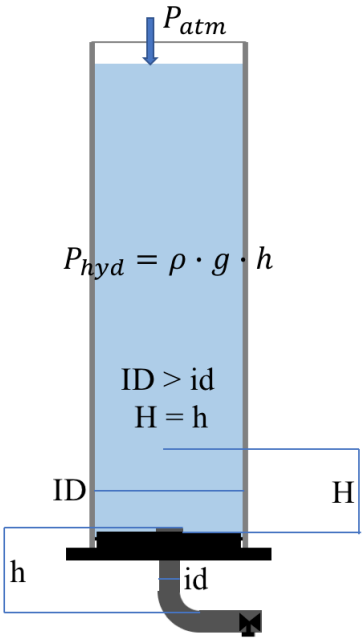

Figure 6.2: Close-up of a water tank with the small pipe connecting the bottom circulation

The hydrostatic pressure is dependent on the density of the fluid and the fluid height. The hydrostatic pressure inside the bottom circulation pipe is therefore expected to decrease more rapidly compared to the hydrostatic pressure inside the tank, since it will take less time for the fluid inside the bottom circulation pipe to be replaced by a fluid with a different density.

The hooded PVC pipe connecting the PVC bend to the bottom plate in the model has a length of 110 mm and an inside diameter of 30 mm. This gives a total volume of 0.078 l. Using the same height, but with the inside diameter of the PMMA cast tubes (284 mm) will result in a total volume of 4.43 l. With an average flow rate of 350 $\mu l/s$, which equals 1.26 l/h, it would only take 3.72 minutes to change the hydrostatic pressure inside the PVC pipe, and over 3.5 hours to change the hydrostatic pressure equally using the same height in the PMMA cast tube. This is why the flow rate was expected to reduce drastically in the start of the experiment before leveling out. Since the heating and cooling systems are continuously heating and cooling the water circulated into each tank respectively, the flow rate will reach a constant when the temperature systems are able to keep the temperature profiles inside each tank constant.

From the flow data presented in chapter 5, it can be seen that the flow rate in two of the experiments, thermal circulation 1 and thermal circulation 2, did not follow the expected development based on theory. In figure 6.3 and 6.4 a 2 hour excerpt of the start of these experiments are shown.

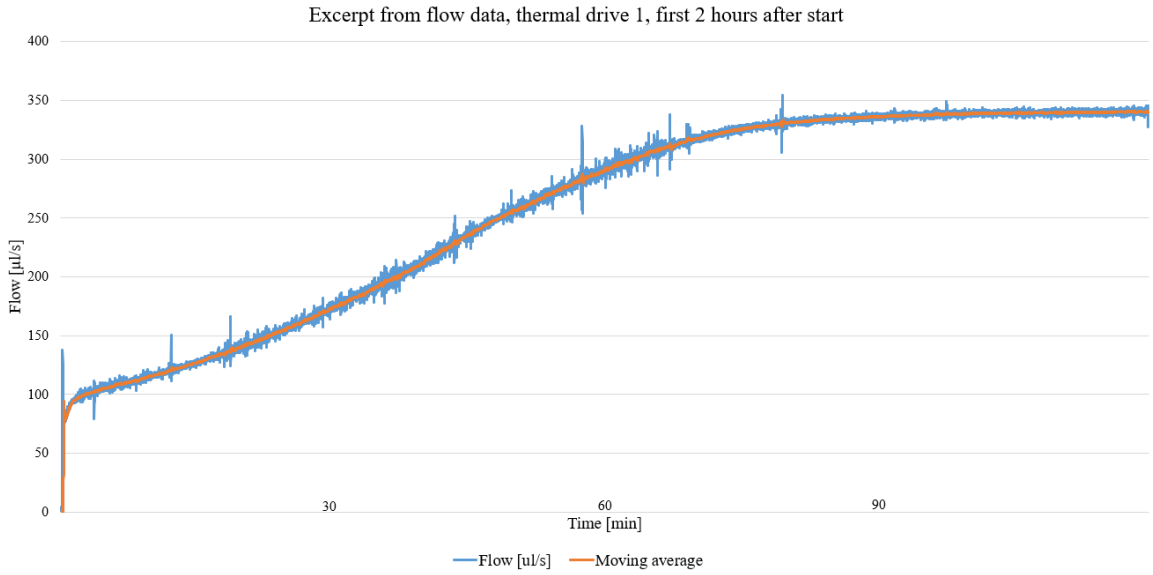

Figure 6.3: Thermal circulation 1, first 2 hours of flow data

Figure 6.3 shows how the flow rate started at a low value and increased for almost 2 hours in the first thermal circulation experiment. Unlike the other experiments, where the flow rate is seen decreasing throughout the experiment, the flow rate here was close to constant for the rest of the experiment. One reason the flow rate appears constant is assumed to be related to the liquid height inside the top circulation pipe not being constant. The hydrostatic pressure in each tank might have been kept constant by the liquid inside the top circulation pipe flowing into the tank where the pressure should have changed.

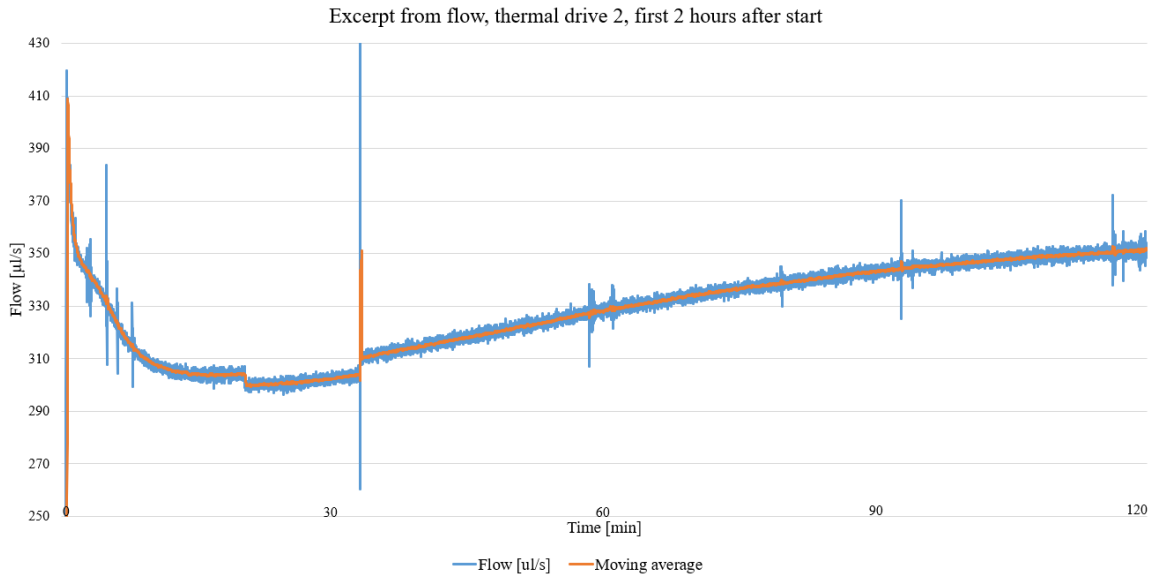

Figure 6.4: Thermal circulation 2, first 2 hours of flow data

Figure 6.4 shows how the flow rate started at a high value and decreased rapidly before starting to increase. During a time period it looks like the graph drops down a notch.

The two experiments where the flow development differed from the theoretical expectation were both performed the first day after the model was filled with water, as explained during the procedure in chapter 4. Although thermally driven circulation is considered a single-phase circulation, air bubbles and air pockets may form during filling and emptying of pipes. Air movement along a pipeline can be slow during filling resulting in a trapped air column adjacent to valves or cross-sectional constrictions. It is therefore assumed that air bubbles or air pockets in the bottom circulation pipeline might have influenced the flow development in these two experiments. The characteristics of bubbles in flowing liquids are complicated due to the effect of drag, fluid viscosity, friction and wall shear stress. Thus, only a general observation of how the air bubbles or air pockets may have influenced the liquid flow in the experiments are mentioned.

The bottom circulation pipe consisted of two ball-valves with two brass hose connections introducing a rapid cross-sectional area reduction, two plastic cartridges introducing a smooth cross-sectional area reduction and a flow meter with the same inside diameter as the smallest inlet/outlet of the plastic cartridges. These parts were all introduced in chapter 4. There are therefore multiple places an air bubble or air pocket may get trapped during filling, and the effect it has on the flow rate may again depend on where the bubble or pocket is situated during the start of experiments. A closeup of the bottom pipeline highlighting the constrictions is shown in figure 6.5.

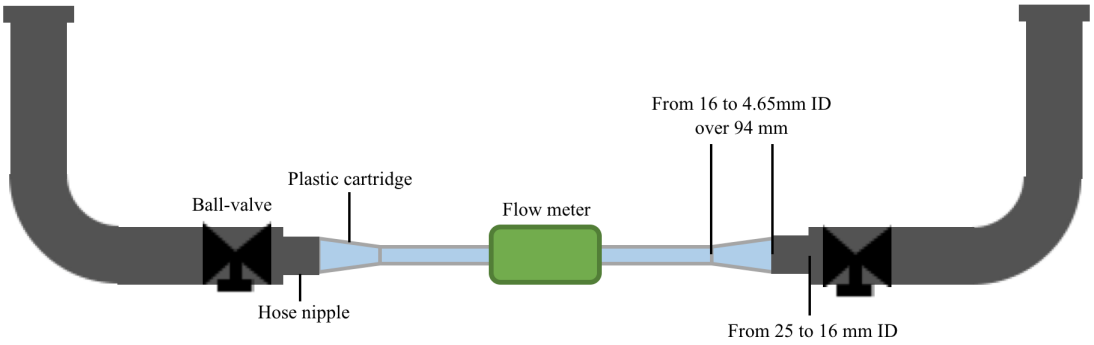

Figure 6.5: Closeup of the bottom circulation pipeline and its constrictions

An air bubble or air pocket situated inside the smallest pipe of the bottom circulation pipeline, namely the flow meter, would take up some of the cross-sectional area, making the area available for liquid flow smaller and thus decreasing the flow rate.

A small air bubble situated inside the valve or hose connection on the high-latitude side of the flow meter could change size going into the flow meter pipe due to the change in diameter. Bubbles are compromised of gases, which as mentioned have a lesser density than water and are considered compressible. Using Bernoulli's principle stating that an increase in the speed of a fluid occurs simultaneously with a decrease in static pressure, the bubble will be subjected to less pressure when entering the reduced cross-sectional area and will therefore be able to increase in size. Inside the flow meter pipe, the bubble may break due to turbulence, or it might just be pushed through by the liquid flow.

In thermal circulation experiment 1 (figure 6.3), it is assumed that an air bubble is situated inside the smallest part of the bottom circulation pipeline. The flow starts at a low value and increases almost linearly, which might be because the bubble is slowly being pushed out by the liquid flow or broken up by turbulence.

In thermal circulation experiment 2 (figure 6.4), it is assumed than an air bubble enters the smallest part of the bottom circulation pipe. The area where the graph jumps down a notch may be due to the bubble entering the measurement chamber. The flow meter is designed to measure liquid flows, not gases, and may be directly affected by having an air bubble inside the chamber.

Since the remaining experiments, which followed the theoretical flow development, were performed the day after another experiment with the same water, it is possible to change the procedure to account for this unexpected error. Avoiding air bubbles can be done by circulating water through the flow meter before starting experiments. When filling up the model, both valves should be kept open and the liquid should be pored into one side. The liquid should be poured carefully to not increase air trapped in the liquid, and should not be filled directly from the tap. During research experiments distilled water should be used. As the method chosen for temperature regulation has the ability to both cool down or heat up the water inside the model, this method could be implemented without changing the setup.

6.4 Impact from surface wind

When introducing wind drive to the water surface, the single-phase flow system became a two-phase flow system. Excerpts from the measurement data showed directly how introducing a surface wind drive affected the flow rate.

When air flow, or wind, is introduced in the same pipe as liquid flow, the wind will directly influence the liquid due to shear stress exerted on the water surface. This is often referred to as wind stress, and it is affected by the wind speed, the wind waves shape and the atmospheric stratification. In figure 6.6 the normal velocity profile of a liquid flowing in a half filled pipe is seen together with how it is assumed surface wind impacted the velocity profile. The green arrows represents the fluid velocity profile while the black arrows represents the wind velocity profile.

(a) Liquid velocity profile, no surface wind

(b) Liquid velocity profile, positive surface wind

(c) Liquid velocity profile, negative surface wind

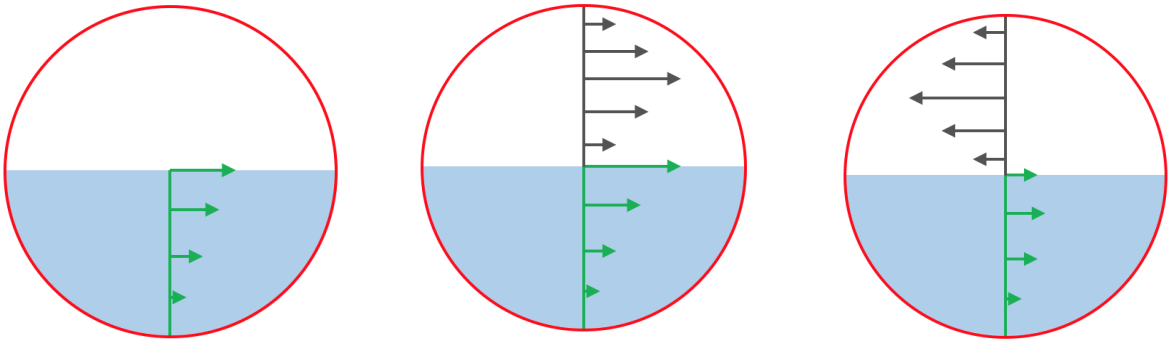

Figure 6.6: The effect of surface wind on liquid velocity profiles

The velocity profile of liquid circulating in a pipe with no wind drive is shown in figure 6.6 (a). The velocity of the fluid will be highest towards the center of the pipe, decreasing towards the pipe walls due to friction. The water surface may be considered a free surface as the surface of the fluid is subject to zero parallel shear stress.

In figure 6.6 (b) the velocity profile of a liquid circulating inside a pipe together with a positive wind drive is shown. The wind velocity profile is similar to a liquid velocity profile for a liquid moving in a completely filled pipe. The velocity will be smaller at the pipe wall and at the liquid surface due to friction. Some of the energy from the wind is transferred to the liquid surface, increasing the velocity of the surface. When wind is blowing over the fluid and disturbing the free surface, small ripples are produced which can develop into large waves once the wind has something to catch on to.

In figure 6.6 (c) the velocity profile of a liquid circulating inside a pipe together with a negative wind drive is shown. The wind velocity profile will be similar as described earlier, but the effect on the liquid velocity profile will be different. The wind will slow down the velocity of the liquid surface as well as create tiny ripples for the wind to catch so that it may create larger waves.

Wind speeds with a power supply of 8 volt, 10 volt and 11.5 volt were used in the experiments. The resulting wind speed based on the power supply was found during one of the tests performed in the feasibility study, showed in chapter 3. To get an inclination of how much of the energy would get transferred to the liquid inside the pipe, the wind speed was not only tested at the location into the pipeline, but also out of the pipeline. The result is presented in table 6.1.

Table 6.1: Comparing Wind speed in and out of top circulation pipe

Power input [V]	Wind speed in [m/s]	Wind speed out [m/s]	ΔWind speed [m/s]
6	1	1	0
8	1.7	1.5	-0.2
10	2.5	1.8	-0.7
11.5	3.1	1.85	-1.25
12	3.3	1.9	-1.4

From table 6.1 one can see how the wind speed into the pipe and out of the pipe was not equal due to energy from the wind being transferred to the liquid surface. When wind speed is low, the disturbance on the liquid surface is so low that only a small amount of energy gets transferred. As the wind speed increases, small ripples are created in the water surface, which the wind then catches. This enables the wind to transfer more energy to the water surface, transforming the small ripples into waves.

6.4.1 Positive wind drive

Air circulating in the same direction as the liquid had a positive impact on the flow rate. The air blowing on the liquid surface dragged up water, creating ripples and waves moving in the same direction as the circulation. These waves created a height difference inside the top circulation pipe, increasing the hydrostatic pressure near the low-latitude ocean, which in turn increased the flow rate. This is shown in figure 6.7. It is assumed that the waves were longer and lower in height compared to the waves created by the negative air circulation based on observations. The excerpt from the figure is taken at random to show how the surface movement might have developed with time, but is not meant to be seen as movement developed with pipe length.

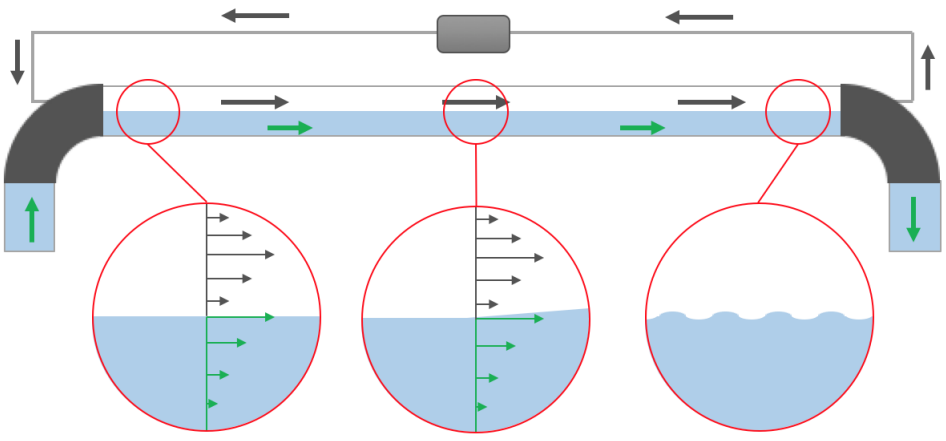

Figure 6.7: Circulation in top pipe, positive wind

In the thermal circulation with positive wind drive experiment, one can see how the flow rate was instantly increased by 1 $\mu l/s$ when a wind drive with a power supply of 8 volt was introduced, and again instantly by 1 $\mu l/s$ when the power supply was increased to 11.5 volt. 1 hour before the end the power supply was turned off, and the flow rate can be seen decreasing by 3.5 $\mu l/s$ instantly. It can also be seen how the flow rate decreased slower during the experiment, and that the flow rate was higher when the experiment ended compared to purely thermal driven circulation.

In thermal circulation experiment 3 a positive wind drive with a power supply of 10 volt was introduced to the surface towards the end of the experiment, and the flow rate was instantly increased by 4.6 $\mu l/s$.

6.4.2 Negative wind drive

Air circulating in the opposite direction as the liquid had a negative impact on the flow rate. The air blowing on the liquid surface dragged up water, creating ripples and movement in the surface. as well as physically slow down the surface speed. The waves observed during experiments seemed to be shorter and taller compared to the waves created by positive wind. The negative wind created therefore a larger liquid height difference inside the top circulation pipe, which in turn had a larger impact on the flow rate. This is shown in figure 6.8.

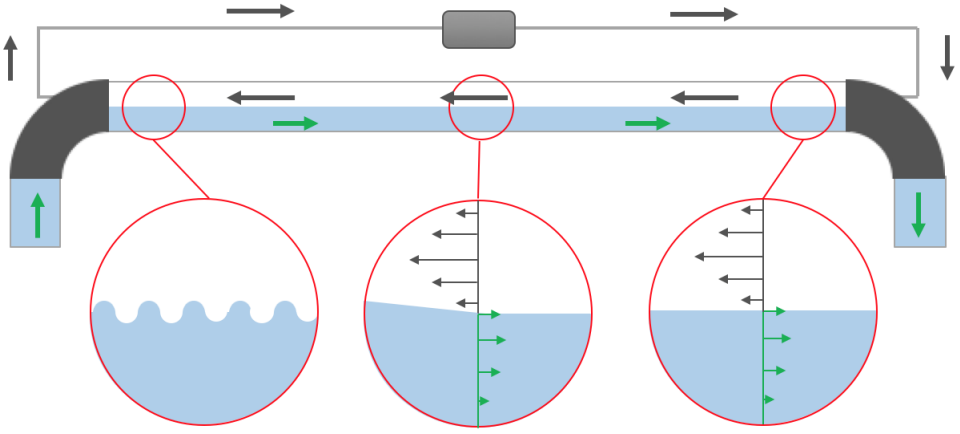

Figure 6.8: Circulation in top pipe, negative wind

In the thermal circulation with negative wind drive experiment, one can see how the flow rate was instantly decreased by 9 $\mu l/s$ when an air flow with a power supply of 8 volt was introduced, and again instantly decreased by 3 $\mu l/s$ when the power supply was increased to 11.5 volt.

6.5 Homogenising the model, Stommel's theory

Although the laboratory model was based on Stommel's two box model, introduced in chapter 2, there were a notable difference. The Stommel's two box model is a homogeneous model, where the fluid inside each tank has a constant temperature and salinity. When the fluid is circulating, the conditioning systems connected to the model keep the conditions constant. The new model, however, allows the circulation to form a temperature gradient in both tanks. Because the heating element inside the low-latitude tank is placed a distance from the bottom plate, it will allow cool water to accumulate at the bottom. As more cool water is circulating into the tank, the heating element will start to heat the cold water as it moves upwards, obtaining the desired temperature gradient. The new model can however be homogenised by simply adding inline pumps in each tank and increasing the size of heating/cooling elements.

6.6 Research limitations

This study had several limitations, both concerning the data collected from the experiments and in terms of the research itself.

The room temperature was seen to vary a lot during the different days the experiments were conducted due to a faulty air conditioner and irregular use of lab equipment that produced a large amount of heat. The room temperature impacted the start conditions in the model, making it harder to compare the results obtained during the different experiments as well as replicate the experiments.

For time and economical reasons the supervisors asked that most equipment used in the new model should be equipment readily available at the multiphase laboratory. This had to be taken into account when designing the model as well as the temperature regulation system. The design will however allow parts to be easily exchanged without affecting the integrity of the structure.

Due to Covid-19 and national rules, the multiphase laboratory was closed down for students in periods. Therefore it took some time before the model could be built and tested. This resulted in a limited time spent performing long term experiments, which gave a small sample size.

Much of the discussion is based on assumptions made during experimentation, especially concerning air bubbles in horizontal pipelines and how surface wind moving in the opposite direction from a liquid impacted the liquid velocity profile.

6.7 Future research

The research question was not to find out how surface wind would impact ocean circulation, but rather to design, build and test a model where such a research question could be investigated. Since much of the discussion is based on assumptions, the new model can be used for more than just thermal circulation with surface wind:

Investigating exactly how a negative wind drive would impact the velocity profile of a liquid circulating is an exciting topic. This can for example be done using PIV with particles, described in chapter 3. In order to use this method, a study researching neutrally buoyant particles has to be conducted in order to find the best particles to use when the fluids density is not constant.

Another interesting research topic can be to identify how large the wind speed would have to be in order to counteract the thermally driven circulation. This would require either a larger air pump or a smaller top circulation pipeline. Since the top circulation pipe used in this thesis is not connected to the model in any way, it can easily be changed with a more appropriate pipeline. With a larger pipeline and larger air pump, one could also investigate how the wind speed would affect the velocity profile when the liquid inside the pipeline had a significant temperature gradient.

The model is intended to be used to research how climate change can affect ocean circulation. An important aspect will therefore be to find a method for desalination, so the thermal circulation experiments can be transformed to thermohaline circulation. To simulate a freshwater influx from ice melting, ice can be added to the high-latitude ocean, which will melt when warmer water is circulated in from the low-latitude ocean. In order to do this, the temperature at the top of the high-latitude ocean has to be cold enough for the ice not to melt due to room temperature.

Chapter 7

Conclusion

This study presents development of a new ocean and climate lab scale model for thermal circulation with surface wind, including a feasibility study with tests, detailed information about the setup and experiments performed in the new model. It was an intensive process with several challenges along the way, which was further complicated due to the Covid-19 pandemic the world was facing in 2021. With the many modifications done throughout the process, the final result was satisfying. The experimental design with its flexible systems functioned as intended, and the measurement data received during the tests held a high quality thanks to the sensitivity of the measurement equipment used. A Sensirion liquid flow meter was used to measure liquid flow while Pasco equipment was used to measure the temperature. Both instruments proved to be fast and highly sensitive to changes, making it possible to note whenever the system was subjected to interference from the outside.

Based on the feasibility study, experimental work and analysis of data, the following conclusions can be drawn:

- Feasibility studies showed that the chosen design would be the most beneficial from a long term perspective. The combined piping system met all the requirements set by the supervisors, and proved to be flexible and easy to work with. Based on research, PIV analyses are deemed to be a good method for visualizing velocity profiles in the top circulation pipeline where wind is introduced. In order for this to be used, a new research must be performed to find the best particles.

- Based on visual analysis during experimentation, the thermal conditioning system seemed to be quite effective and did not influence the circulation in a negative way. The system was flexible and can easily be altered should a larger heat transfer be needed. A second cooling element should also be added to the top of the high-latitude ocean in order to counteract the temperature gradient forming during experiments.

- Flow meter from Sensirion appeared to be a good choice for flow measurement for very low flow velocities, but the sensitivity introduced some restrictions on movement around the model during experiments. Equipment from Pasco performed satisfactory during experiments after it was taken into account where the sensors measured from. Both instruments were easy to use and calibrate.

- The MATLAB script used to predict flow rates in the new model showed a higher flow rate compared to experiments. The MATLAB script took only into account how the density would change with temperature and salinity, and not how the viscosity would change. The script was also based on the assumption that the smallest cross-sectional area would be the source of the dominant friction, and that friction in the rest of the model could therefore be ignored. The script could still be used to ensure the flow rate would not surpass the maximum flow rate measured by the Sensirion flow meter, if equipment or model parts were to be changed.

- Based on analysis of flow rate it can be concluded that an air flow introduced in the same direction as a liquid surface moving due to thermal circulation would result in a positive impact on the flow rate. Air flow introduced in the opposite direction as a liquid surface moving due to thermal circulation would result in a negative impact on the flow rate. Experiments also proved that a higher wind speed introduced to a water surface allowed a higher amount of energy to be transferred from the wind to the liquid.

- As Stommel's model is used as a preliminary study, the results gathered so far can be used to acknowledge that surface wind drive does affect thermal circulation. Given the complexity and diversity of surface wind impact on ocean circulation, the experiments performed in this thesis does not provide a comprehensive picture, but they may be used to determine how a difference in wind strength impacts the flow rate.

- Experiments showed some unforeseen results which can be considered a drawback of the new setup. The small cross-sectional area of the bottom circulation pipe made it possible for air to get trapped during filling of the model, but a detailed method on how to avoid this was presented in chapter 6.

The main goal of developing a new model was to enable students, teachers and professors at the multiphase laboratory to do research and studies on thermal circulation with surface wind. By using the guide presented in appendix C, the model can be put to use as it stands. Suggestions of how to further develop the model was given in chapter 6. In conclusion, the developed model can already be used for thermal circulation with surface wind, and the thesis can be used as a precursor when the model is to be furthered developed. Parameters which can be changed during experimentation ranges from wind speed and wind direction, to liquid height and temperature.

References

[1] Stefan Rahmstorf. Thermohaline ocean circulation. *Encyclopedia of Quaternary Sciences*, 2006.

[2] Henry Stommel. Thermohaline convection with two stable regimes of flow. *In: Tellus 13.2, pp. 224–230.*, 1961.

[3] John P. Bentley. *Principles of Measurement Systems*. Pearson Education Limited, 4 edition, 2005.

[4] Rune W. Time. Two-phase flow in pipelines, course compendium with matlab examples and problems. *University of Stavanger*, 2017.

[5] Joan Shanita Wanyenze. Small scale thermohaline ocean circulation (master thesis). *University of Stavanger*, 2020.

[6] Sensirion the sensor company. Slq-qt500 liquid flow meter datasheet. `https://www.sensirion.com/fileadmin/user_upload/customers/sensirion/Dokumente/4_Liquid_Flow_Meters/Liquid_Flow/Sensirion_Liquid_Flow_Meters_SLQ-QT500_Datasheet.pdf`, 2018.

[7] Engineering ToolBox. Water - density, specific weight and thermal expansion coefficient. `https://www.engineeringtoolbox.com/water-density-specific-weight-d_595.html`, 2003.

[8] Y.A. Cengel, J.M. Cimbala, and R.H Turner. *Fundamentals of Thermal-Fluid Sciences*. PMcGraw-Hill Education, 5 edition, 2012.

[9] M.L. Parry, O.F. Canziani, J.P. Palutikof, P.J. van der Linden, and C.E. Hanson. Climate change 2007: Impacts, adaptation and vulnerability. *Fourth Assessment Report of the Intergovernmental Panel on Climate Change*, 2007.

[10] T.F. Stocker, D. Qin, G.-K. Plattner, M. Tignor, S.K. Allen, J. Boschung, A. Nauels, Y. Xia, V. Bex, and P.M. Midgley. Climate change 2013: The physical science basis. *Fifth Assessment Report of the Intergovernmental Panel on Climate Change*, 2013.

[11] Rich Pawlowicz. Key physical variables in the ocean: Temperature, salinity and density. *Nature Education Knowledge*, 4(4), 2013.

[12] Britannica T. Editors of Encyclopedia. Latitude and longitude. `https://www.britannica.com/science/latitude/additional-info#history`, July 20, 1998.

[13] National Geographic Society. Ocean currents. *Resource library, encyclopedic entry*, 2019.

[14] Carl Wunsch. Thermohaline loops, stommel box models, and the sandstrom theorem. *Department of Earth, Atmospheric and Planetary Sciences, Massachusetts Institute of Technology, Cambridge*, 2004.

[15] T. D. Østevold and E. Marvik. "north - stommel eksperimentet" eksperiment oppsett og manual. *University of Stavanger*, 2019.

[16] W. Thielicke and E.J. Stamhuis. Pivlab - towards user-friendly, affordable and accurate digital particle image velocimetry in matlab, 2014.

[17] J. Westerweel, G. Elsinga, and R. Adrian. Particle image velocimetry for complex and turbulent flows. *Annual Review of Fluid Mechanics*, 45:409–436, 01 2013.

[18] Britannica T. Editors of Encyclopedia. Copper. `https://www.britannica.com/science/copper`, October 28, 2020.

[19] S.A. Sulaiman and N.A.Z Kamarudin. Bubbles size estimation in liquid flow through a vertical pipe. *Journal of Applied Sciences*, 12, 2012.

Appendix A

MATLAB scripts

A.1 Fluid flow script

```
% Calculate Sea water density difference and pressure for two sea water
% columns of height H
% SW_Density and SW_Psat is copied from
% http://web.mit.edu/seawater/
% MATLAB, EES, and VBA files in a zip archive
% (Version: 20 February 2017. Version history.)

clear all
g = 9.81 % g constant m/s^2
H = 1    % (m) Height of tank
T1= 10 %Temperature in tank 1 - deg C
uT = 'C'
S1 = 0  % Salinity in tank 1 -
uS = 'ppt'
P = 1 % Approximate abolute pressure in bar
uP = 'bar'

rho1 = SW_Density(T1,uT,S1,uS,P,uP)

T2 = 25 %Temperature in tank 1
S2 = S1
rho2 = SW_Density(T2,uT,S2,uS,P,uP)

drho = rho1-rho2
DP = drho*g*H

rho_ave = 0.5*(rho1+rho2)

% Flowrate:
% DPdx = (32/d^2)*my*U
my = 1.150e-3
d = 4.35e-3
L = 0.95
DPL = DP/L

' With MIT density'
```

```
' With MIT density - Laminar solution '
% Flow speed U:
U = DPL*d^2/my
Reyn = rho_ave*U*d/my
Areal=pi*d^2/4
% Flowrate:
Q = U*Areal % m^3/s
Qmlprsek = Q*1e6
Qmlprmin = Qmlprsek*60

' With MIT density - Turbulent solution '
% If Reyn>4.000 --> turbulent f =0.046*Reyn^-0.2
% define the constant including d, my,rho into F
F=0.092*d^-1.2*rho_ave^0.8*my^0.2
Uturb =sqrt(DPL/F)^1/1.8
%Turbulent solution:
Qturb = Uturb*Areal % Turbulent solution
QTurbmlprsek = Qturb*1e6
QTurbmlprmin = QTurbmlprsek*60

% ********************************************
% Med Stommel istf
' With Stommel density'
rhoSt1 = density_Stommel(S1,T1)
rhoSt2 = density_Stommel(S1,T2)
drhoSt = rhoSt1-rhoSt2
DPSt = drhoSt*g*H

rhoSt_ave = 0.5*(rho1+rho2)
' With Stommel density - Laminar solution '
% Flowrate:
% DPdx = (32/d^2)*my*U
% Flow speed U:
USt = (DPSt/L)*d^2/my

% Flowrate:
QSt = USt*Areal % m^3/s
QStmlprsek = QSt*1e6
QStmlprmin = QStmlprsek*60

'With Stommel density - Turbulent solution'
% If Reyn>4.000 --> turbulent f =0.046*Reyn^-0.2
% define the constant including d, my,rho into F
F=0.092*d^-1.2*rho_ave^0.8*my^0.2
DPStL = DPSt/L
USt_turb =sqrt(DPStL/F)^1/1.8
%Turbulent solution:
QSt_turb = USt_turb*Areal % Turbulent solution
QSt_Turbmlprsek = QSt_turb*1e6
QSt_Turbmlprmin = QSt_Turbmlprsek*60
```

A.2 Stommels Density script

```
function rho = densityStommel(S,T)

% Function for water density versus temperature and salinity (g salt/kg vann)

Alfa = 1.3e-4; %K^-1
Beta = 7.9e-4; % Non-dimensional
rho0 = 1000;
rho = rho0*(1-Alfa*T+Beta*S);
```

The MIT density script used can be found and copied from http://web.mit.edu/seawater/

Appendix B

Results

B.1 Feasibility test

Figure B.1 shows one of the results when the Sensirion liquid flow meter was tested in a small U-pipe.

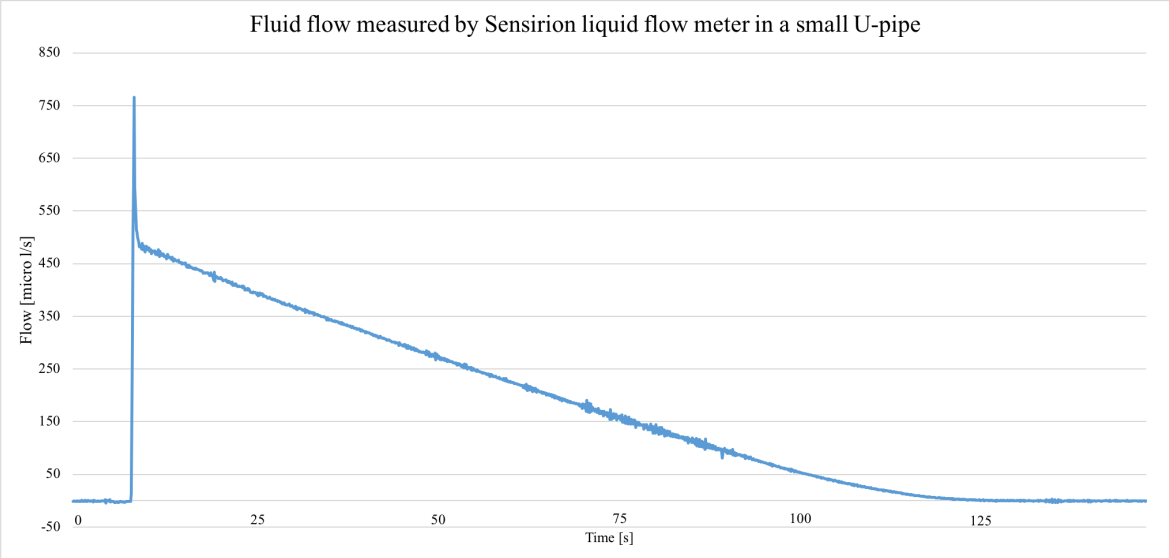

Figure B.1: Sensirion test in small U-pipe

The flow rate decreases linearly throughout the time period, as the pressure decreases until it equalizes. From analysing the data, one can see that the flow meter measured the liquid flow rate accurately down to +/- 0.5 $\mu l/s$.

B.2 Experimental results

Figure B.2 shows how the temperature developed during the first thermally driven circulation experiment. The development followed the same trend as for the other experiments.
Figure B.3 shows how the temperature developed during the second thermally driven circulation experiment. The development followed the same trend as for the other experiments.

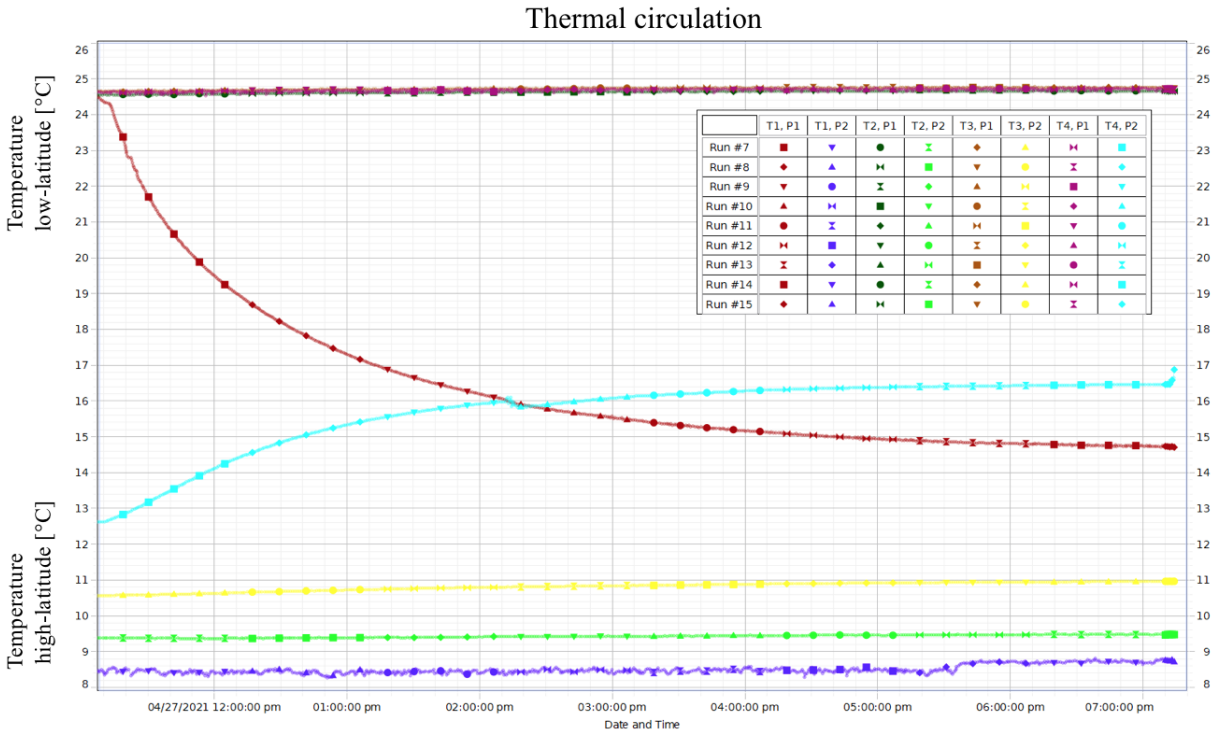

Figure B.2: Temperature development, thermal circulation first time

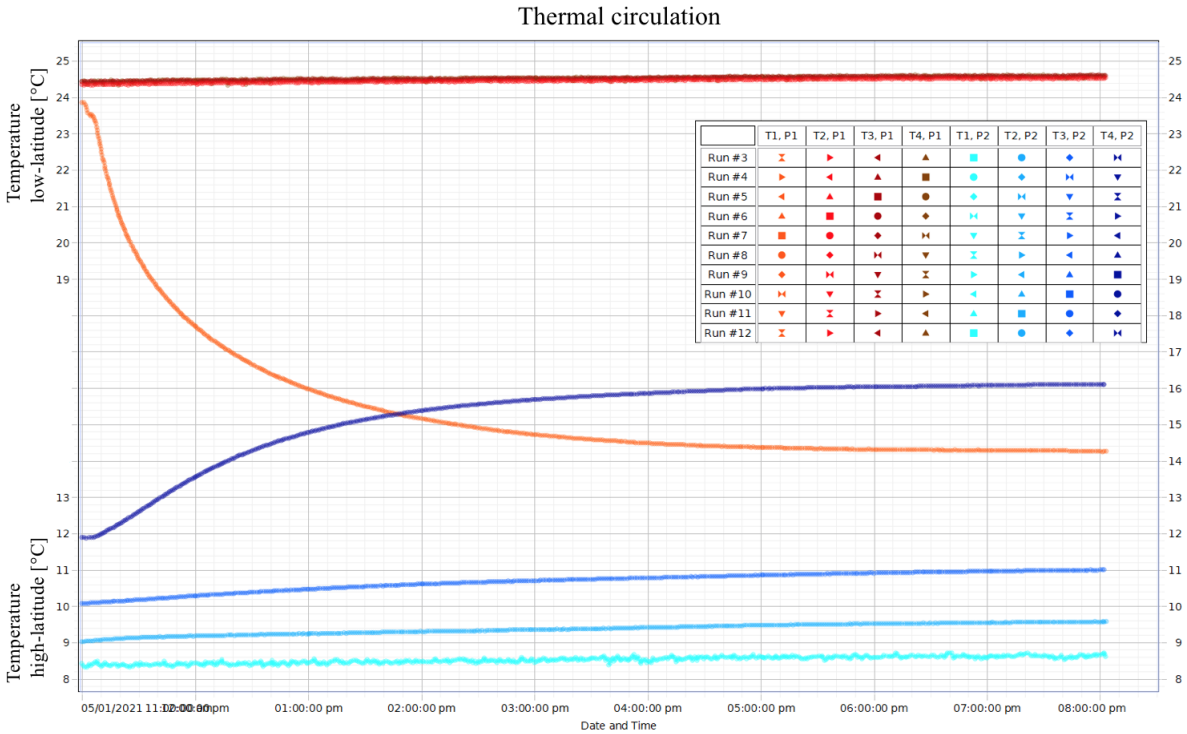

Figure B.3: Temperature development, thermal circulation second time

Figure B.4 shows a 2 hour excerpt of the fluid flow data for the third thermally driven circulation experiment.

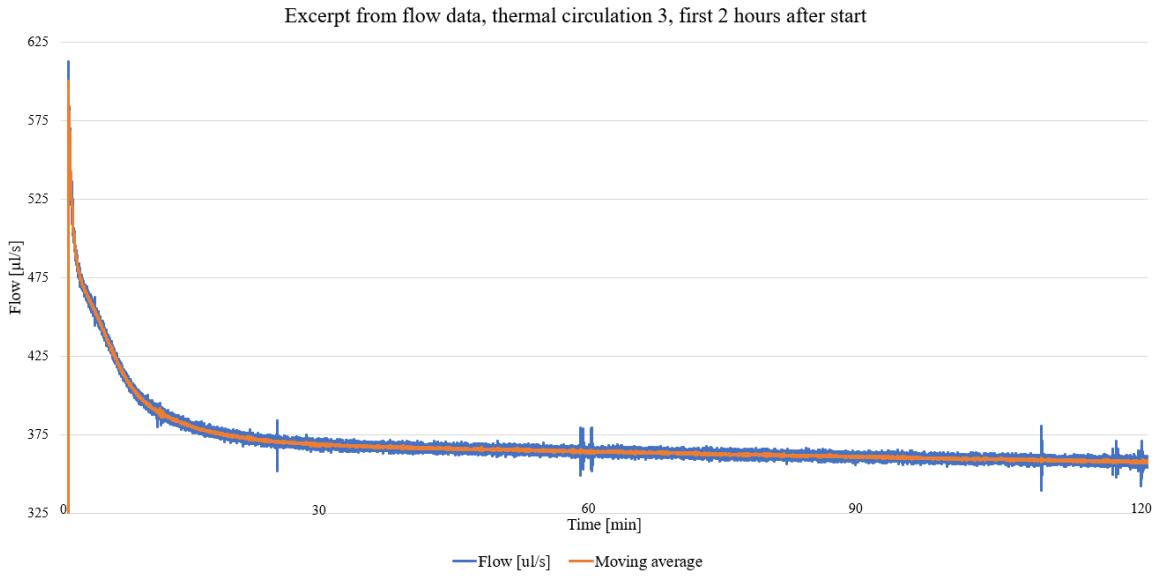

Figure B.4: Thermal circulation 3, first 2 hours of flow data

Figure B.5 shows a 2 hour excerpt of the fluid flow data for the thermally driven circulation with positive wind experiment.

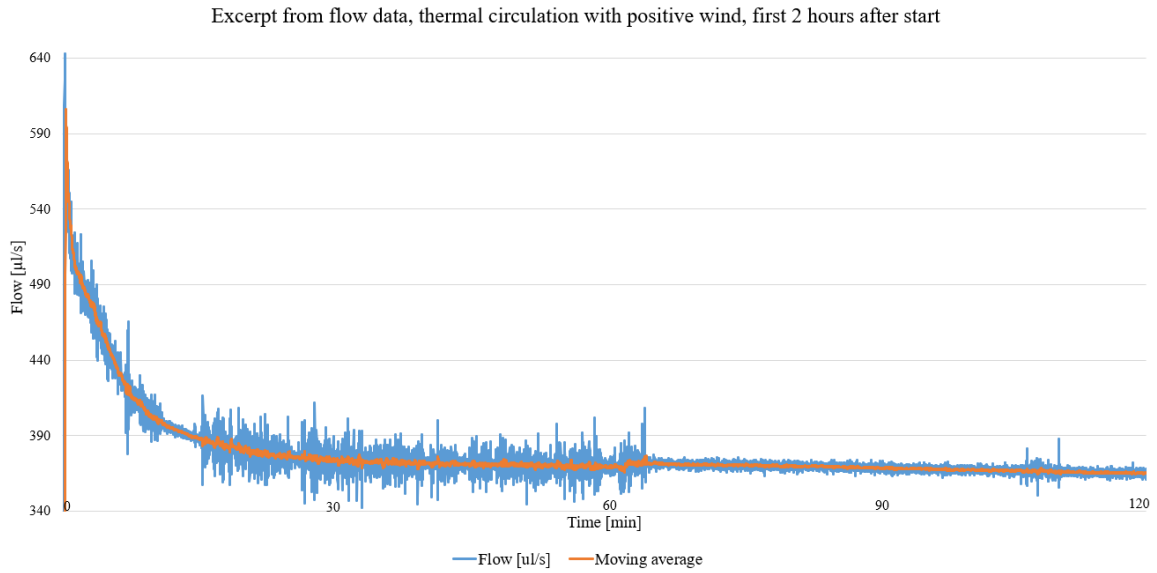

Figure B.5: Thermal circulation with positive wind, first 2 hours of flow data

Figure B.6 shows a 2 hour excerpt of the fluid flow data for the thermally driven circulation with negative wind experiment.

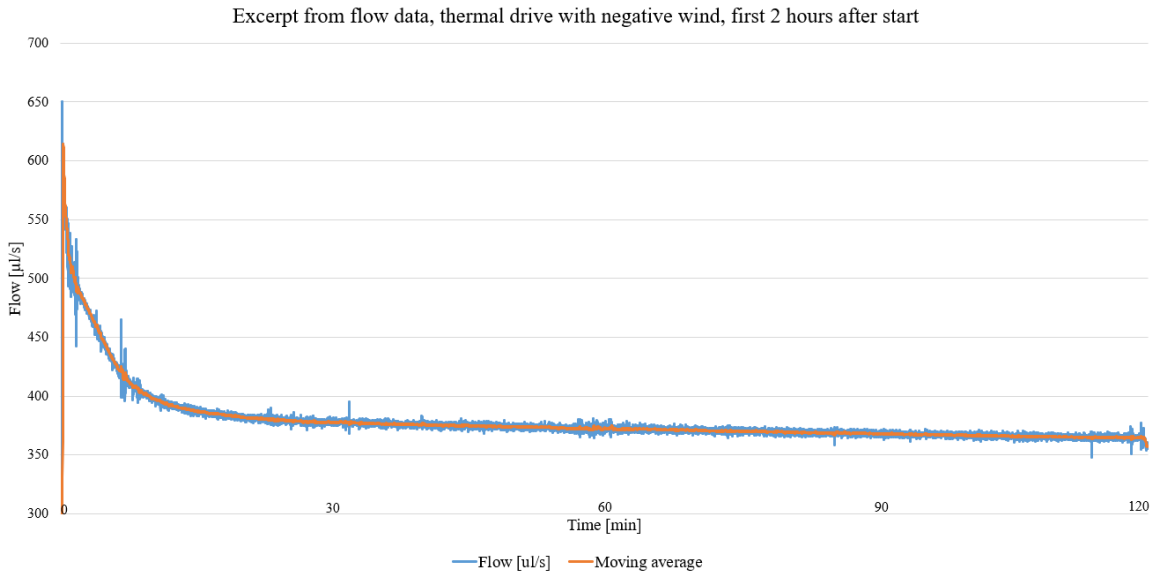

Figure B.6: Thermal circulation with negative wind, first 2 hours of flow data

Appendix C

Model structure, equipment specifications, calibration and setup

This appendix is meant to be a user guide for future use of the model, both in terms of experimentation and further development. The chapter includes detailed information about everything related to the model.

C.1 Model structure

The model was based on two PE100 plates (figure C.1) and two PMMA cast tubes (figure C.2).

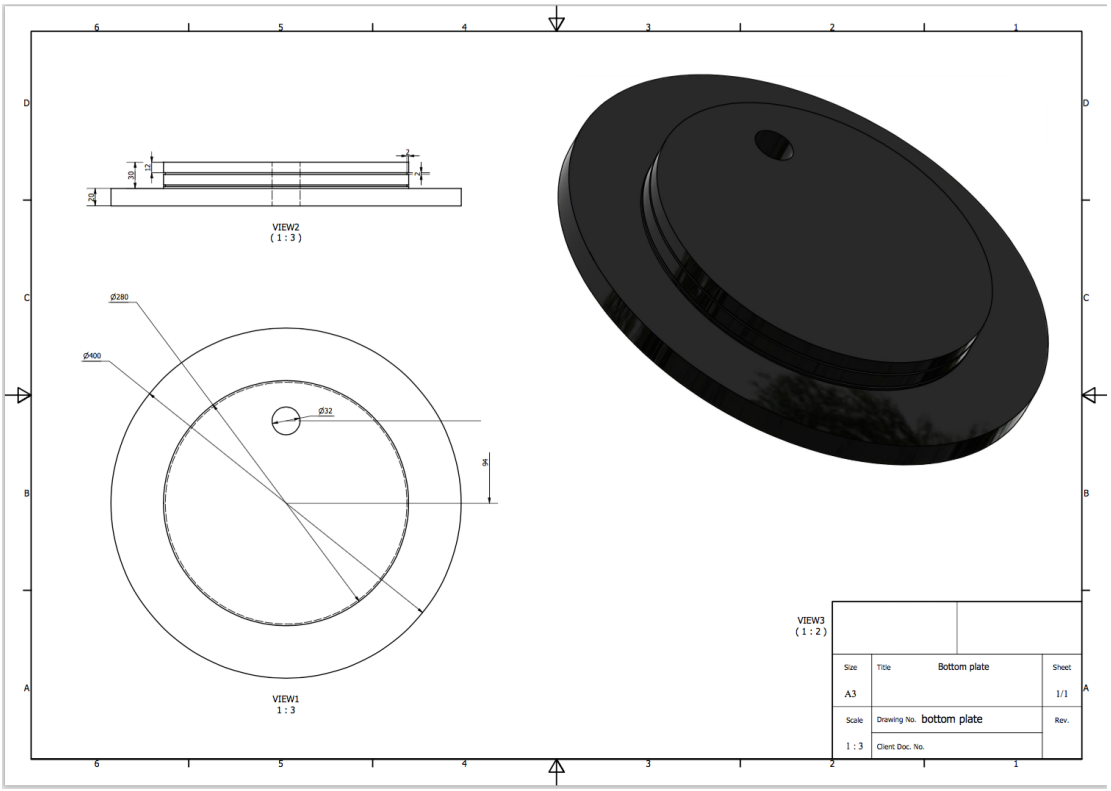

Figure C.1: Inventor drawing of PE100 plates, [Ida Haug Færøy]

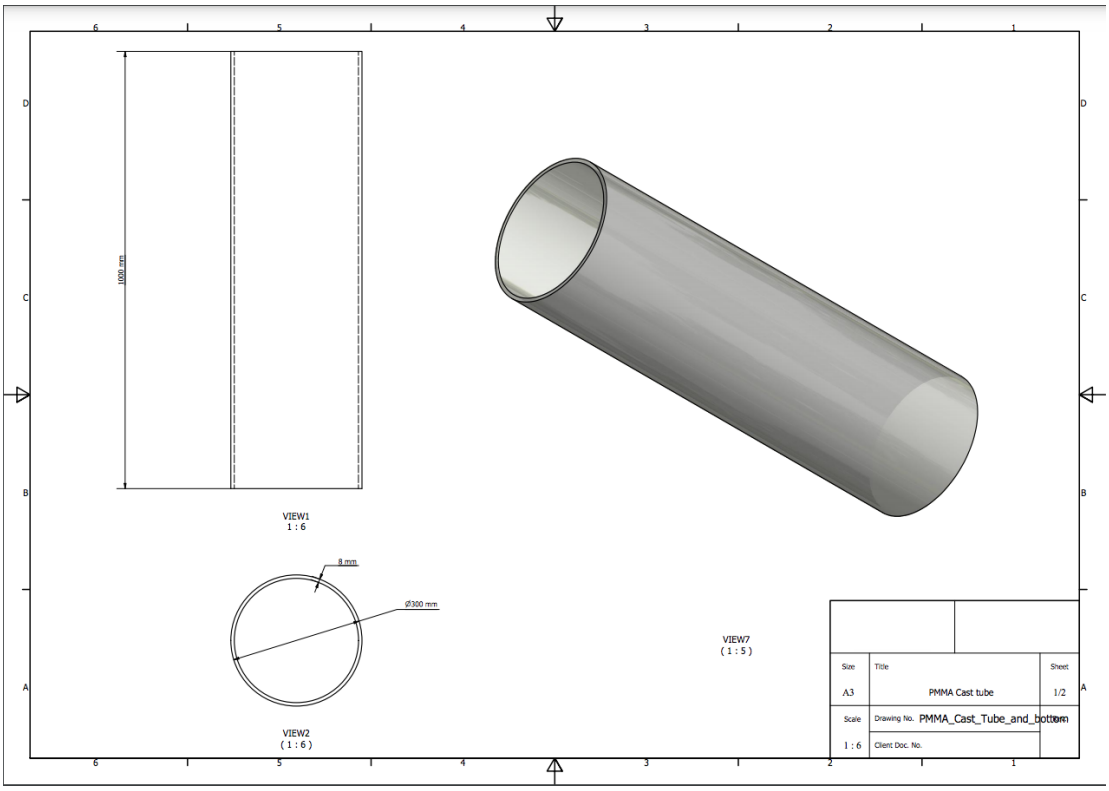

Figure C.2: Inventor drawing of PMMA cast tubes, [Ida Haug Færøy]

The Inventor drawings were made before the holes were drilled in the bottom plates, in order to ensure that they would be drilled correctly. The bottom plates came with two milled tracks, as shown in figure C.1. Due to the placement of the milled tracks, mainly the lowest one, it was decided to only use one rubber packing. The bottom milled track were filled with a large amount of flexible silicon before connecting the PE100 plates to the PMMA cast tubes.

Illustration of the new model is presented in figure 4.1. The different components are listed in table 4.1 with their respective dimensions, and some special components are highlighted in figure 4.2. A general descrition of how the model was built is listed below.

- Holes were drilled in the bottom plates using a 32 mm hole saw. The hole was then expanded slightly using a coars, semicircular file, and sanded using fine grained sandpaper. The hole was sanded until the hooded PCV pipe was situated straight through the bottom plate with a 90° angle relative to the plate.
- The hooded PVC pipe was connected to the bottom plate using both black and clear flexible silicon. The silicon was added around the hood of the PVC pipe before it was placed through the hole. The plate was then put on a table with the hood of the PVC pipe down, in order to put pressure on it. To make sure the pressure distribution was even, two items with the same thickness as the hood was placed under the plate. From the bottom of the plate, the space between the PVC pipe and the bottom plate was filled with silicon. The silicon was left to harden for the appropriate time, estimated based on the thickness of silicon.

- Rubber packing were fitted in the laboratory from rubber wire. The packing were then placed in the top, milled out track, and the bottom milled out track was filled with a large amount of flexible silicon. The cast tubes were placed over the bottom plates and pressed down. Lead weights were used to keep the pressure while the silicon hardened. The silicon was left to harden for the appropriate time, estimated based on the thickness of silicon.

- One of the 45° angled PVC bends had a hole in the bend. This was sealed with a rubber stopper. The PVC bends were then connected to each other by the rubber packing inside to make a 90° angle. The now 90° bends were connected to the hooded PVC pipe by the rubber packing.

- The brass ball valve was directly inserted into the now 90° bend, and held there by the rubber packing.

- The brass hose connection was connected to the valve by treads and sealed using thread tape. Pressure tested.

- The plastic cartridges, which were cut to ensure the outlet diameter would be equal to the inlet diameter of the flow meter, was connected to the brass hose connector using a clear PVC hose. This had a smaller ID than the OD of the brass hose connector and plastic cartridge, but was heated up to fit. Hose clamps were used on both sides to seal it.

- Holes were drilled in the large 90° bends, 12.5 mm from the top, on the backside. Placement is showed in figure C.5. The holes were threaded to connect plastic hose connectors to the bends. Clear, flexible silicon was used to ensure no air leakage.

- The acrylic pipes were connected to the 90° bends with clear, flexible silicon. The silicon was left to harden for the appropriate time, estimated based on the thickness of silicon.

- The model was connected to a table, which in turn was attached to the floor, with four table clamps and two lead weights to ensure it would not tip over. The flow meter was used to connect the model.

- The bottom circulation pipeline was secured by a metal profile attached to the table underneath it.

The final setup is shown in figure C.3.

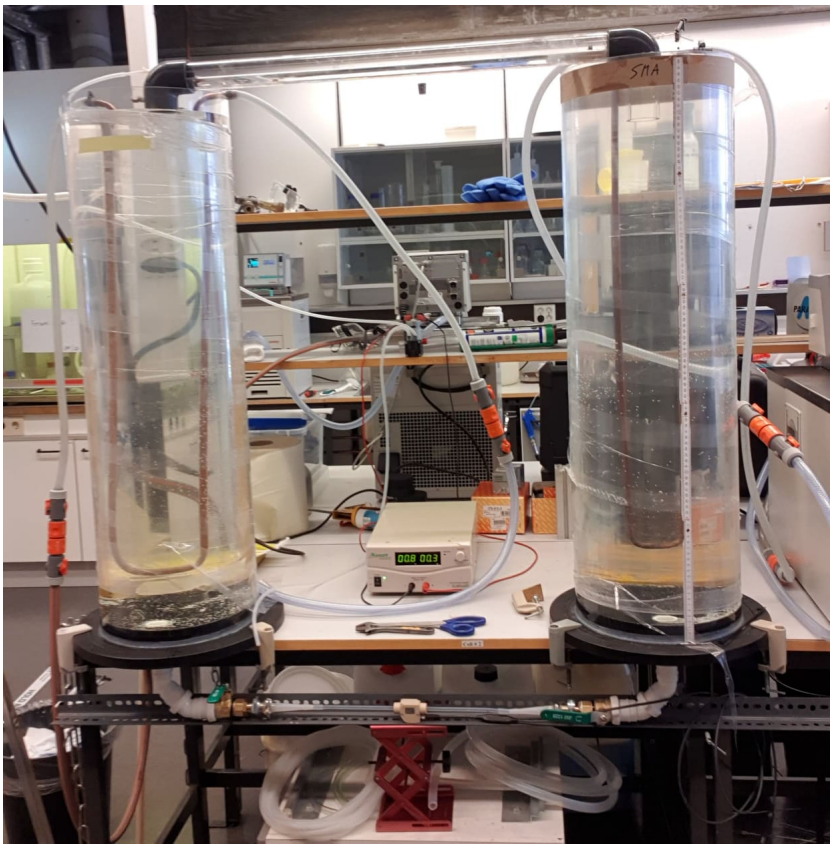

Figure C.3: New model setup

Insulation:
The model was insulated using bubble wrap. Two to three layers were used around the tanks, and four to six layers were used around the bottom circulation pipe. To replicate the natural surroundings, the top circulation pipe was not insulated. Figure C.4 shows the model after it was insulated. The figure shows also how the tanks were marked based on the water temperature, how the bottom circulation pipe was kept up using a metal L-profile connected to the table, the power supply used for the vacuum pump, the Pasco 850 universal interface and the vacuum pump. The large hoses were connected to the water baths and the copper pipes.

Figure C.4: New model insulated

Vacuum pump connection:
Figure C.5 shows the inlet/outlet of the top circulation pipe, and how the pipe was laying on top of the model. On top of the model, the pipeline was kept in place using tape. The pipeline was also checked to ensure it was level.

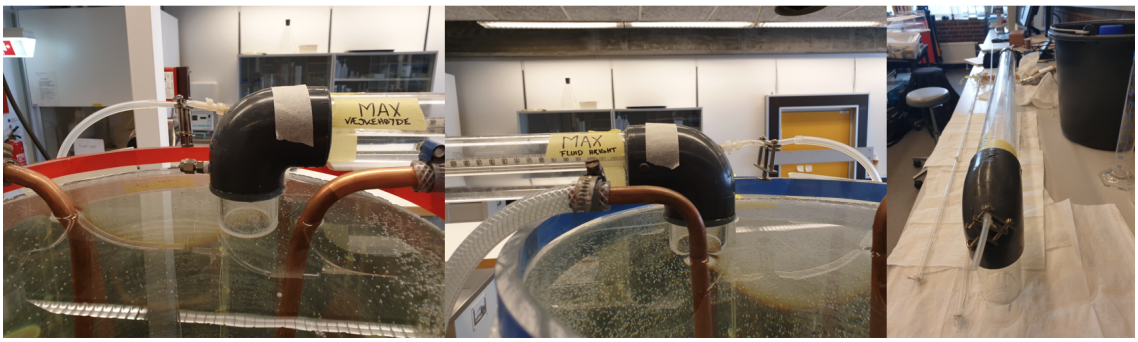

Figure C.5: Top circulation pipe, hose connectors

Figure C.6 shows a picture of the original crocodile clips used on the left, and the new clamps with a closing mechanism on the right. The new clamps ensured that the pump would not stop during experiments.

Figure C.6: Clamps used to connect the vacuum pump to the power source

Temperature sensors:
The temperature sensors were coiled around a plastic rod with an interval of 30 cm. This can be seen in figure C.7, together with how they were marked.

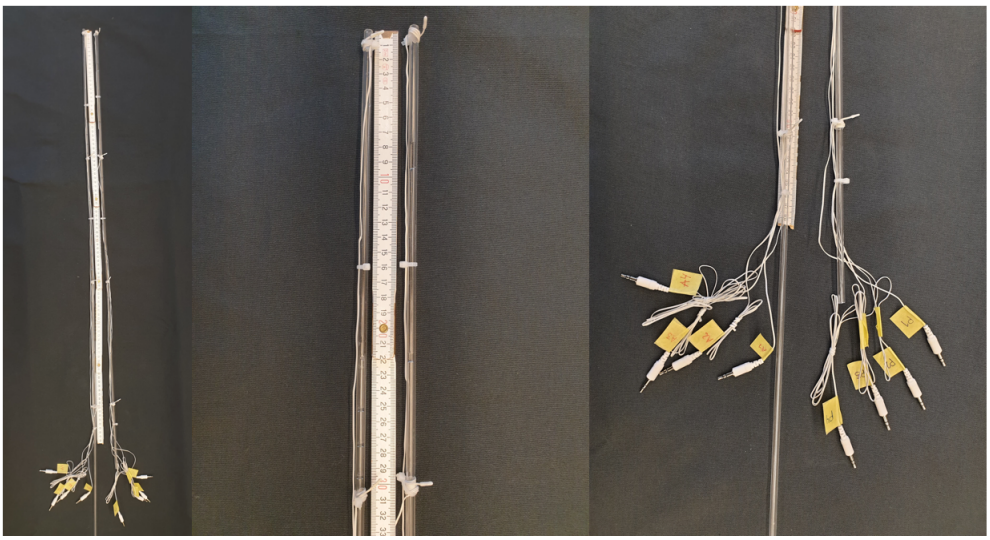

Figure C.7: Temperature sensors coiled on rod

A closeup of how the sensors were coiled is showed in figure C.8. A metal screw was attached close to the bottom of the poles, in order to limit the movement induced by the liquid circulating in/out of the tanks.

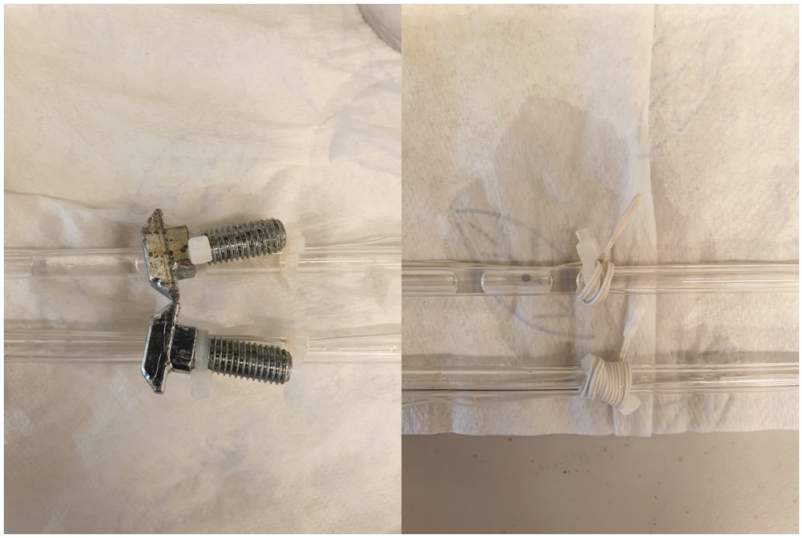

Figure C.8: Close-up temperature sensor coiled on rod and weights

From the figure, one can clearly see how the steel screws have already been affected by being in water over time.

The numbering of each sensor made it easy to identify the sensor placements during logging and analyzing. Figure C.9 shows how the Pasco Quad Sensors were attached to the model using double sided tape and masking tape. From the picture, one can clearly see how each sensor was marked to see which port it was connected to.

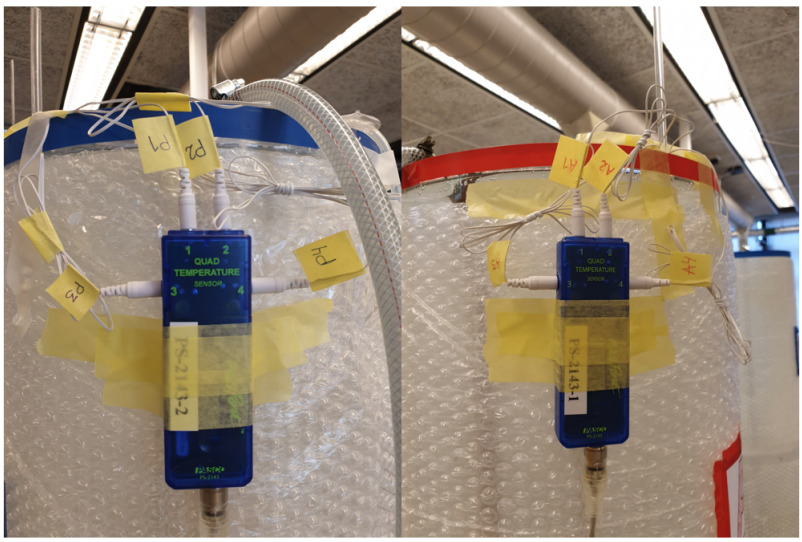

Figure C.9: Pasco Quad Sensors connected to the model

Emptying the model:
The model was emptied by closing both valves, removing the flow meter and connecting a hose to the plastic cartridge. The hose end was then placed in a drain in the floor, and the valves were opened. In the picture one can also see the clamps used to attache the model to the table and the yellow weights used. This is showed in figure C.10.

Figure C.10: Illustration of how to empty the new model

The method made it possible to do other things while the model was being emptied. In the picture one can also see the clamps used to attache the model to the table and the yellow weights used.

C.2 equipment specification

This section presents the specifications of the different sensors and measurement equipment used in the model.

Sensirion SLQ-QT500 Liquid Flow Meter:

- Liquid flow rates up to 120 ml/min
- Flow detection response time < 50 ms
- Operating temperature +5 - +50 °C
- Max operating pressure 12 bar
- Accuracy below full scale 5 % of measured value
- Repeatability below full scale 0.5 % of measured value

Online source: https://www.sensirion.com/

PASPORT QUAD Temperature Sensor PS-2143:

- Accuracy: -35 to +135 °C at +/- 0.5 °C
- Displays °C, K and °F
- Resolution: 0.0025 °C
- Maximum Sample Rate: 100 Hz

Online source: https://www.pasco.com/

Manson SPS-9602 Power Supply:

- Total max. continuous output current: 30A
- Precise Load Point Voltage: 1-30 V
- Remote Sensing
- Low ripple and noise
- Analogue remote control
- Thermostat control fan cooling
- High RFI stability

Online source: https://www.manson.com.hk/

AIRPRO D2028B Vacuum Pump 12 V:

- Operating range: 0 - 220 kPa
- Free flow range: 12-15 LPM
- Vacuum range: 0-16 ”Hg
- Pressure range: 0-32 PSI
- Operating temperature range 0-50 °C
- Power: 12W
- Standard motion voltage options: 12VDC

Julabo F34-HE Refrigerated/heating circulator:

- Working temperature range: -30 ... +150 °C
- Temperature stability: +/- 0.01 °C
- Heating capacity: 2 kW
- Cooling capacity: 0.45 kW
- Pump capacity flow rate: 22...26 l/min
- Pump capacity flow pressure: 0.4...0.7 bar
- Filling volume: 14...20 l

Online source: https://www.julabo.com/en

Julabo F33-HE Refrigerated/heating circulator:

- Working temperature range: -30 ... +250 °C
- Temperature stability: +/- 0.01 °C
- Heating capacity: 2 kW
- Cooling capacity: 0.5 kW
- Pump capacity flow rate: 22...26 l/min
- Pump capacity flow pressure: 0.4...0.7 bar
- Filling volume: 12...16 l

Onine source: https://www.julabo.com/en

PASPORT Weather Anemometer Sensor PS-2174:

- Wind Speed Range: 0.5 - 29 m/s
- Wind Speed Resolution: 0.1 m/s
- Wind Speed Accuracy: +/- (3 % of reading + 0.2 m/s)

Online source: https://www.pasco.com/

C.3 equipment calibration

This section presents the calibration method used for the different sensors and the result.

Sensirion SLQ-QT500 Liquid Flow Meter:
A gravimetric calibration method was used to calibrate the flow meter. The method is cost-effective and ideal for liquid flow meters, and involves using a calibrated scale to measure the fluid passing through the flow meter and then comparing the cumulated flow measured by the flow meter to the cumulated weight measured by the scale. The setup is showed in figure C.11.

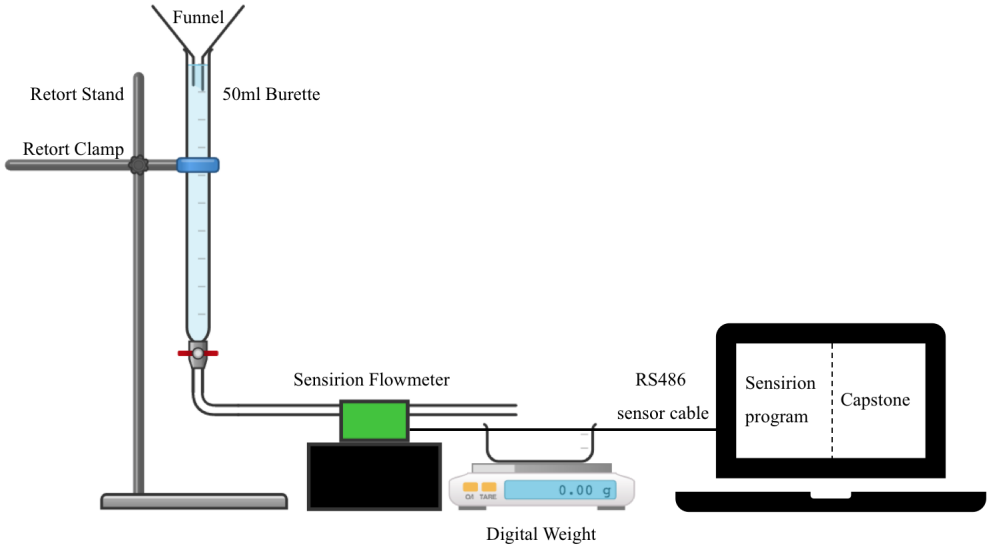

Figure C.11: Experimental setup for gravimetric calibration

The digital weight was wireless connected to Capstone by Bluetooth on the same computer as the Sensirion flow meter. A known amount of distilled water was poured into the burette to make sure the experiment could be repeated. The valve was kept closed until the logging programs were turned on and the logging started.

The volumetric flow, measured by the Sensirion flow meter, is showed in figure C.12. The water weight, measure by the digital weight, is showed in figure C.13.

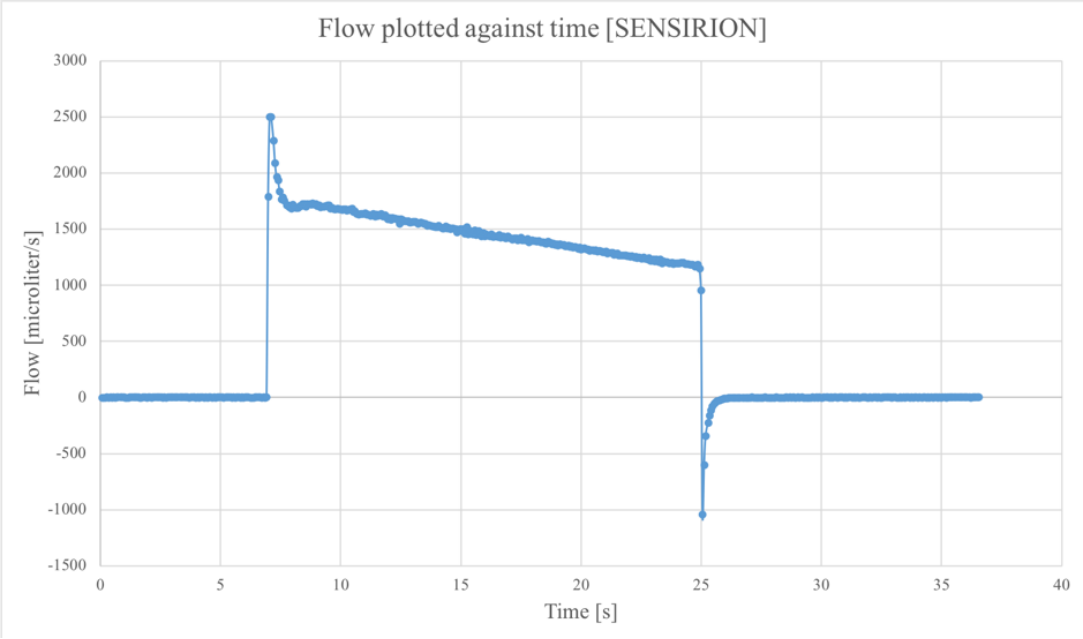

Figure C.12: Volumetric flow plotted against time, calibration

The volumetric flow decreases linearly as the hydrostatic pressure decreases in the burette.

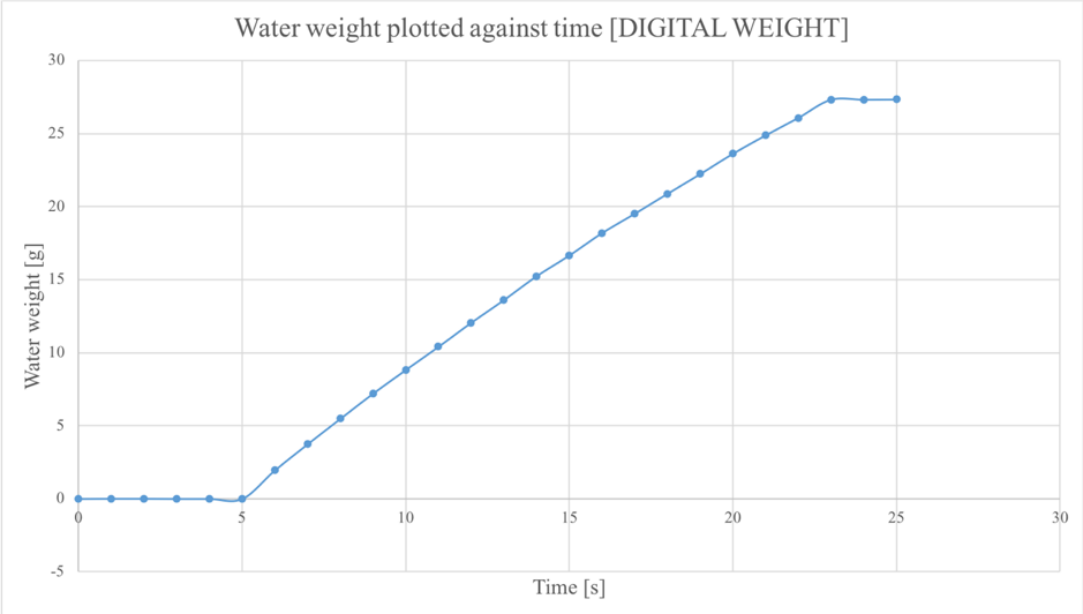

Figure C.13: Liquid weight plotted against time, calibration

The water weight increases linearly as the burette was emptying.

The measured fluid flow was plotted against the measured fluid weight. The result is presented in figure C.14.

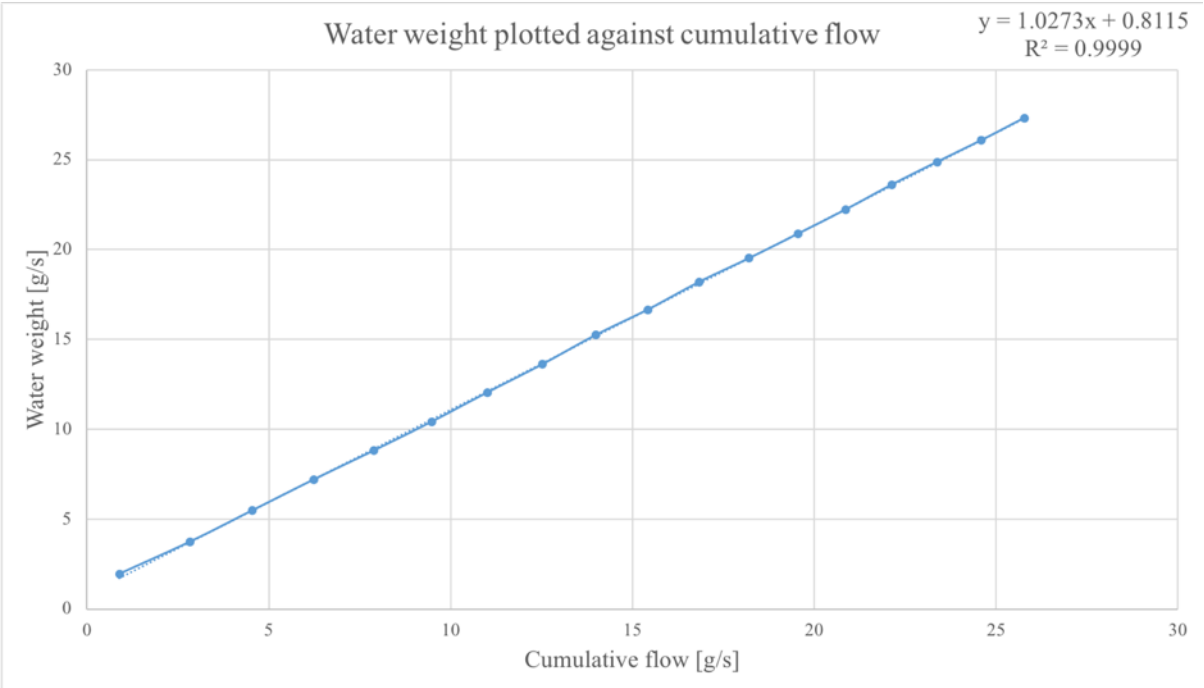

Figure C.14: Liquid weight plotted against cumulative flow, calibration

From the figure, one can see the result was a linearized trendline. The small difference in cumulative weight and cumulative volumetric flow may be due to friction in tubes or some unseen air bubbles.

Pasco QUAD Temperature Sensor PS-2143:
Using Fluke Calibration 9102S Dry-well and a standard two-point method. This method involves resetting two points to define a new calibration line that affects both the slope and the offset which are both used when raw data from the sensors are being calibrated.

The sensors were connected to Capstone by Pasco 850 universal interface. The Fluke Calibration Dry-well was turned on, and a set temperature was chosen to be 30 °C. The calibration dry-well was left to heat up and stabilize (approximately 10-15 minutes). Calibration was chosen from the tools palette in the Capstone program, and temperature was chosen as measurement type. Standard two-point method was chosen as calibration type. The temperature read from the calibration dry-well was entered in the Standard Value text box in Capstone, and the temperature sensor was placed inside the dry-well. After letting the Current Value stabilize, current value was set to standard value. The set temperature of the dry-well was then reduced to 10 °C, and the procedure was done again. Capstone calculates the new calibration line. The method is showed by figure C.15.

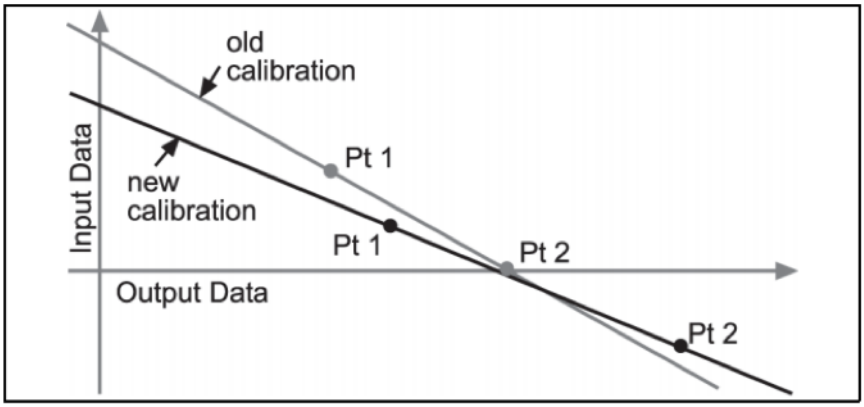

Figure C.15: Two-point calibration method, temperature

C.4 equipment setup

This section is a supplement to the experimental method in this thesis, and presents how the different measurement equipment was set up together with the logging programs.

Sensirion SLQ-QT500 Liquid Flow Meter:
The Sensirion flow meter was connected to a laptop situated beside the model with a RS485/ USB sensor cable. The program "USB RS485 Sensor Viewer" was opened, which gives the window "Product Selection", shown in figure C.16.

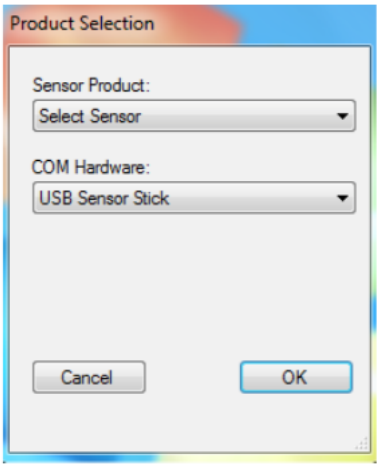

Figure C.16: Sensirion setup: Product Selection window

Liquid flow sensor is chosen under "Sensor Product", and 485/ USB sensor cable under "COM Hardware". An extended window appears where one has to choose the correct COM port used. When the connection is established, the "Liquid Flow Viewer" is opened, shown in figure C.17.

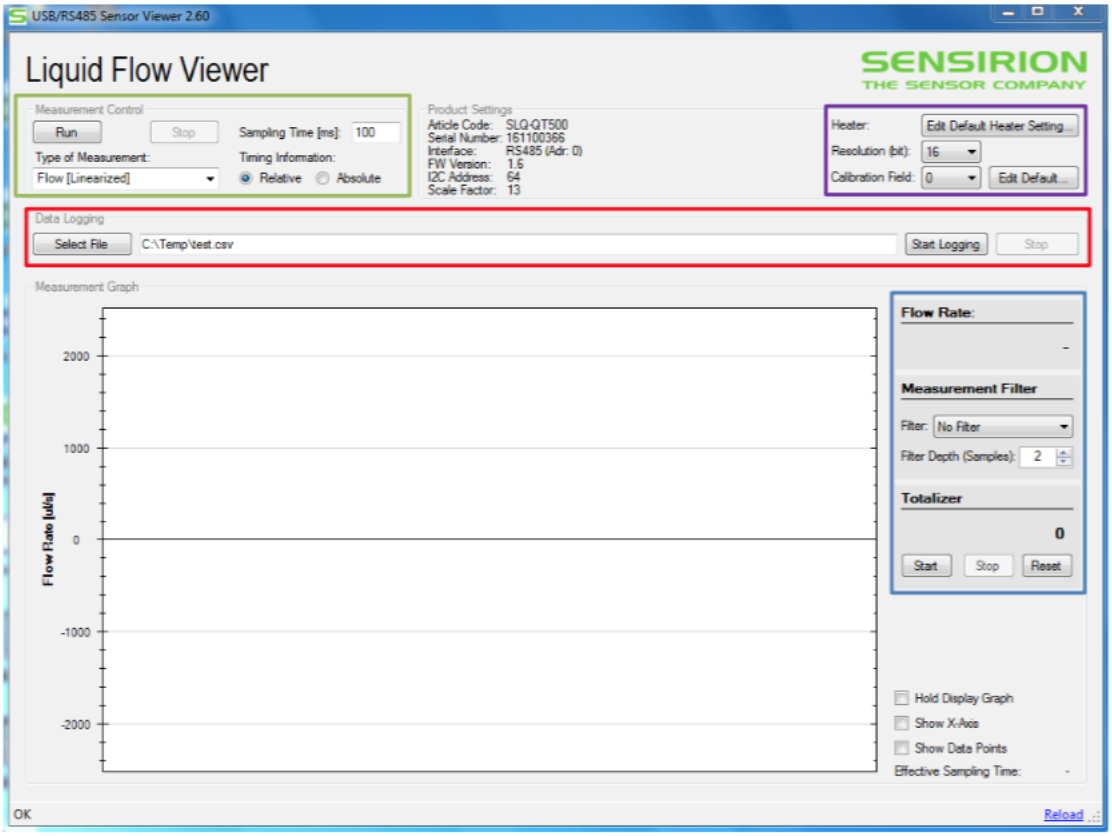

Figure C.17: Sensirion setup: Liquid Flow Viewer

In "Data logging", one can either choose a file where one wants the data to be saved, or write in a new file name. Log parameters which can be altered includes resolution, calibration field and measurement type as well as filtering.The following settings were used during the experiments:

- Sampling Time (ms): 500 (converts to 2 Hz)
- Timing Information : Relative
- Type of Measurement: Flow [Linearized]
- Heater: Default
- Resolution (bit) : 16
- Calibration field: 2

The default calibration field is 0, which is calibrated for IPA. It is therefore important to change to calibration field 2, which is for water.

Press "Run", shown inside the green square in figure C.17, to start the sensor. Press "Start Logging", inside the red square in figure C.17 to start storing measured data in the requested file. "Totalizer", inside the blue square, can be started to calculate the total liquid flow, but this value does not get stored in the chosen logging file and has to be manually written down.

Pasco QUAD Temperature Sensor PS-2143:
Fast responding temperature sensors were connected to the Pasco QUAD Temperature Sensor PS-2143, which in turn was connected to the Pasco 850 Interface with the included cable. The interface was connected to a computer with two independent displays using a USB cable, and the program Capstone was started. A detailed guide how to use Capstone can be found on pasco.com. The capstone program is opened over two screens, where the table is shown on one, and the graph on the other.

Appendix D

Illustrations

Liquid flow in the top circulation design A could be measured by a flow meter by introducing a valve, as showed in figure D.1.

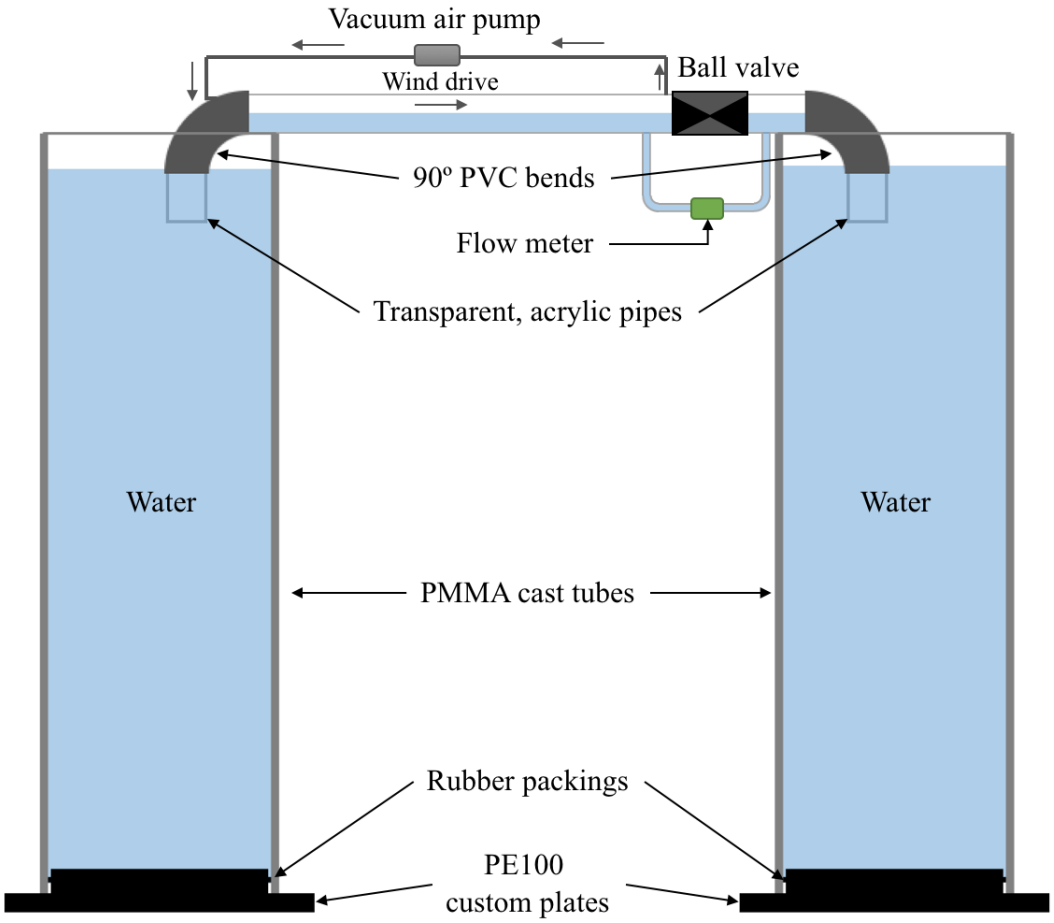

Figure D.1: Top Circulation A design whit flow meter

Liquid flow in the top circulation design B could be measured by a flow meter by introducing a valve, as showed in figure D.2.

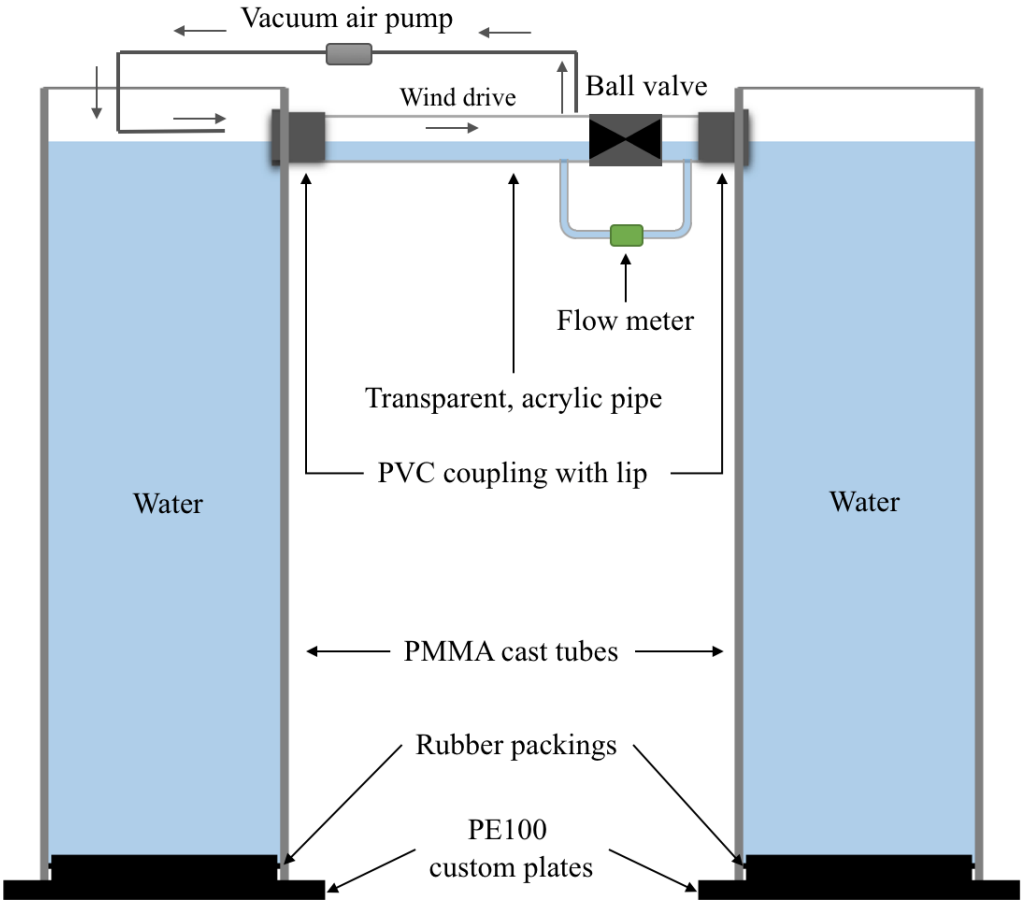

Figure D.2: Top Circulation B design whit flow meter

The heating/cooling element chosen in the temperature regulation system can be shaped differently. Two alternative shapes than what was chosen in the model can be seen in figure D.3.

(a) Long copper pipe, bent

(b) Long copper pipe, coiled

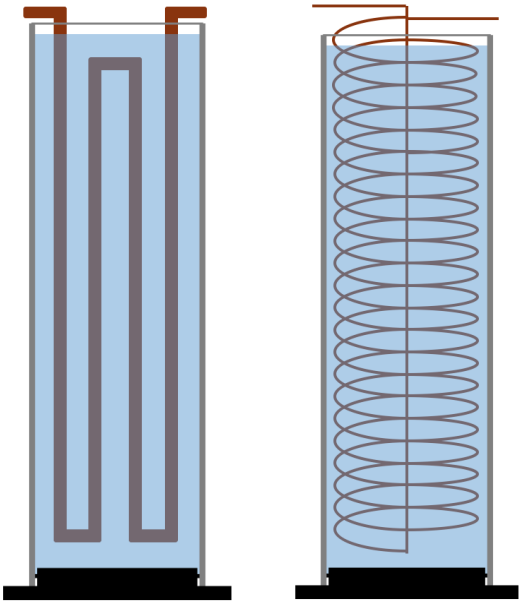

Figure D.3: Alternative shapes for heating/cooling element

The Sensirion flow meter was tested in a small scale U-pipe, showed in figure D.4.

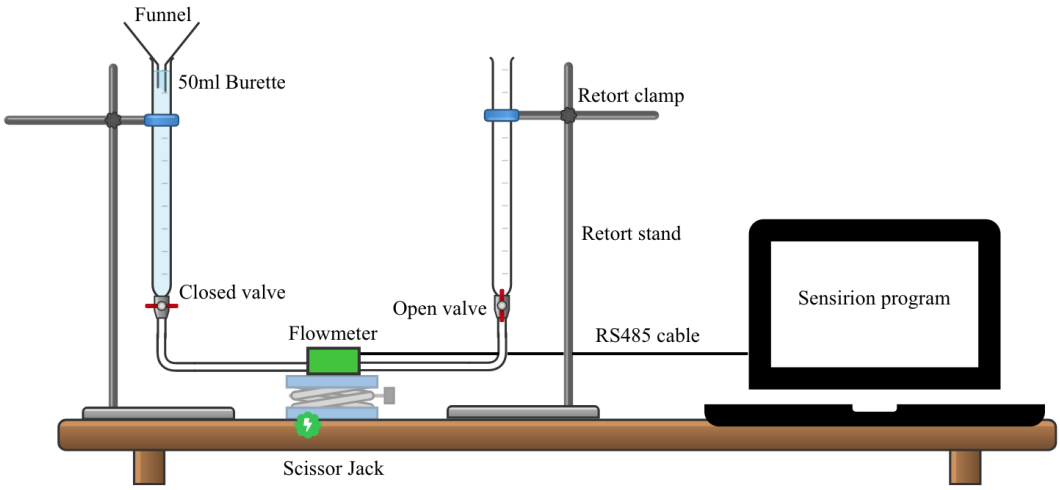

Figure D.4: Small scale U-pipe for testing Sensirion

Three tests were performed on the Pasco small scale circulation model. Some snapshots of the experiment are shown in figure D.5, D.6 and D.7.

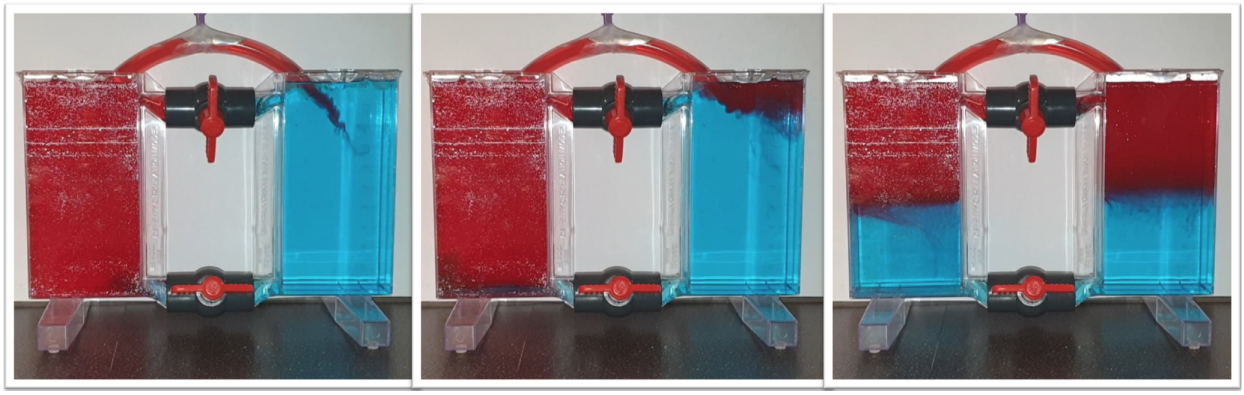

Figure D.5: Pasco model with large PVC hose

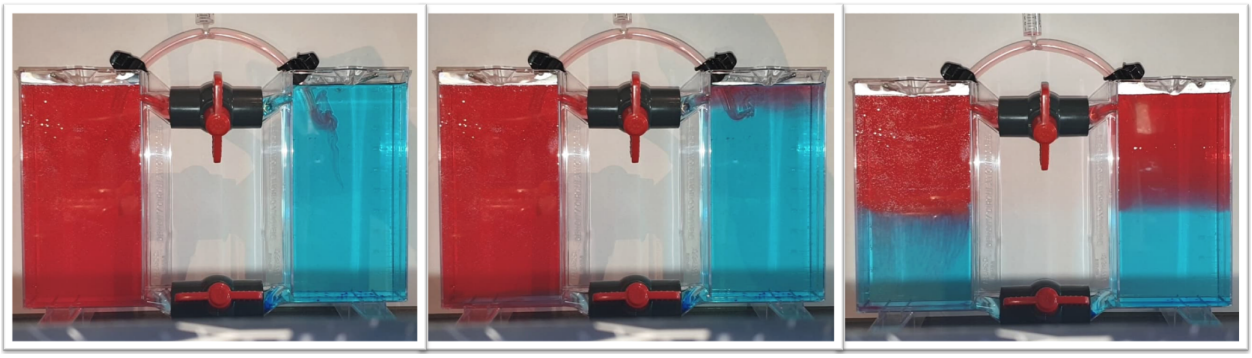

Figure D.6: Pasco model with small PVC hose

Figure D.7: Pasco model with no PVC hose